

Adsorption of organic micropollutants onto activated carbon and zeolites

Water management academic press

Published by
Water Management Academic Press
PO Box 5048
2600 GA Delft
the Netherlands
Tel.: +31 15 278 3347

Author D.J. de Ridder
Printed Gildeprint Drukkerijen BV
ISBN 978-94-6186-068-2

Adsorption of organic micropollutants onto activated carbon and zeolites
Copyright © 2012 by Water Management Academic Press

All rights reserved. This book, or parts thereof, may not be reproduced in any form or by any means, electronic or mechanical, including photocopying, recording or any information storage and retrieval system now known or to be invented, without written permission from the Publisher.

Adsorption of organic micropollutants onto activated carbon and zeolites

Proefschrift

ter verkrijging van de graad van doctor
aan de Technische Universiteit Delft;
op gezag van de Rector Magnificus prof.ir. K.C.A.M. Luyben;
voorzitter van het College voor Promoties
in het openbaar te verdedigen op donderdag 15 november 2012 om 15:00 uur

door
David Johannes DE RIDDER

civiel ingenieur

geboren te Utrecht

Dit proefschrift is goedgekeurd door de promotoren:

Prof.ir. J.C. van Dijk

Prof.dr.ir. G.L. Amy

Samenstelling promotiecommissie:

Rector Magnificus

voorzitter

Prof.ir. J. C. van Dijk

Technische Universiteit Delft, promotor

Prof.dr.ir. G.L. Amy

King Abdullah University of Science and Technology, promotor

Prof.dr.ir. R Denoyel

Université de Provence

Prof.dr.ir. A.R.D. Verliefde

Universiteit van Gent

Prof.dr.ir. J.P. van der Hoek

Technische Universiteit Delft

Prof.dr.ir. W.G.J. van der Meer

Technische Universiteit Delft

Dr.ir. S.G.J. Heijman

Technische Universiteit Delft

Prof.dr.ir. L.C. Rietvelt

Technische Universiteit Delft, reservelid

S.G.J. Heijman heeft als begeleider in belangrijke mate aan de totstandkoming van het proefschrift bijgedragen.

De Vereniging van Waterleidingbedrijven in Nederland (VEWIN) heeft met haar financiële ondersteuning dit proefschrift mogelijk gemaakt.

ISBN: 978-94-6186-068-2

Summary

Numerous organic micropollutants are present in water sources used to produce drinking water, and this suite of organic micropollutants is constantly changing as new products (i.e. pesticides, pharmaceuticals, industrial additives) are introduced, while other products are phased out. Organic micropollutants that adsorb poorly on activated carbon can potentially end up in finished drinking water. As such, a modeling approach is required that can give a quick indication of the adsorption efficacy of organic micropollutants. This would allow drinking water treatment plant operatives to make an informed decision on plant operation when specific organic micropollutants are found in their source water, and enables policy makers to include “treatment efficacy” as a criterium when deciding if new products should be introduced.

In order to identify which mechanisms dominated in the adsorption of organic micropollutants (i.e. solutes) onto activated carbon, the adsorption of a wide range of solutes onto F400 activated carbon was investigated. It was found that hydrophobic partitioning, as represented by the solutes log D value (the pH-corrected octanol-water partitioning coefficient) was an important mechanism which especially dominated the removal of relatively hydrophobic solutes. For more hydrophilic solutes, hydrogen bond formation between the solute and the activated carbon surface strongly affected solute removal. Aromatic solutes showed slightly better adsorption than aliphatic solutes, due to the potential to form pi-pi bonds with the basal planes of activated carbon. No significant influence of solute charge or size was observed. This approach was reversed; the adsorption efficacy of two probe solutes, hexanol and 1,3-dichloropropene, on a wide range of commercial activated carbons was investigated. Activated carbon hydrophobicity was measured with various methods; mass increase due to water vapour uptake, oxygen surface density of the activated carbon, contact angle measurements using the capillary rise approach and immersion calorimetry of activated carbon in water. It was found that the water vapour uptake correlated to the oxygen surface density, indicating that the oxygen surface density is a good indicator for the amount of adsorption sites for water. However, the oxygen surface density correlated poorly with the enthalpy of immersion of activated carbon in water, indicating that the oxygen surface density did not give information on the interaction strength between water and activated carbon. Nevertheless, activated carbon hydrophobicity (i.e. activated carbon-water interaction) *alone* could not explain the observed adsorption. According to thermodynamics, the interaction energy between solute and activated carbon, and solute and water have to be included as well. After deriving these from immersion calorimetry and the literature, respectively, and calculating the (3-phase) interaction of solute and activated carbon in water matrix, a good correlation ($r^2=0.82$) with the observed adsorption is found. Hexanol showed higher solute-carbon interaction than 1,3-dichloropropene, which could be related to the potential of hexanol to form hydrogen bonds with the activated carbon surface, while 1,3-dichloropropene was unable to do so, confirming the previous finding that hydrogen bonding can be an important mechanism in adsorption.

The thermodynamic approach was further refined by introducing surface tension components that correspond with van der Waals interaction, and electron donor-acceptor interactions (which also include hydrogen bond formation). Furthermore, it allows to determine solute-activated carbon interactions for solid solutes, which is not possible with the original approach. The surface tension components were determined independently on six activated carbons (using immersion calorimetry) and sixteen solutes (using contact angle measurements on compressed plates). We found that the donor and acceptor surface tension components of activated carbon correlated to the activated carbon oxygen content. Solute-water interaction

correlated well to their solubility, although four solutes deviated from the trend. In the interaction between solute and activated carbon, van der Waals interactions were dominant and explained 65-94% of the total interaction energy, depending on the hydrophobicity of the activated carbon and solute. A reasonable relationship ($r^2=0.70$) was found between the calculated (3-phase) interaction between solute and activated carbon in water and the experimentally determined activated carbon loading.

In practice, solutes are removed from natural waters, and the presence of natural organic matter (NOM) can significantly affect solute adsorption by either competing for adsorption sites, or restricting access to (micro)pores. Preloading activated carbon with surface water or waste-water resulted in a reduction in BET surface area of 24-28%. The reduction in solute adsorption was far more extensive; where 80-100% of positively and negatively charged solutes was removed on 6.7 mg/l fresh activated carbon in demineralized water, only 23-98% (positively charged solutes) and 0-58% (negatively charged solutes) removal was observed on 6.7 mg preloaded activated carbon. In contrast to the previous experiences with fresh activated carbon, charge interactions *did* affect solute adsorption significantly. NOM has a negative charge at neutral pH, and after preloading with NOM, the surface of activated carbon obtains a negative charge as well. This resulted in reduced adsorption of negatively charged solutes and increased absorption of positively charged solutes. The influence of charge repulsion or attraction on solute removal onto preloaded activated carbons was strongest in demineralised water. This influence was lower in surface- or waste-water, due to charge shielding by ions.

The efficacy of high-silica zeolites for solute removal was investigated. It was found that, in contrast to activated carbon, there was no influence of NOM on adsorption as NOM molecules were unable to penetrate the pores of the zeolites. The relative hydrophilic zeolites (as determined by immersion calorimetry) DAY and Mordenite (Si/Al 30) were ineffective for solute removal, but the more hydrophobic zeolites ZSM5 (Si/Al 80) and Mordenite (Si/Al 200) outperformed activated carbon. Solutes with a Stokes diameter closer to the zeolite pore dimension showed higher adsorption (“close fit mechanism”). Charge repulsion of negatively charged solutes was observed for ZSM5 (Si/Al 80), while this was not the case for Mordenite (Si/Al 200), as in the latter zeolite the content of negatively charged Al in its framework was lower. An important consideration for applying zeolites in drinking water treatment practice is that their size exclusion and close fit adsorption mechanism makes them effective for the removal of specific solutes. A great application would be for polluted groundwater, as the pollutant is specific (i.e. with MTBE), and pollutant plumes can affect the source water for extended periods of time.

The original goal to develop a model to predict the adsorption efficacy of organic micropollutants is within closer reach. The thermodynamic approach can predict solute adsorption reasonably well, although still some experimental input is required to determine the surface tension components of each new activated carbon and each new solute. The predicted adsorption is for demineralized water and fresh activated carbon. As such, the model can give a “best case” removal efficacy, which can be used in a relative comparison. Pharmaceuticals which showed poor adsorption according to the model are Lincomycine and Cyclophosphamide and care should be taken to prevent these pharmaceuticals to enter source waters for drinking water production.

Based on *equilibrium* experiments with *fresh* powdered activated carbons in *demineralised* water, the activated carbon types F400 and SN4 proved to be most effective for both solutes with and without hydrogen bond donor/acceptor groups. AC1230C and ROW were effective

for both solute classes as well, although F600 and W35 outperformed AC1230C and ROW for solutes without hydrogen bond donor/acceptor groups.

Samenvatting

In waterbronnen die gebruikt worden voor de productie van drinkwater worden talloze organische microverontreinigingen gevonden. Deze set van organische microverontreiniging verandert continu omdat nieuwe producten (b.v. bestrijdingsmiddelen, geneesmiddelen, industriële additieven) worden geïntroduceerd, terwijl andere producten worden uitgefaseerd. Organische microverontreinigingen die slecht adsorberen op actieve kool kunnen in het gezuiverde drinkwater terecht komen. Hierdoor is een modelmatige benadering nodig die een snelle indicatie kan geven van de adsorptie-effectiviteit van organische microverontreinigingen. Dit zou waterleidingbedrijven de mogelijkheid geven om een geïnformeerd besluit te nemen over de bedrijfsvoering van de zuivering wanneer specifieke verontreinigingen zijn aangetroffen in het bronwater, en maakt het mogelijk voor beleidsmakers om “zuiveringseffectiviteit” als criterium mee te nemen bij de beslissing of nieuwe producten worden ingevoerd.

Om te kunnen vaststellen welke mechanismen dominant zijn in de adsorptie van organische microverontreinigingen (stoffen) op actieve kool, is de adsorptie van een groot aantal stoffen op F400 actieve kool onderzocht. Het bleek dat hydrofobe partitie, uitgedrukt in de log D waarde van een stof (de pH-gecorrigeerde octanol-water partitiec coefficient) een belangrijk mechanisme dat vooral dominant was bij de verwijdering van relatief hydrofobe stoffen. Voor meer hydrofiele stoffen werd de verwijdering sterk beïnvloed door de vorming van waterstofbindingen tussen de stof en het oppervlak van de actieve kool. Aromatische stoffen gaven een licht betere adsorptie dan alifatische stoffen, omdat deze pi-pi interacties konden aangaan met het actieve kool oppervlak. Er werd geen significante invloed waargenomen van de lading of grootte van een stof op de adsorptie.

Deze aanpak werd omgekeerd, en de adsorptie-effectiviteit van twee stoffen, hexanol en 1,3-dichloorpropeen, op een breed scala aan commerciële actieve kool werd onderzocht. De hydrophobiciteit van actieve kool werd gemeten met verschillende methoden; massatoename door opname van waterdamp, de dichtheid van zuurstof op het oppervlak van de actieve kool, contacthoekmetingen a.d.h.v. de capillaire opstijging en immersiecalorimetrie van actieve kool in water. Het bleek dat de waterdamp opname gecorreleerd is met de oppervlaktedichtheid van zuurstof, wat aangeeft dat de oppervlaktedichtheid van zuurstof een goede indicator is voor het aantal adsorptieplaatsen voor water. De oppervlaktedichtheid van zuurstof correleerde slecht met de immersie-enthalpy van actieve kool in water, wat aangeeft dat de oppervlaktedichtheid van zuurstof geen informatie geeft over de interactiesterkte tussen water en actieve kool.

Toch kan de hydrophobiciteit (dwz actieve kool-water interactie) alléén geen verklaring geven voor de waargenomen adsorptie. Volgens de thermodynamica moeten ook de interactie-energie tussen de stof en actieve kool, en de stof en water worden meegenomen. Na deze te bepalen uit de literatuur of met immersiecalorimetrie, en vervolgens de (3-fase) interactie tussen de stof en actieve kool in een watermatrix te berekenen, wordt een goede correlatie ($r^2=0.82$) met de waargenomen adsorptie gevonden. Hexanol had een sterkere interactie tussen stof en actieve kool dan 1,3-dichloorpropeen omdat hexanol de mogelijkheid heeft om waterstofbruggen te vormen met het actieve kooloppervlak en 1,3-dichloorpropeen niet. Dit bevestigt de eerdere bevinding dat de vorming van waterstofbruggen een belangrijk adsorptiemechanisme kan zijn.

De thermodynamische benadering werd verder verfijnd door het introduceren van oppervlaktespanning componenten voor van der Waals interactie en electron donor-acceptor interacties (waaronder ook waterstofbindingen). Bovendien is het mogelijk om hiermee stof-actieve kool interactie te bepalen voor vaste stoffen, wat niet mogelijk is met de eerdere

benadering. De oppervlaktespanning componenten werden onafhankelijk van elkaar bepaald op zes actieve kool (met behulp van immersiecalorimetrie) en zestien stoffen (met behulp van contacthoekmetingen op gecompriëerde platen). We vonden dat de donor en acceptor oppervlaktespanning componenten van actieve kool gecorreleerd zijn aan het zuurstofgehalte van de actieve kool. Stof-water interactie was gecorreleerd aan de oplosbaarheid van stoffen, hoewel vier stoffen van de trend afweken. Van der Waalsinteracties domineerden de stof-actieve koolinteracties, met een bijdrage van 65-94% van de totale interactie-energie. Deze bijdrage was afhankelijk van de hydrophobiciteit van de actieve kolen en de stoffen. Een redelijke relatie ($r^2=0.70$) werd gevonden tussen de berekende (3-fase) interactie tussen stof en actieve kool in water en de experimenteel bepaalde koolbelading.

In de praktijk worden opgeloste stoffen verwijderd uit natuurlijke wateren, en de aanwezigheid van natuurlijk organisch materiaal (NOM) kan een aanzienlijke invloed hebben op de adsorptie van stoffen door competitie om adsorptieplaatsen of het beperken van de toegang tot (micro) poriën. Het voorbeladen van actieve kool met oppervlaktewater of afvalwater resulteerde in een vermindering van 24-28% van het BET oppervlak. De afname van de adsorptie van stoffen was veel groter. Terwijl in gedemineraliseerd water en met 6.7 mg/l verse kool 80-100% van positief en negatief geladen stoffen werden geadsorbeerd, was slechts 23-98% (positief geladen stoffen) en 0-58% (negatief geladen stoffen) verwijderd op 6.7 mg/l voorbeladen actieve kool. In tegenstelling tot de bevindingen met verse actieve kool hebben ladingsinteracties hier *wel* significante invloed op adsorptie. NOM heeft bij neutrale pH een negatieve lading, en bij het voorbeladen van actieve kool met NOM krijgt actieve kool eveneens een negatieve lading. Dit resulteerde in verminderde adsorptie van negatief geladen stoffen en verbeterde adsorptie van positief geladen stoffen. De invloed van ladingsafstoting en -aanrekening op stofverwijdering op voorbeladen actieve kool was het sterkst in gedemineraliseerd water. Deze invloed was minder in oppervlaktewater of afvalwater als gevolg van ladingsafscherming door ionen.

De effectiviteit van zeolieten met hoge silicaverhouding is onderzocht voor de verwijdering van stoffen. Het bleek dat NOM, in tegenstelling tot bij actieve kool, geen invloed heeft op adsorptie omdat NOM moleculen de poriën van de zeolieten niet konden binnendringen. De relatief hydrofiele zeolieten (zoals bepaald met immersiecalorimetrie) DAY en Mordeniet (Si/Al 30) waren niet effectief voor het verwijderen van stoffen, maar de meer hydrofobe zeolieten ZSM5 (Si/Al 80) en Mordeniet (Si/Al 200) waren effectiever dan actieve kool. Stoffen met een Stokes diameter die dichtbij de poriediameter van de zeoliet lag werden beter geadsorbeerd. Ladingsafstoting voor negatief geladen stoffen werd waargenomen voor ZSM5 (Si/Al 80), maar niet voor Mordeniet (Si/Al 200) omdat deze een kleinere hoeveelheid negatief geladen Al atomen bevatte. Een belangrijke overweging voor het toepassen van zeolieten voor drinkwaterzuivering is dat zeolieten effectief zijn voor enkel specifieke stoffen. Een zeer goede toepassing zou de behandeling van verontreinigd grondwater zijn, waarbij de verontreiniging (bv. MTBE) specifiek is en de verontreiniging voor langere tijd van invloed kan zijn.

Het oorspronkelijke doel om een model te ontwikkelen om de adsorptie-effectiviteit te voorspellen van organische microverontreinigingen is dichterbij gekomen. De voorspelling van stofadsorptie met de thermodynamische benadering redelijk goed, hoewel nog enige experimentele inspanning nodig is om de oppervlaktespanning componenten van elke nieuwe actieve kool en elke nieuwe stof te bepalen. De voorspelde adsorptie is gebaseerd op gedemineraliseerd water en verse actieve kool en als zodanig geeft het model een "best case" voorspelling van de adsorptie-effectiviteit welke bruikbaar is voor relatieve vergelijkingen.

Geneesmiddelen die volgens het model slecht adsorberen zijn Lincomycine en Cyclofosfamide, en het dient voorkomen te worden dat deze stoffen in het bronwater terecht komen dat wordt gebruikt voor drinkwaterproductie.

Op basis van *evenwichtsexperimenten* met *verse* poederkool in *gedemineraliseerd* water bleek dat de actieve koolsoorten F400 en SN4 het meest effectief waren voor zowel de stoffen met als zonder functionele groepen voor waterstofbrugvorming. AC1230C en ROW waren effectief voor beide stofsoorten, maar F600 en W35 presteerden beter dan AC1230C en ROW voor de verwijdering van stoffen zonder functionele groepen voor waterstofbrugvorming.

Table of contents

Summary	v
Samenvatting	ix
1. Introduction	1
2. Modeling equilibrium adsorption of organic micropollutants onto activated carbon	17
Supporting information chapter 2	32
3. Determining activated carbon hydrophobicity and its importance for organic solute adsorption	39
Supporting information chapter 3	52
4. Relation between interfacial energy and adsorption of organic micropollutants onto activated carbon	59
Supporting information chapter 4	73
5. Influence of natural organic matter on equilibrium adsorption of neutral and charged pharmaceuticals.	85
6. Zeolites for nitrosamine and pharmaceutical removal from demineralised and surface water: Mechanisms and efficacy	95
Supporting information chapter 6	107
7. Conclusions and recommendations	109
Acknowledgements	115
CV	117
Publications	118

Chapter 1

Introduction

1. Drinking water treatment in the Netherlands

Clean drinking water is a basic need for any society. Lack thereof will lead to exposure to waterborne diseases such as Cholera, Typhoid, Hepatitis and Diarrhea. According to the World Health Organisation (WHO), waterborne diseases are the world's leading killer, claiming over 3.4 million lives each year [1]. Naturally, access to treated drinking water is included in the Millenium Development Goals of the United Nations.

Besides removing the disease-causing micro-organisms from water, also suspended solids, iron, ammonium, methane, calcium and organic micropollutants (such as pesticides, pharmaceuticals or industrial waste products) are removed in water treatment processes, either for health, operational and/or aesthetic reasons. In this thesis, the focus will be on (predicting) the removal of organic micropollutants.

In the Netherlands, 63% of our drinking water is produced from groundwater, while 37% is produced from surface water (www.vewin.nl; drinking water statistics 2012). The advantage of groundwater is that the soil itself can be regarded as a treatment process. Groundwater is hygienically reliable, of constant composition, and requires only limited treatment [2] (Figure 1). Groundwater abstraction will, however, also lower the ground water table, which can adversely affect agriculture and nature. Surface water quality shows larger variation than groundwater, resulting in a more extensive treatment to ensure an excellent drinking water quality (Figure 2).

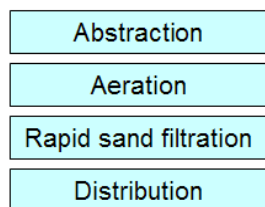


Figure 1. Typical treatment scheme for groundwater.

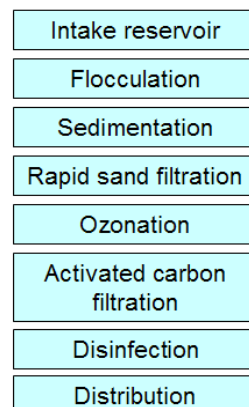


Figure 2. Typical treatment scheme for surface water

An overview of the treatment techniques used at various locations in the Netherlands where surface water is treated is shown in Table 1. This table shows that virtually all locations use activated carbon to adsorb organic micropollutants. As such, it is of great practical value to know which organic micropollutants are effectively removed with activated carbon, and which are not.

Table 1. Overview treatment techniques used by Dutch water companies that treat surface water. Derived from [3].

Water company	Location	Intake reservoir	Infiltration	Aeration	Coagulation + flocculation	Rapid sand filtration	Softening	Ozone	Activated carbon	Advanced oxidation	Membrane filtration	UV disinfection	Chlorination	Slow sand filtration
WML	Heel													
	Roosteren													
Evides	Kralingen													
	Berenplaat													
	Ouddorp													
Dunea	Baanhoek													
	Katwijk													
	Scheveningen													
Vitens	Monster													
	Weerseloseweg													
PWN	Andijk													
	Bergen													
	Mensink													
	Heemskerk													
Waternet	Leiduin													
	Weesperkarspel													
Waterbedrijf Groningen	De punt													

While the combination of treatment processes provides a robust barrier against contamination in drinking water, the drinking water companies follow a broader (multibarrier) approach. Water sources are protected by defining groundwater protection areas where waste discharges are prohibited (groundwater), or to stop surface water intake when a contamination incident is noticed upstream, and temporarily use the water storage capacity of the intake reservoir (surface water). Recontamination of finished water in the distribution network is prevented by selecting pipe materials that don't leech harmful substances, designing it such that sedimentation and accumulation of particles is limited.

2. Organic micropollutants

Traditionally, the safety of treated drinking water was related to microbiological parameters. However, a survey of US groundwaters in 1982 revealed the presence of pesticides, petroleum products and other industrial products [4]. The concentrations measured were in the order of $\mu\text{g/l}$, often close to the detection limit of the analytical equipment used. Nowadays, the detection limits of current analytical methods reach to several ng/l [5]. Also, a far broader set of contaminants is detected in surface waters besides the pesticides and industrial products mentioned in the 1982 survey, including endocrine disrupting compounds (EDC's), pharmaceuticals, flame retardants, perfluorinated compounds, artificial sweeteners and personal care products such as fragrances, cosmetics and sunscreen. A general term for all these different pollutants is "organic micropollutants", referring to their organic nature and low concentrations in water sources. A schematic overview of the pathways that lead to the contamination of drinking water sources by these organic micropollutants is shown in Figure 3.

The impact on human health at ng/l concentrations is considered low, but there is still uncertainty concerning long term and synergetic effects (mixture toxicity) [6]. From an ethical point of view, the mere presence of organic micropollutants, even at low concentrations, is undesirable for drinking water companies.

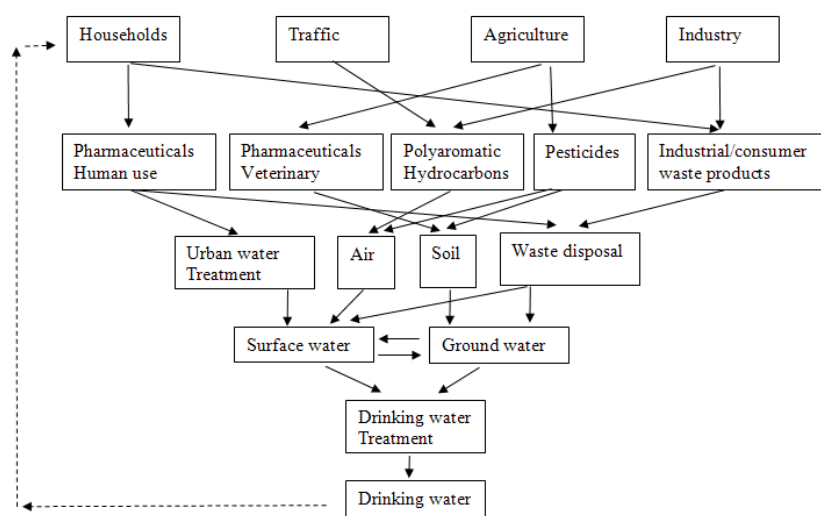


Figure 3. Pollution pathways; Partially based on [7].

2.1 Micropollutants and legislation

Regulation of organic micropollutants on the European level is necessary, as rivers and river basins have an international character. Waste discharges of a European member state upstream can force a member state downstream to use more extensive water treatment techniques or to temporarily stop surface water intake for drinking water production. This is especially relevant for the Netherlands, which is a delta country with 4 European member states laying upstream of its rivers (River Meuse; France and Belgium. River Rhine; Germany and Switzerland).

In the European Water Framework Directive (WFD; Directive 2000/60/EC), 33 individual or groups of organic micropollutants are classified as priority or priority hazardous substances (Table 2). The monitoring of these micropollutants is mandatory in EU member states, maximum concentrations limits are derived and, in the case of priority hazardous substances, their use must be phased out. Every four years, the list of priority and priority hazardous substances is revised. For this purpose, an elaborate procedure, called COMMPS (Combined Monitoring-based and Modeling based Priority Setting) was developed by the Fraunhofer Institute. The monitoring-based approach is used for micropollutants that are measured regularly in surface waters. When monitoring data is limited, the environmental concentrations are estimated based on production/import/use data in the modeling-based approach. Monitoring data is only considered sufficient when more than three EU member states offer monitoring data and the analytical limit of detection is low. For micropollutants with limited or no available monitoring data, the modeling-based approach is used. In both approaches, the priority rating of a pollutant is the quotient of its environmental concentration (PEC; Predicted Environmental Concentration), divided by the concentration at which no harmful effects are expected (PNEC; Predicted No Effect Concentration). After ranking the micropollutants and merging the highest ranked pollutants from both approaches, a selection of 10-15 micropollutants is made by expert review that can be included as priority (hazardous) substances in the WFD.

The WFD states in article 7 (part 1 and 2) that water bodies that are used for drinking water production have to be identified. Stricter legal limits apply to these water bodies (directive 80/778/EEC) and deterioration of the water quality should be prevented.

VEWIN, the association of Dutch water companies, defends the interests of water companies in this (interdisciplinary) procedure to classify unregulated organic micropollutants. Apart from involvement in the COMMPS procedure, VEWIN also supports other initiatives, such as reducing emissions at the source (e.g. by more efficient pesticide spraying techniques in agriculture) and regulation for introduction of new products.

Table 2. European limits for priority (hazardous) pollutants in surface water
Limit: Annual Average Environmental Quality Standard (AA-EQS) as proposed in Directive 2008/105/EC

Substance	Limit (µg/l)	Substance	Limit (µg/l)
Alachlor	0.3	Hexachlorocyclohexane	0.02
Anthracene	0.1	Isoproturon	0.3
Atrazine	0.6	Lead	7.2
Benzene	10	Mercury	0.05
Brominated diphenylether	0.0005	Naphthalene	2.4
cadmium	0.08	Nickel	20
chloroalkanes	0.4	Nonylphenol	0.3
Chlorfenvinphos	0.1	Oxtylphenol	0.1
Chlorpyrifos	0.03	Pentachlorobenzene	0.007
1,2-dichloroethane	10	Pentachlorophenol	0.4
Dichloromethane	20	Polyaromatic hydrocarbons (PAH)	<0.05
DEHP	1.3	Simazine	1.0
Diuron	0.2	Tributyltin	0.0002
Endosulfan	0.005	Trichlorobenzenes	0.4
Fluoranthene	0.1	Trichloromethane	2.5
Hexachlorobenzene	0.01	Trifluralin	0.03
Hexachlorobutadiene	0.1		

Dutch national regulation on drinking water quality (as shown in table 3) is typically more strict than the European regulation in the water framework directive. This is understandable when considering that the national regulation involves *finished* drinking water, while the European regulation involves *source* water. However, article 7 (part 3) of the water framework directive states that the water quality of source water for drinking water production should be *improved*, in order to *reduce* the required treatment. To meet this goal, the limits for surface water should be lowered, and include a broader set of pollutants. This can for example be done by following the example of the Dutch national limits and adding a limit for generic groups of pollutants (“pesticides”) rather than only several specifically, and adding a limit for the accumulated total.

Table 3. Dutch national limits for organic micropollutants in drinking water (Drinking water decree, appendix A)

Organic Substance	Limit (µg/l)	Substance	Limit (µg/l)
Acrylamide	0.1	Polyaromatic hydrocarbons (PAH) (total)	0.1
N-nitrosodimethylamine (NDMA)	0.012	PCB's (individual)	0.1
Epichlorohydrine	0.1	Polychlorobiphenyls (PCB's) (total)	0.5
Benzene	1.0	Pesticides (individual)	0.1
Benzo(a)pyrene	0.01	Pesticides (total)	0.5
Bromate	1.0	Trihalomethanes (total)	25
1,2-dichloroethane	3.0	Cyanids (total)	50
Cadmium	5.0	Tri- & tetrachloroethene (sum)	10
Vinylchloride	0.1		

2.2 Monitoring

In the Netherlands, the quality of the source water and finished drinking water is reported by RIWA (River waterworks association; river Rhine, Meuse, Scheldt), RIVM (National institute for public health and the environment; groundwater) and VROM (Ministry of traffic, spatial planning, environment; finished drinking water).

In Lobith, 273 organic micropollutants are measured on a monthly basis in the river Rhine. IAWR (International Association or Waterworks in the Rhine catchment area) have proposed guideline values for organic micropollutants for which no legal standard exists. This corresponds to a majority of the measured pollutants; in the European Water Framework directive, only 33 pollutants have legal standards. IAWR maintains a precautionary limit of 0,1 µg/l for pollutants that can affect biological systems, a limit of 1 µg/l for pollutants that have passed toxicological tests, and a temporary limit of 5 µg/l for complexing agents. In Table 4, a selection of organic micropollutants is shown which have been found at higher levels than the guideline values in the Rhine river basin. This table shows that, with the exception of AMPA, the concentrations of the pesticides monitored seem to reduce to levels lower than the IAWR guideline. This is, however, not the case for the pharmaceuticals and industrial waste products. Furthermore, it should be noted that Table 4 shows concentrations measured in *surface*water. Pesticides are also prevalent in *groundwater*, with bentazon reaching a concentration of 0.5 µg/l and mecoprop reaching a concentration of 0.2 µg/l in ground water in 2006 (RIVM, REWAB database), while their concentrations did not surpass 0.1 µg/l in Rhine river water in the same period. Also, the water flow in rivers is on the order of meters/second, while the water flow in ground water is on the order of meters/day. As such, any changes that may lead to a reduction of pesticides in the environment will show their effect faster in surface water systems compared to ground water systems.

Table 4. Maximum concentrations of organic micropollutants measured in surface waters in the Rhine river basin. Source: RIWA Rhine (www.riwa-rijn.org)

	IAWR guideline (µg/l)	2009	2008	2007	2006
Pharmaceuticals and X-ray contrasts					
Amidotrizoic acid	0.1	0.62	1.2	0.53	0.25
Iomeprol	0.1	1.3	0.8	0.97	0.36
Iopamidol	0.1	0.53	0.45	0.45	0.44
Iopromide	0.1	0.49	0.67	0.31	0.32
Caffeine	0.1	0.29	0.23	0.48	0.51
Diclofenac	0.1	0.12	0.11	0.11	0.13
Carbamazepine	0.1	0.16	0.12	0.21	0.16
Metoprolol	0.1	0.25	0.18	0.14	0.20
Pesticides and metabolites					
AMPA	0.1	0.90	0.92	0.92	0.87
Glyphosate	0.1	0.11	0.11	0.21	0.59
Isoproturon	0.1	<0.1	0.17	0.26	0.12
Diuron	0.1	<0.1	<0.1	0.17	0.14
2,4-D	0.1	<0.1	0.14	<0.1	<0.1
Mecoprop	0.1	<0.1	0.19	<0.1	<0.1
Industrial waste products					
Diglyme	1	5.30	3.76	4.41	12.00
MTBE	1	5.12	6	5.56	2.44
ETBE	1	5.41	2.58	5.78	2.83
EDTA	5	16.5	23.7	14.8	19
DTPA	5	5.4	8.7	7.5	13
Toluene	1	1.4	1.3	0.39	0.5

3. QSAR and water treatment

Organic micropollutants pose a serious threat to water treatment companies. In the previous section, it is established that the generic term “organic micropollutants” includes a vast amount of different substances. Changing consumption patterns and innovations in the agricultural and industrial sectors lead to the use of new and different products which can pollute drinking water sources. Drinking water companies need to know how effective their treatment techniques are to remove the organic micropollutants, but given their large quantity, it is impossible to do this all experimentally. Quantitative Structure Activity Relationships (QSAR) are originally used in drug development, where molecular properties are related to pharmaceutical action. With this approach, it was possible to reduce the effort and costs of pharmaceutical synthesis and testing. Such an approach is helpful for drinking water companies as well; it can provide a quick answer whether the current treatment can remove specific organic micropollutants sufficiently, can be used in designing new treatment plants or extending and optimizing existing ones to be more robust and effective for a broader range of organic micropollutants. QSAR models can even be used in a preventive way: In the procedure of admitting new products, the removal efficacy of these products in water treatment processes can be included as a decision factor as well.

In a QSAR model, the pollutant properties are used as input, and referred to as “descriptors”. The variable that is predicted should be meaningful and measurable, and the descriptors should preferably be physicochemical parameters that can be related to relevant mechanisms [8]. This does not only increase the insight into which mechanisms define the efficacy of water treatment processes, but is also important to explain outliers (i.e. pollutants with poor model predictions) and consequently for which pollutant types the QSAR model is valid, and for which pollutant types it is not.

4. Activated carbon adsorption for organic micropollutant removal

4.1 Production of Activated carbon

According to reference [9], almost any carbonaceous material can be used to produce activated carbon. Materials with high carbon content and low inorganic components, like wood, coconut shells, peat, coal and lignite can be used. Also, more unconventional materials like straw and automobile tires can also be used [10]. The main criteria for these materials are [9, 11]:

- low inorganic matter (ash content)
- high carbon content
- ease of activation
- availability and low cost
- low degradation

Activated carbon can be produced using either physical or chemical processes ([9, 12]). In the physical process, the raw material is first “carbonized”. In this process, volatile matter and non-carbon species are eliminated at high temperatures (700-800 °C). Subsequently, steam or CO₂ is added, resulting in partial gasification of the carbon and an increase in porosity. This process step is called “activation”. In the chemical process, compounds like H₃PO₄ or ZnCl₂ are added and the material is heated. This results in charring and aromatization of the carbon skeleton and creation of the porous structure.

4.2 Properties of activated carbon

4.2.1 Framework

Activated carbon is highly heterogeneous, both in morphology and in surface characteristics. In Figure 4 (l), a microscope image of a peat-based activated carbon is shown, visualizing the heterogeneity in pore sizes. An elemental analysis indicated that the main elements in the activated carbon framework are carbon (92 % w/w) and oxygen (7% w/w) (Figure 4 (r)). For commercial activated carbons, the amount of oxygen can vary between <1 % to up to 16%.

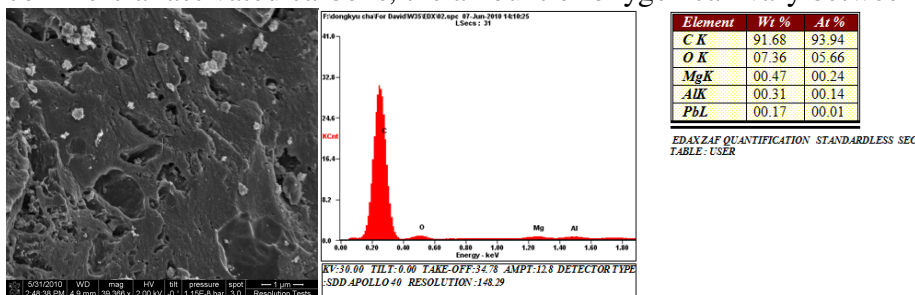


Figure 4. (l) SEM image of a peat-based activated carbon (Norit W35) (r) EDX results of this carbon

On an atomic level, activated carbon is considered to consist of graphene layers – layers of interlocking aromatic rings, which are also referred to as “basal planes” [13]. At the edges of a basal plane, various oxygen- or nitrogen-containing functional groups can be present, as shown schematically in Figure 5 (l). In the activated carbon framework, these basal planes are stacked randomly (Figure 5 (r)), although the structure becomes more ordered when higher temperatures are used when heat-treating activated carbon, as visualized in Figure 6 [14].

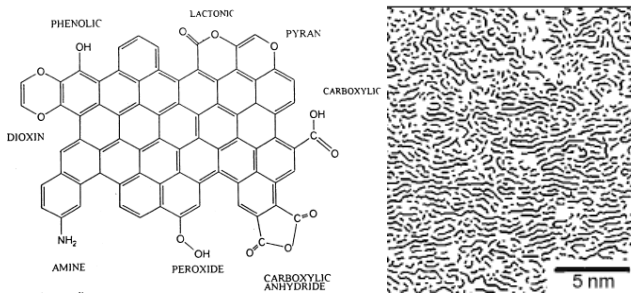


Figure 5. (l) Activated carbon basal plane with functional groups on the edges (source: [13]) (r) Random stacking of basal planes. source: [14]

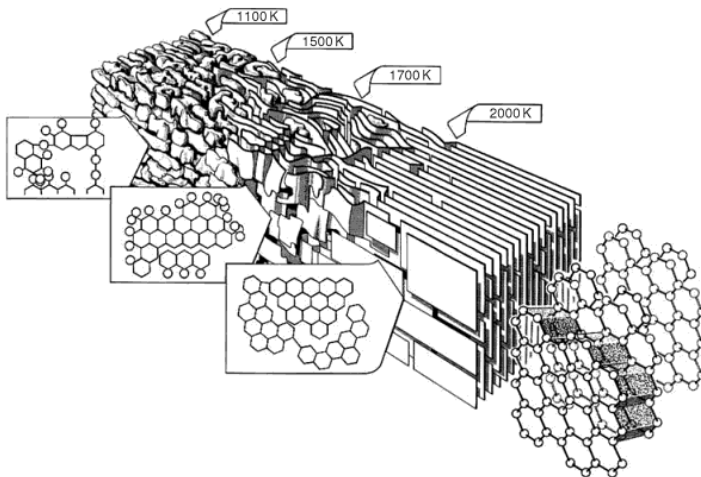


Figure 6. Structural changes which occur during heat treatment of graphitizable carbon. Source: [14].

4.2.2 Pore size

Activated carbon contains pores of various sizes, as illustrated in Figure 7. These have been categorized by IUPAC (International Union of Pure and Applied Chemistry) into micropores (diameter <2 nm), mesopores (diameter 2-50 nm) and macropores (diameter >50 nm). Micropore and mesopore surface areas can be determined with N_2 and CO_2 adsorption isotherms. Macropore surface area can be determined with mercury porosimetry [15]. Typically, the internal surface area of activated carbon is dominant for the total available adsorption surface area (internal+external). Of the internal surface area, micropore surface area mostly determines the adsorption capacity for micropollutants [16, 17]. This can be explained by:

- 1) Stronger van der Waals interaction as the distance between solute molecule and carbon surface is shorter [18].
- 2) Size exclusion may occur at the pore entrance. As larger molecules are retained, there is less competition for adsorption sites for the smaller molecules.

However, larger molecules may also block the entrance to the micropore. For a target solute dissolved in a natural surface water, the optimal pore size corresponds to 1.3-2 times the target solute diameter [17, 19].

Pore shape (slit, elliptic, cylindrical) is also expected to play a role in size exclusion, but no analytical methods are known to determine this.

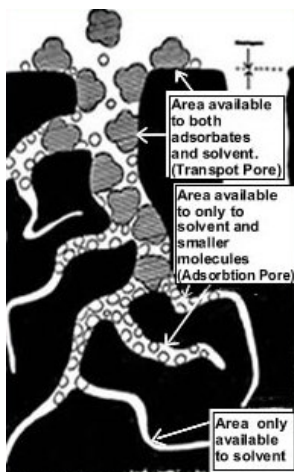


Figure 7. Pore structure of activated carbon. Source: www.aurocarbon.com

4.2.3 Charge

Solute adsorption can be influenced by electrostatic repulsion or attraction when both solute and carbon have a certain electrostatic charge. The charge of activated carbon is dependant on pH as is illustrated in Figure 8. Functional groups with an acid character, such as phenol (-OH) and carboxyl (-COOH), may dissociate at higher pH, releasing their proton (H^+) and obtaining a negative charge. A positive surface charge can be attributed to basic functional groups, such as amine (-NH₂), chromene and pyrene (both O-containing) as these functional groups protonate at lower pH, taking up H^+ and obtaining a positive charge. Electron-rich areas on the graphene plates also increase activated carbon basicity [20].

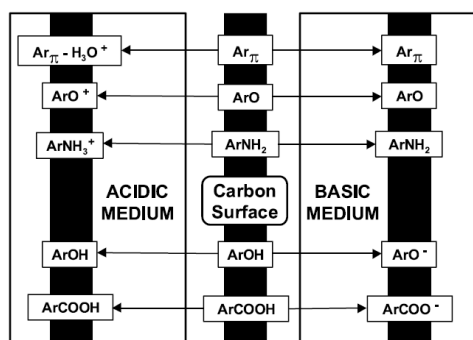


Figure 8. pH effects on activated carbon surface charge. source: Moreno-Castilla 2004

4.2.4 Hydrophobicity

Acidic, basic, and neutral functional groups can bind to water molecules through hydrogen bond formation. Activated carbons with higher quantities of O-containing or N-containing functional groups have a higher affinity for water, and are considered “hydrophilic” [17, 19]. As hydrophilic carbons promote bonding with water, the number of available adsorption sites for the solute is reduced. Also water clusters can be formed, which can block the entrance of micropores [21, 22].

Li et al. (2002) found that the removal of solutes was lower with more hydrophilic activated carbons, even when the solutes were also able to form hydrogen bonds with the functional groups. These solutes did, however, show higher removal on hydrophilic activated carbons when they were dissolved in cyclohexane, which is a solvent that cannot form H-bonds [22].

4.3 Adsorption

4.3.1 Basics adsorption

Adsorption is the attachment of a chemical species (adsorbate) onto the surface of a material (adsorbent). When the chemical species is dissolved in a liquid (i.e., a solute which is dissolved in a solvent), molecules of both the solute and the solvent may adsorb onto the adsorbent, and compete for the available surface area. Adsorption should not be confused with absorption. In the latter process, the adsorbate diffuses into the adsorbent (see Figure 9).

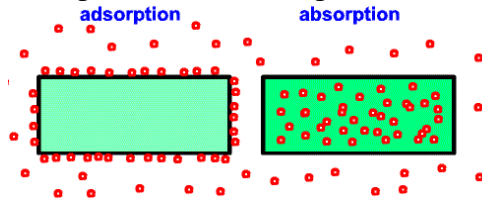


Figure 9. Adsorption vs absorption

In drinking water treatment, the water is contacted with granular activated carbon in packed (fixed) bed reactors. During the process, three dynamic zones can be delineated (Figure 10):

- 1) Saturated (exhausted) zone: the maximum *equilibrium* adsorption capacity of the activated carbon has been reached. No solute will be adsorbed in this zone.
- 2) Mass Transfer Zone (MTZ): Solute has adsorbed onto the activated carbon, but the maximum equilibrium adsorption capacity has not yet been reached.
- 3) Clean (fresh) zone: No solute has adsorbed onto the activated carbon.

During the filter run, the saturated zone will increase and the clean zone will decrease. The size of the mass transfer zone will remain the same during the filter run, and depends on the hydraulic load and solute adsorption kinetics [23]. The filter run ends when the solute concentration in the effluent exceeds a set threshold. The filter is then emptied and refilled with fresh activated carbon, and spent (exhausted) activated carbon is regenerated. In this process, a typical carbon loss of 4-8 % is accounted for [23].

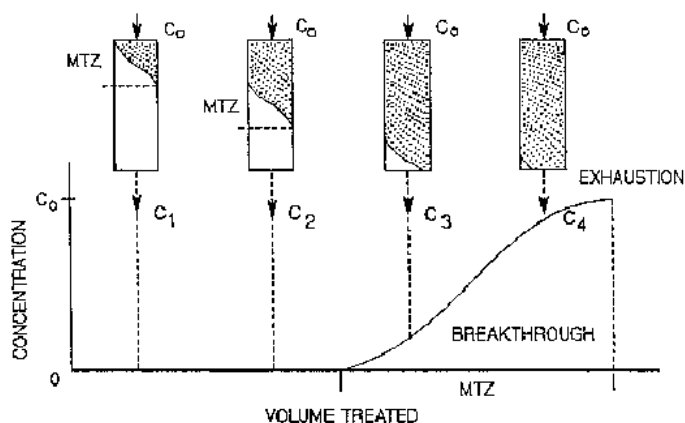


Figure 10: Solute breakthrough curve during activated carbon filtration. source: www.activated-carbon.com

4.3.2 Equilibrium adsorption

Adsorption is a dynamic process, where solute continuously adsorbs onto and desorbs from the activated carbon. When the amount adsorbed equals the amount desorbed, the system is at equilibrium. This equilibrium depends on the solute concentration and water temperature. The Freundlich, Langmuir and Polanyi models are often used to describe adsorption isotherms, i.e., the relation between aqueous solute concentration (C_e) versus adsorbed solute quantity, or carbon loading (q_e), at equilibrium and at a specific temperature. The equations of these

models are shown in table 5. The linearized form of the Langmuir and Freundlich equation can be used to derive q_{\max} , K_L and $1/n$, K_F , respectively.

Table 5. Models for adsorption isotherm at equilibrium

	equation	Linearized equation
Langmuir	$q_e = \frac{q_{\max} K_L C_e}{1 + K_L C_e}$	$\frac{C_e}{q_e} = \frac{1}{q_{\max}} C_e + \frac{1}{K_L q_{\max}}$
Freundlich	$q_e = K_F C_e^{1/n}$	$\log q_e = \log K_F + \frac{1}{n} \log C_e$
Polanyi-Dubinin-Manes (PDM)	$W = W_0 \exp \left[-a \left(\frac{\varepsilon}{N} \right)^b \right]$ $\varepsilon = RT \ln \left(\frac{C_s}{C_e} \right)$	

q_e (mmol/g) is the amount of solute adsorbed onto the activated carbon in equilibrium, C_e (mmol/l) is the solute concentration in water phase at equilibrium, q_{\max} (mmol/g) is the maximum monolayer adsorption capacity, K_L (L/mmol) is a Langmuir empirical constant, K_F (mmol/g^{1/n}/mmol) and $1/n$ (dimensionless) are Freundlich empirical constants, W (ml/g) is the volume of solute adsorbed, W_0 (ml/g) the maximum volume of solute adsorbed, ε (cal/mol) the adsorption potential, N a normalizing factor, a and b empirical constants, R (1.987 cal/mol*K) the universal gas constant, T (K) the absolute temperature and C_s (mmol/l) the solubility of the solute.

In the *Langmuir* model, it is assumed that (i) the surface is homogeneous with respect to the energy of adsorption, (ii) there is no interaction between adsorbed species, (iii) adsorption sites are equally available to all species and (iv) the adsorbed layer is a monolayer [24]. The *Freundlich* model assumes heterogeneity of adsorption sites, and is considered as an empirical model which can only be used at lower and intermediate solute concentrations, as the model doesn't include a maximum adsorption capacity [25]. The empirical constants K_L and K_F indicate adsorption affinity of the solute onto the activated carbon, while $1/n$ is an indication of the heterogeneity of the adsorption sites as well as favorability of adsorption. The Langmuir constant K_L can also be related to the Gibbs free energy of adsorption (ΔG) [25]:

$$\Delta G = RT \ln K_L$$

Also, a general adsorption isotherm model was developed, in which both the Langmuir as the Freundlich model are specific cases [26] :

$$q_e = q_{\max} \left(\frac{C_e^n}{K_{ads} + C_e^n} \right)$$

When $n=1$ (i.e. single type of adsorption sites), the Langmuir equation is obtained, with $K_{ads}=1/K_L$. When the value of C_e^n is considered small compared to K_{ads} , this equation can be simplified to:

$$q_e = \frac{q_{\max}}{K_{ads}} C_e^n$$

Where $q_{\max}/K_{ads}=K_F$, or $q_{\max} * K_L = K_F$.

In the *Polanyi-Dubinin-Manes (PDM)* model, a pore filling mechanism is assumed instead of a surface coverage mechanism. More specifically, pore filling of the *micropores* is assumed [27]. The benefit of the PDM model is that a characteristic curve can be obtained when plotting q_e (volume) versus ε/N . Different solutes may follow the same characteristic curve, provided that ε and N represent the solute properties that relate to the dominant adsorption mechanism.

The normalization factor N in the PDM model was traditionally molar volume, polarizability or parachor, i.e., parameters that only describe non-specific van der Waals-interactions [28]. Crittenden et al. (1999) used parameters of the Linear Solvation Energy Relationship (LSER) to calculate the normalization factor. This way, specific hydrogen bond donor/acceptor interaction is included.

In another approach, molar volume is used as normalization factor, but ϵ is corrected with ϵ_w , i.e., with the water affinity of the specific activated carbon [29, 30]. This way, activated carbon hydrophobicity is specifically included in the model, although the model is only valid for solutes which mainly adsorb by non-specific interaction.

5. Thesis research framework

5.1 Problem statement

Numerous organic micropollutants are present in water sources used to produce drinking water, and this suite of organic micropollutants is constantly changing as new products are introduced, while other products are phased out. Typically, batch or column experiments are carried out to assess the efficacy of activated carbon to remove organic micropollutants, but given the large amount of current and future drinking-water relevant pollutants, a modelling approach to predict activated carbon efficacy is highly needed. While this doesn't replace the need for experimental work, it does allow for fast identification of solutes which are expected to show poor removal with activated carbon, and which can consequently be a potential health hazard. If the input of the model can even be deduced from only the chemical structure of organic micropollutants, this model can even provide an "early warning" for poor removal efficacy of organic micropollutants in drinking water treatment even before they are introduced on the market. Currently, such a model does not exist.

5.2 Research questions and approach

The goal is to develop a *mechanistic model*, rather than a statistical model, to predict the adsorption of organic micropollutants onto activated carbon. Hereby, the focus is on predicting *equilibrium adsorption*.

Research question: What solute and activated carbon properties can be related to adsorption mechanisms to determine removal efficacy? (Chapters 2, 3, 4)

An overview of known adsorption mechanisms is made. Subsequently, a large existing database, containing equilibrium adsorption data of a wide range of solutes onto one specific activated carbon type in demineralized water is analyzed. Solute properties are chosen which can be related to adsorption mechanisms, and solutes are categorized in groups (or "bins") of other solutes with similar properties (Chapter 2). Based on these findings, hydrophobic interaction appeared -as expected- to be an important adsorption mechanism, but hydrogen bond formation between solute and activated carbon appeared to be important as well. Outside the work of this thesis, this adsorption mechanism has not been considered to be relevant in existing literature.

Following this, the surface chemistry of a broad set of activated carbons is analyzed, and compared to the affinity for water, solute-activated carbon interaction, and solute removal from water (Chapter 3). Two probe solutes were studied with similar hydrophobicity, but differing in their ability to form hydrogen bonds. Indeed, it was confirmed that the probe solute with the ability to form hydrogen bonds also showed higher adsorption on all activated carbons. Furthermore, knowing only the hydrophobicity (i.e. affinity for water) of activated

carbon or the solute was insufficient to explain adsorption; solute-activated carbon interaction has to be known as well.

Solute and activated carbon characteristics are integrated (Chapter 4). With the surface tension component approach of Van Oss, Chaudhury and Good (1988), the interactions between solute-water, activated carbon-water and solute-activated carbon are related to van der Waals - and acid-base interactions. These surface tension components can be determined relatively easily for solutes and activated carbon alike, and allow for both determining 2-phase interactions (i.e. only solute-water) and 3-phase interactions (solute-activated carbon-water).

Research question: What is the influence of natural organic matter on solute adsorption? (Chapter 5)

Previous chapters focused on adsorption mechanisms of solutes onto activated carbon types in *demineralized water*, but in practice, surface- ground- or waste water will be treated which contains natural organic matter (NOM). NOM can reduce solute adsorption either by competing for adsorption sites and/or by reducing access to (micro)pores due to pore blockage. In order to separate these two mechanisms, activated carbon was preloaded with natural organic matter in an attempt to maximize pore blockage, and experiments with fresh activated carbon, but in natural water, were done to maximize adsorption competition (Chapter 5). Two different water types, surface water and waste water, were studied.

Research question: Are zeolites an effective alternative adsorbent to remove organic micropollutants that are removed poorly on activated carbon? (Chapter 6)

Zeolites are alternative adsorbents. They are minerals, and have a highly defined and structured (micro)pore network, with pores with limited variation in size. NOM cannot enter the zeolite pores, and consequently, adsorption competition and (internal) pore blockage by NOM will not occur. The efficacy of several high-silica (low polarity) zeolites for solute removal is investigated in demineralized and natural water (Chapter 6). It is investigated whether zeolite hydrophobicity or a close fit of the solute in the zeolite pore (and thus stronger van der Waals interaction) determines solute removal with zeolites.

References

- [1] Berman J. WHO: Waterborne disease is world's leading killer. Journal [serial on the Internet]. 2005.
- [2] De Moel PJ, Verberk JQJC, Van Dijk JC. Drinking water, principles and practices. World Scientific Publishing Co. Pte. Ltd.; 2006.
- [3] Zwolsman JGG, Van den Berg GA. Bescherming drinkwaterfunctie oppervlaktewater door KRW en Nederlands beleid: KWR watercycle research institute; 2006.
- [4] Cotruvo JA. Organic micropollutants in drinking water: an overview. The science of the total environment. 1985;47:7-26.
- [5] Richardson SD, Ternes TA. Water Analysis: Emerging contaminants and current issues. Analytical chemistry. 2011;83:4614-48.
- [6] Schwarzenbach RP, Escher BI, Fenner K, Hofstetter TB, Johnson CA, Von Gunten U, et al. The challenge of micropollutants in aquatic systems. Science. 2006;313(5790):1072-7.
- [7] Heberer T. Occurrence, fate, and removal of pharmaceutical residues in the aquatic environment: a review of recent research data. Toxicology letters. 2002;131:5-17.
- [8] Eriksson L, Jaworska J, Worth AP, Cronin MTD, McDowell RM, Gramatica P. Methods for reliability and uncertainty assessment and for applicability evaluations of

- classification- and regression-based QSARs. *Environmental health perspectives*. 2003;111(10):1361-75.
- [9] Dabrowski A, Podkoscielny P, Hubicki Z, Barczak M. Adsorption of phenolic compounds by activated carbon - a critical review. *Chemosphere* 2005;58:1049-70.
- [10] Streat M, Patrick JW, Camporro Perez MJ. Sorption of phenol and para-chlorophenol from water using conventional and novel activated carbons. *Water Research*. 1995;29:467-72.
- [11] Moreno-Castilla C, Rivera-Utrilla J, Lopez-Ramon MV, Carrasco-Marin F. Adsorption of some substituted phenols on activated carbons from a bituminous coal. *Carbon*. 1995;33:845-51.
- [12] McElroy JA. Adsorption of substituted aromatic compounds by activated carbon: A mechanistic approach to quantitative structure activity relationships: University of Florida; 2005.
- [13] Brennan JK, Bandosz TJ, Thomson KT, Gubbins KE. Water in porous carbons. *Colloids and Surfaces A: Physicochemical and Engineering Aspects*. 2001;187-188:539-68.
- [14] Marsh H, Rodriguez-Reinoso F. *Activated carbon*. Elsevier; 2006.
- [15] Rodriguez-Reinoso F, Molina-Sabio M, Gonzalez MT. The use of steam and CO₂ as activating agents in the preparation of activated carbons. *Carbon*. 1995;33(1):15-23.
- [16] Bautista-Toledo I, Ferro-Garcia MA, Rivera-Utrilla J, Moreno-Castilla C, Vegas Fernandez FJ. Bisphenol A removal from water by activated carbon. Effects of carbon characteristics and solution chemistry. *Environmental science and technology*. 2005;39:6246-50.
- [17] Li L, Quinlivan PA, Knappe DRU. Effects of activated carbon surface chemistry and pore structure on the adsorption of organic contaminants from aqueous solution. *Carbon*. 2002;40:2085-100.
- [18] Anderson MA. Removal of MTBE and other organic contaminants from water by sorption to high silica zeolites. *Environmental science and technology*. 2000;34:725-7.
- [19] Quinlivan PA, Li L, Knappe DRU. Effects of activated carbon characteristics on the simultaneous adsorption of aqueous organic micropollutants and natural organic matter. *Water Research*. 2005;39:1663-73.
- [20] Moreno-Castilla C. Adsorption of organic molecules from aqueous solutions on carbon materials. *Carbon*. 2004;42:83-94.
- [21] Villacanas F, Pereira MFR, Orfao JJM, Figueiredo JL. Adsorption of simple aromatic compounds on activated carbons. *Journal of colloid and Interface Science*. 2006;293:128-36.
- [22] Franz M, Arafat HA, Pinto NG. Effect of chemical surface heterogeneity on the adsorption mechanism of dissolved aromatics on activated carbon. *Carbon*. 2000;38:1807-19.
- [23] Tchobanoglous G, Burton FL, Stensel HD. *Wastewater engineering, treatment and reuse*. 4th ed.: McGraw-Hill; 2003.
- [24] Choy KKH, Porter JF, McKay G. Langmuir isotherm models applied to the multicomponent sorption of acid dyes from effluent onto activated carbon. *Journal of chemical and engineering data*. 2000;45:575-84.
- [25] Pikaar I, Koelmans AA, van Noort PCM. Sorption of organic compounds to activated carbons. Evaluation of isotherm models. *Chemosphere*. 2006;65:2343-51.
- [26] Liu Y, Xu H, Tay J-H. Derivation of a general adsorption isotherm model. *Journal of environmental engineering*. 2005;131(10):1466-8.
- [27] Long C, Li A, Wu H, Liu F, Zhang Q. Polanyi-based models for the adsorption of naphthalene from aqueous solutions onto nonpolar polymeric adsorbents. *Journal of colloid and Interface Science*. 2008;319:12-8.
- [28] Crittenden JC, Sanongraj S, Bulloch JL, Hand DW, Rogers TN, Speth TF, et al. Correlation of aqueous-phase adsorption isotherms. *Environmental science and technology*. 1999;33:2926-33.

[29] Li L, Quinlivan PA, Knappe DRU. Predicting adsorption isotherms for aqueous organic micropollutants from activated carbon and pollutant properties. *Environmental science and technology*. 2005;39:3393-400.

[30] Mezzari IA, Speth TF, Knappe DRU, editors. Predicting the adsorption capacity of activated carbon for organic contaminants from adsorbent and adsorbate properties. *AWWA ACE2006* 2006; San Antonio.

Chapter 2

Modeling equilibrium adsorption of organic micropollutants onto activated carbon

D.J. de Ridder^{1)*}, L. Villacorte²⁾, A.R.D. Verliefde¹⁾³⁾⁴⁾, J.Q.J.C. Verberk¹⁾, S.G.J. Heijman¹⁾, G.L. Amy¹⁾²⁾⁵⁾, J.C. van Dijk¹⁾

1) Delft University of Technology, P.O. box 5048, 2600 GA Delft, The Netherlands

2) Unesco-IHE, P.O. Box 3015, 2601 DA Delft, The Netherlands

3) University of New South Wales, Sydney, Australia

4) KWR Watercycle Research Institute, P.O. Box 1072, 3430BB Nieuwegein

5) King Abdullah University of Science and Technology, Thuwal, Saudi Arabia

* Corresponding author

Water research 44 (2010) 3077-3086

Abstract

Solute hydrophobicity, polarizability, aromaticity and the presence of H-bond donor/acceptor groups have been identified as important solute properties that affect the adsorption on activated carbon. However, the adsorption mechanisms related to these properties occur in parallel, and their respective dominance depends on the solute properties as well as carbon characteristics. In this paper, a model based on multivariate linear regression is described that was developed to predict equilibrium carbon loading on a specific activated carbon (F400) for solutes reflecting a wide range of solute properties. In order to improve prediction accuracy, groups (bins) of solutes with similar solute properties were defined and solute removals were predicted for each bin separately. With these individual linear models, coefficients of determination (R^2) values ranging from 0.61 to 0.84 were obtained. With the mechanistic approach used in developing this predictive model, a strong relation with adsorption mechanisms is established, improving the interpretation and, ultimately, acceptance of the model.

Keywords: Activated carbon, QSAR, binning

1. Introduction

Since the presence of low concentrations of pesticides, pharmaceuticals, industrial waste constituents and personal care products has been confirmed in water sources, their occurrence levels, effects on (human) health and efficacy of treatment processes for their removal from drinking water have been of primary concern to water utilities and environmental agencies (Schwarzenbach et al. (2006)). It is a time-consuming and expensive process to experimentally determine all these different aspects for every individual micropollutant. The number of organic micropollutants present in water sources not only is vast, but also variable as new products are continuously introduced.

In order to minimize experimental work in drug design, the pharmaceutical industry applies quantitative structure activity relationship (QSAR) models, which can predict drug metabolic activity and toxicity a priori, based only on chemical structure (Kruhlak et al. (2007)). Environmental protection agencies, such as the U.S. EPA and the Danish EPA, also apply QSAR models to predict micropollutant toxicity. QSAR models to predict micropollutant removal in water treatment processes, however, have rarely been used, although some models have been proposed for membrane filtration (Yangali-Quintanilla et al. (2008); Verliefde et al. (2009)), ozonation (Lei and Snyder (2007)) and adsorption (Blum et al. (1994); Luehrs et al. (1996); Brasquet and Le Cloirec (1999); Crittenden et al. (1999)). These

types of models are considered necessary, as experimental data is often not available to determine process efficacy for micropollutant removal.

This study focuses on the development and use of QSAR models to determine organic micropollutant removal by activated carbon adsorption, as activated carbon filtration is a widely used treatment method for removal of pesticides as well as taste and odor compounds. Early QSAR models for activated carbon adsorption had the limitation of being based only on van der Waals attraction forces (Crittenden et al. (1999)), normally dominant for adsorption of gases or vapors on hydrophobic activated carbon. In aqueous solutions, however, this premise is no longer valid because also hydrophobic partitioning, electrostatic attraction or repulsion, and H-bond donor/acceptor interactions may occur. More recently, QSAR models have been proposed that include parameters related to these adsorption mechanisms (Luehrs et al. (1996); Crittenden et al. (1999); Magnuson and Speth (2005)). These models yielded better predictions than the models which were previously available. However, specific solute classes that could not accurately be predicted using these models were polysulfonated aromatics, polyfunctional organic solutes (Crittenden et al. (1999)) and dinitro solutes (Magnuson and Speth (2005)).

When a QSAR model is developed for a varied dataset, prediction accuracy can be improved by classifying the solutes in this dataset into specific groups – bins – that contain similar solutes (Xu and Gao (2003)). These bins are typically based on specific solute classes, limiting the applicability of the QSAR model. In this article, *solute properties* are used to define the bins. With this approach, the model is applicable for a broader range of solutes.

An important step in QSAR model development is the choice for the dependent variable, i.e., the parameter that is estimated by the model, as it should be representative of the adsorption process. The following dependent variables have been used in the literature when predicting equilibrium solute removal;

- (i) Carbon loading (q_e)(Crittenden et al. (1999); Li et al. (2005)) in equilibrium with aqueous concentration (C_e)
- (ii) Freundlich capacity constant ($\log K_F$)(McElroy (2005))
- (iii) Water/carbon partitioning constant ($\log q_e/C_e$; $\log K_D$)(Blum et al. (1994); Luehrs et al. (1996); Brasquet and Le Cloirec (1999); Nguyen et al. (2005); Shih and Gschwend (2009))

The relationship between q_e and C_e can be included in the different models as follows:

- (i) q_e is specific for a single equilibrium concentration (C_e). The models can also be used to predict the entire isotherm(Crittenden et al. (1999); Li et al. (2005)). This is done by measuring the adsorption isotherm of a specific solute (e.g. benzene). The removal of other solutes is predicted using the measured isotherm and a normalizing factor which is based on solute properties and calculated for all solutes.
- (ii) q_e is related to C_e by the Freundlich isotherm. However, in this relation the Freundlich intensity factor, $1/n$, also has to be known, or assumed constant.
- (iii) The relation between q_e and C_e is expressed in the predicted (linear) coefficient, and is constant. As such, these types of models are only valid to predict the linear part of the (curvilinear) adsorption isotherm.

In this article, q_e will be predicted directly, approach (i), as (iii) would limit the amount of information obtained from the isotherm, and (ii) is an indirect way to determine q_e . q_e and C_e will be related by multivariate linear regression, with q_e as dependent variable (variable to be predicted) and C_e as one of the independent variables (variables used for prediction).

2. Relevant solute and carbon properties

In the literature, several solute properties that influence organic solute adsorption onto activated carbon are discussed. These properties include solute hydrophobicity, charge, size and presence of specific functional groups. The influence of each of these properties on organic solute adsorption can only be assessed when carbon characteristics are known. When the adsorbent surface is hydrophilic, lower solute removal has been observed than when the adsorbent surface is hydrophobic (Pendleton et al. (1997); Quinlivan et al. (2005)). These authors determined surface hydrophobicity by water vapor adsorption and by the enthalpy of (water) displacement with calorimetry. Adsorbent surface hydrophobicity was related to total oxygen content, as determined with elemental analysis. Solute hydrophobicity is often represented by the octanol-water partitioning coefficient ($\log K_{ow}$). Several authors have tried to directly relate $\log K_{ow}$ to observed adsorption rates. Good relations between $\log K_{ow}$ and adsorption rates were found in a system containing hydrophobic solutes and a hydrophobic adsorbent (Chiou (1979); Hu et al. (1997); Westerhoff et al. (2005)). A poor correlation was found when hydrophobic partitioning is less relevant, i.e., when the solutes are small, hydrophilic and/or charged/polar (Southworth and Keller (1986); Calvet (1989); Westerhoff et al. (2005); Chen et al. (2007); Zwiener (2007)).

Adsorbent surface hydrophobicity is related to the presence of oxygen-containing functional groups. However, while these functional groups promote water adsorption, they can also facilitate H-bond donor and –acceptor interactions between solutes and adsorbent surface. Increasing the amount of oxygen-containing functional groups on the activated carbon surface decreases the adsorption of organic solutes, indicating preferential adsorption of water molecules over organic solutes at these sites (Pendleton et al. (1997); Franz et al. (2000); Li et al. (2002)). In non-polar solvents (e.g., cyclohexane), the presence of oxygen containing functional groups on the carbon surface enhanced removal of MTBE (Li et al. (2002)), phenol and aniline (Franz et al. (2000)).

In addition to the effect on solute-adsorbent interactions, the presence of H-bond donor/acceptor groups in a solute also results in a lower solute hydrophobicity and thus a reduced expulsion in the solute-water system (Li et al. (2002)).

Depending on the pH of the solution, either the solute and/or the adsorbent can be charged as a result of dissociation or protonation (Moreno-Castilla (2004)). For a solute, its acid dissociation constant (pK_a) represents the pH at which 50% of the solute is dissociated or protonated. Within 2 pH units deviation of the pK_a , more than 99% of the solute is dissociated or protonated, according to the Henderson-Hasselbalch equation (1).

$$pH = pKa - \log \frac{[AH]}{[A^-]} \quad (1)$$

For bases, $[AH]$ and $[A^-]$ can be replaced for $[AH^+]$ and $[A]$, respectively. Clear effects of molecule dissociation and subsequent charge repulsion were found for phenol and aniline. For phenol ($pK_a=9.95$), a reduction of 47% of carbon loading was found at pH 12 as compared with removal at pH 2. At pH 12, both (dissociated) phenol and the carbon surface were negatively charged (Moreno-Castilla (2004)). The basic solute Aniline ($pK_a=4.6$) is positively charged at pH 2. At this pH, a 14-38% decrease of aniline carbon loading was found when using carbon types which were positively charged at that pH as compared to carbon loading at a pH of 12. At a pH of 12, the solute is neutral and no charge interactions are observed (Villacanas et al. (2005)).

One of the van der Waals bonding mechanisms is dipole interaction between a surface and a solute with either permanent (polar molecule) and/or induced (polarizable molecule) dipole moment. The influence of solute *polarity* was investigated by comparing removal of TCE (dipole moment 0.95 D) and MTBE (dipole moment 1.37 D)(Li et al. (2002)), both solutes having similar sizes, but MTBE was more hydrophilic than TCE with a $\log K_{ow}$ 0.89

and 2.42, respectively. TCE carbon loading was considerably higher than MTBE carbon loading. This is expected based on log K_{ow} values, and as such, no conclusions can be made with respect to the effect of polarity for aliphatic solutes. For aromatic solutes, it was found that the polar solutes nitrobenzene and nitrotoluene were removed more effectively than their non-polar counterparts benzene and toluene (Chen et al. (2007)). The non-polar aromatic solutes 1,2,4 trichlorobenzene and benzene had different *polarizability* (10.86 and 8.28 D^*C/N , respectively), but showed similar removal when n-hexadecane was used as solvent to rule out the hydrophobic effect (Chen et al. (2007)).

3. Materials and methods

The experimental basis for this article consists of a study of Freundlich isotherm constants for 71 organic micropollutants, as determined by batch equilibrium experiments in US EPA technical documents (Speth (1990))(Speth (1998)). The experiments were conducted at room temperature (24 °C) using organics-free water. The measured pH values varied between 5.3 and 8.0. The adsorbent used was F400 activated carbon (Calgon Carbon Corp., Pittsburgh).

Solute properties related to hydrophobicity (log K_{ow}), charge (pK_a), polarity (dipole moment), solute polarizability and functional group counts (H bond donor/acceptor groups) were obtained using Internet databases or calculated using commercial software. Log K_{ow} values were obtained from ChemIDplus Advanced (US National Library of Medicine, Bethesda), or calculated using ADME (Pharma-algorithms, Toronto) when experimental values were not available. pK_a values were calculated using ADME. Aromaticity ratio (ARR, the ratio of number of aromatic bonds to total number of bonds in a molecule), the number of H-bond donor/acceptor groups and the total polarizability were calculated using Dragon (Talete, Milan). The dipole moment was calculated using Chem3D Ultra (Cambridge Software, Cambridge), after importing 2D structures from ChemDraw and calculating the 3D configuration with minimized energy using MOPAC (Molecular Orbital PACKage). Model and parameter significance were determined with SPSS 16, and Mobydigs (Talete, Milan) was used for model cross validation.

The solute parameters were used to construct a QSAR predictive model, based on multivariable linear regression (MLR). The experimental database (Speth (1990); Speth (1998)) only provided Freundlich constants K_F , the capacity factor, in $((\mu\text{g/g})*(L/\mu\text{g}))^{1/n}$ and $1/n$, the intensity factor (unitless) for solute equilibrium adsorption. For this paper, neither of these constants was selected as the model-dependent variable, since *both* parameters are required to describe the equilibrium curve, and there is no strict relationship between them (Figure S.1, supporting information). Instead, carbon loading (q_e , in $\mu\text{mol/g}$), was selected as the dependent variable for the QSAR model. The carbon loading was calculated for each solute from the corresponding K_F and $1/n$ values provided by Speth (1990) and Speth (1998), at equilibrium concentrations of 1 and 0.1 $\mu\text{mol/l}$. Both concentration levels were in the measured range of most solutes within the experimental database. In the model, carbon loading is calculated on a logarithmic scale, because this increased linearity between dependent and independent parameters, which is a requirement for MLR-type models. Furthermore, at log scale, higher model sensitivity is reached for solutes with low carbon loading. Solutes which show poor removal are typically more critical for activated carbon reactor design than solutes which show good removal.

4. Results and discussion

In order to determine the importance on adsorption of the solute parameters as described before, the different solute properties were correlated to q_e . For ionic solutes, log K_{ow} values were corrected for pH with respect to their H^+ dissociation/uptake. The pH-corrected log K_{ow}

values are referred to as log D (distribution coefficient). Log D values can be determined from log K_{ow} values and the pK_a values of the solute, using equations (2) and (3) (Schwarzenbach et al. (2003)).

$$\text{Acids: } \log D = \log K_{ow} - \log(1 + 10^{(pH - pK_a)}) \quad (2)$$

$$\text{Bases: } \log D = \log K_{ow} - \log(1 + 10^{(pK_a - pH)}) \quad (3)$$

For neutral solutes, $\log K_{ow} = \log D$; for ionic solutes $\log D < \log K_{ow}$. Only polarizability and log D show clear trends, as shown in Figure 1.

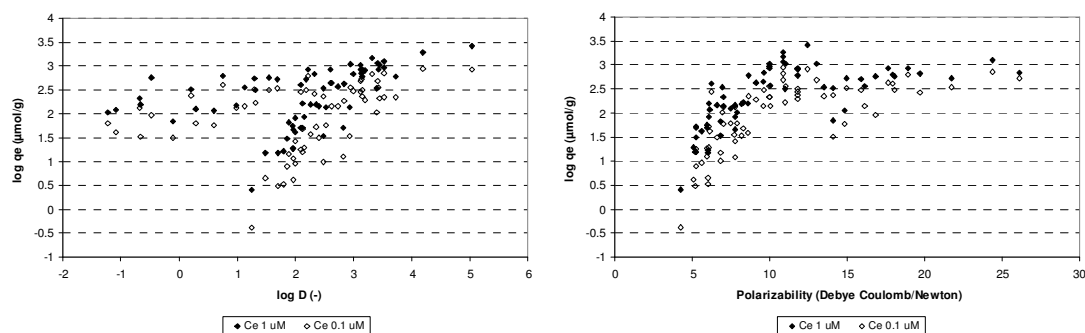


Figure 1: Relation between $\log q_e$ and solute $\log D$ (left), polarizability (right) at C_e 1 μM and 0.1 μM (no binning)

The relations between $\log q_e$ and the amount of H-bond donor/acceptor groups, the dipole moment and the aromaticity ratio can be found in the supporting information (Figure S.2 - S.4). No trend is observed between these three parameters and $\log q_e$. While these parameters are not *dominant* in the prediction of $\log q_e$, they can still be *relevant*, and help explain observed variations in Figure 1. As such, four bins were formed, containing (i) aliphatic solutes with H-bond d/a groups, (ii) aliphatic solutes without H-bond d/a groups, (iii) aromatic solutes with H-bond d/a groups, (iv) aromatic solutes without H-bond d/a groups. When creating bins which separated solutes based on dipole moment, no clear trends were observed. In Figure 2 and 3, the relations between $\log D$ vs. $\log q_e$ and polarizability vs. $\log q_e$ are shown for $C_e=1 \mu\text{mol/l}$, based on these four bins.

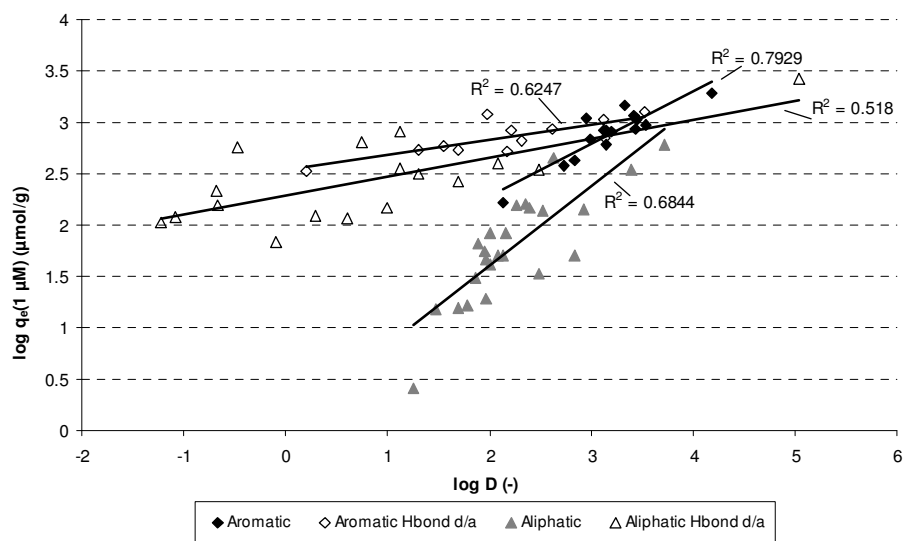


Figure 2: Effect of presence or absence of aromatic rings and Hbond d/a groups on relationship between $\log D$ and $\log q_e$ (1 μM)

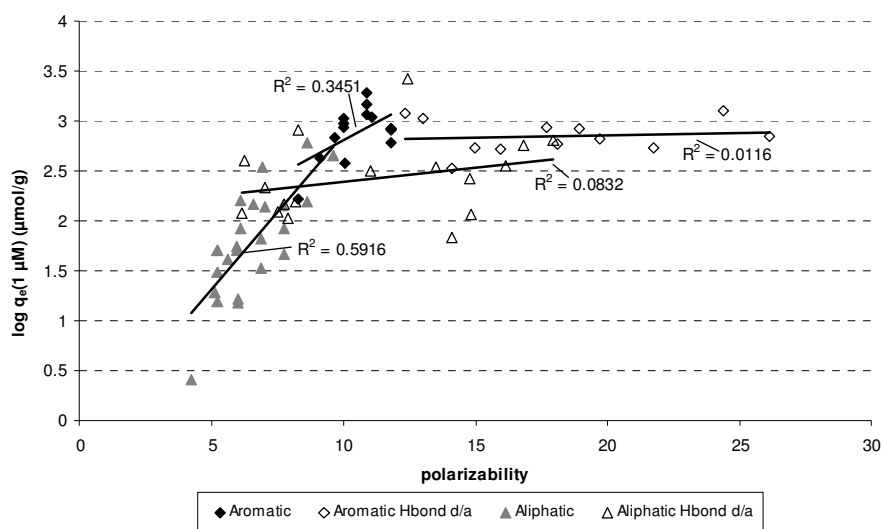


Figure 3: Effect of presence or absence of aromatic rings and Hbond d/a groups on relationship between polarizability and $\log q_e$ (1 μM)

From Figure 2, it was observed that each of the bins correlated reasonably well with $\log D$, with coefficients of determination varying between 0.52 and 0.79 and visually even distribution of data points around the trend line. At the same $\log D$, higher carbon loadings were observed for aromatic solutes than aliphatic solutes, both for the bins with and without H-bond d/a groups. Differences in aromaticity of the solutes within the aromatic bins had no significant influence for aromatic solutes with H-bond d/a groups (Figure S4, Supporting information, solutes with $\text{ARR} < 0.6$). ARR appeared to have a strong influence for aromatic solutes without H-bond d/a groups (Figure S4, Supporting information, solutes with $\text{ARR} > 0.6$), but in this dataset there was a strong correlation between $\log D$ and aromaticity ($R^2 = 0.80$).

Both aliphatic and aromatic solutes with H-bond d/a groups showed higher carbon loading *at similar* $\log D$ than the solutes without these groups. At higher $\log D$ values, the influence of the presence of H-bond d/a groups was less obvious. Apparently, hydrogen bond formation between functional groups on the carbon surface and the solute is a very relevant removal mechanism for solutes with relatively low $\log D$ values, but hydrophobic partitioning is more relevant at higher $\log D$ values. According to the observed trends, carbon loading is similar for all solute bins at a $\log D$ of approximately 3.7. This indicates that hydrophobic partitioning is the dominant removal mechanism at that $\log D$ value, overruling the influences of pi-pi-interaction and H-bond formation.

Within the bins of aromatic and aliphatic solutes with H-bond d/a groups in their molecular structure, no influence was observed regarding the number these groups.

As activated carbon has a limited number of carbonyl and carboxyl groups on the carbon surface (the O content of carbon is typically $< 5\%$), it is unlikely that for a single solute, more than one carbon surface groups are available to form H-bonds with. As such, the *total* number of solute H-bond d/a groups is irrelevant for H-bond formation.

Polarizability is correlated less strongly to $\log q_e$ than $\log D$, as shown in Figure 3.

However, it should be noticed that higher polarizability can be the result of either:

- 1) solute chemical constitution – some atoms have higher polarizability than others;
- 2) solute size – larger solutes contain more atoms, resulting in higher total polarizability.

Indeed, a strong relation was found between polarizability and solvent (water) accessible surface (SAS) of the solutes (S.5, appendix). Solute without H-bond d/a groups showed a stronger increase of carbon loading with increasing polarizability/SAS than those with H-

bond d/a groups. This might be related to the bonding mechanism. For solutes without H-bond d/a groups, the main bonding mechanisms are London dispersion forces and/or pi-pi-interaction, and for these mechanisms, a higher contact surface between solute and carbon would increase bonding strength. H-bond formation is an interaction between functional groups, and in principle independent of solute size, resulting in a less significant relation to polarizability/SAS.

Within both bins containing solutes with H-bond d/a groups, neutral and ionic solutes were present, and significant differences in solute dipole moment (0–5.3 Debye) were observed in these bins. However, no conclusive influence was observed for solute charge (Figure S.6-S.9) or dipole moment (Figure S.10-S.13) in both bins. Values for the pH_{pzc} of F400 activated carbon are reported between 6.5 and 10.5 (Bjelopavlic et al. (1999); Strelko and Malik (2002); Iriarte-Velasco et al. (2008)). The pH_{pzc} of F400 was not measured for the database used in this work, and the large spread in pH_{pzc} values reported by other authors indicate that either the analysis method is very sensitive and/or there is considerable variation in carbon properties for different batches of F400 activated carbon. Although it cannot be concluded that the carbon surface is charged or not, it was observed that ionic solutes showed similar removal as neutral solutes in the same bin, which suggests that the influence of charge interactions was limited.

5. QSAR construction

A commonly used algorithm for QSAR models is multiple linear regression (MLR), which is popular for its ease of interpretation (Gramatica (2007)). In this algorithm, the parameter that should be predicted ($\log q_e$ in equation (4)) has a linear relationship with parameters relevant to it, which are referred to as “descriptors” (polarizability, $\log C_e$ and $\log D$ in equation (4)). $\log C_e$ is, in contrast to polarizability and $\log D$, no solute property and inclusion of this parameter might contradict the core principle of a QSAR: relating activity (adsorption onto carbon) to structure related parameters (polarizability, $\log D$) only. However, q_e is related to C_e . Consequently, when C_e is not introduced into the model explicitly, the model will only be valid for q_e at a single specific C_e .

The importance (or weight) of the descriptors (a, b and c in equation (4)) is determined by finding the best fit of the model to the experimental data set using the method of least squares.

$$\log q_e = a * \text{polarizability} + b * \log D + c * \log C_e + d \quad (4)$$

In order to use solute parameters as descriptors in multivariable linear regression, these parameters should be linearly related to $\log q_e$. Furthermore, descriptors should be independent of each other. For all bins, co-linearity between $\log D$ and polarizability is limited, with all values for the coefficient of determination under 0.34. This justifies the use of both descriptors in the QSAR model.

In Table 1, the solute properties and calculated $\log q_e$ values used in the model construction are shown. A QSAR model was constructed for each bin, and the model equations are shown in Table 2.

Model significance of the integrated models including $\log C_e$ was determined with the F-test, and significance of individual parameters with the t-test. All models had a significance < 0.005 , indicating that with $> 99.5\%$ confidence, the models are statistically significant; i.e., the relations found are representative for the dataset. Results from the t-test indicated that polarizability was only significant for the bin with aliphatic solutes without H-bond d/a groups; for the other bins, significance varied between 0.104 and 0.247. As the solutes in the bin with aliphatic solutes without H-bond d/a groups can neither form pi-pi bonds or H-bonds,

the weaker London dispersion forces become more dominant for solute removal, which explains why polarizability is only significant for this bin. The parameters $\log D$ and $\log C_e$ were significant in all models (significance <0.004).

Table 1: Compound properties; outliers marked as lightly shaded. K_F and n values derived from Speth and Miltner 1990 and Speth and Miltner 1998. Log D and pKa values with asterisk (*) are calculated using ADME (Pharma-algorithms)

Solute	K_F ($\mu\text{g/g}$) L/ μg	1/n	log D (pH 7)	Polarizability (Debye C/N)	ARR	Dipole moment (Debye)	Nr. H-bond donor+acceptor groups	pKa	Log $q_e(0.1)$ ($\mu\text{mol/g}$)	Log $q_e(1)$ ($\mu\text{mol/g}$)
Aromatic, no Hbond d/a										
1,2-Dichlorobenzene	19300	0.378	3.43	10.00	0.75	1.97	0	n/a	2.56	2.94
Benzene	1260	0.533	2.13	8.28	1.00	0.00	0	n/a	1.68	2.22
1,3,5-Trichlorobenzene	63800	0.324	4.19	10.86	0.67	0.00	0	n/a	2.95	3.28
1,3-Dichlorobenzene	5910	0.630	3.53	10.00	0.75	1.23	0	n/a	2.34	2.97
1,4-Dichlorobenzene	4970	0.691	3.44	10.00	0.75	0.00	0	n/a	2.34	3.03
Ethylbenzene	9270	0.415	3.15	11.80	0.75	0.32	0	n/a	2.37	2.78
m-Xylene	4930	0.614	3.20	11.81	0.75	0.29	0	n/a	2.30	2.91
o-Chlorotoluene	23200	0.378	3.42	10.90	0.75	1.21	0	n/a	2.68	3.06
o-Xylene	9760	0.474	3.12	11.81	0.75	0.44	0	n/a	2.45	2.92
p-Xylene	12600	0.418	3.15	11.81	0.75	0.06	0	n/a	2.50	2.92
Styrene	12200	0.479	2.95	11.05	0.75	0.01	0	n/a	2.56	3.04
Toluene	5010	0.429	2.73	10.05	0.86	0.26	0	n/a	2.15	2.58
p-Chlorotoluene	35900	0.340	3.33	10.90	0.75	1.62	0	n/a	2.83	3.17
Bromobenzene	17200	0.364	2.99	9.64	0.86	1.52	0	n/a	2.47	2.84
Chlorobenzene	9170	0.348	2.84	9.10	0.86	1.54	0	n/a	2.28	2.62
Aromatic, Hbond d/a										
2,4,5-Trichlorophenoxyacetic acid	43000	0.210	1.31	14.98	0.43	2.31	4 (3a+1d)	2.8 (acid)	2.52	2.73
Acifluorofen	60200	0.198	1.70	21.76	0.48	0	9 (8a+1d)	1.8 (acid)*	2.53	2.73
Dicamba	33100	0.147	0.21	14.12	0.46	4.51	4 (3a+1d)	2.0 (acid)	2.37	2.52
Dinoseb	30400	0.279	1.56	18.09	0.35	1.38	6 (5a+1d)	4.6 (acid)	2.49	2.77
Pentachlorophenol	42600	0.339	3.12	13.03	0.5	1.24	2 (1a+1d)	4.7 (acid)	2.69	3.03
Alachlor	81700	0.257	3.52	24.39	0.33	4.34	3 (3a)	n/a	2.85	3.11
Cyanazine	102000	0.126	2.22	18.94	0.38	4.59	8 (6a+2d)	1.7 (base)*	2.80	2.93
Metolachlor	98200	0.125	3.13	26.15	0.32	3.90	3 (3a)	n/a	2.72	2.85
Simazine	31300	0.227	2.18	15.93	0.46	3.96	7 (5a+2d)	1.7 (base)*	2.49	2.71
Atrazine	38700	0.291	2.61	17.69	0.43	2.68	7 (5a+2d)	1.7 (base)*	2.64	2.93
Carbofuran	16400	0.408	2.32	19.7	0.35	2.25	5 (4a+1d)	n/a	2.42	2.83
2,4-Dinitrotoluene	96100	0.157	1.98	12.35	0.46	1.00	4 (4a)	n/a	2.92	3.08
Aliphatic, no Hbond d/a										
1,1,1,2-Tetrachloroethane	1070	0.604	2.93	7.72	0	1.44	0	n/a	1.54	2.15
1,1,1-Trichloroethane	335	0.531	2.49	6.86	0	1.75	0	n/a	1.00	1.53
1,1-Dichloroethylene	470	0.515	2.13	5.24	0	1.22	0	n/a	1.19	1.71
1,1-Dichloropropene	2670	0.374	2.53	7.00	0	1.16	0	n/a	1.77	2.15
1,2,3-Trichloropropane	1080	0.613	2.27	8.62	0	1.40	0	n/a	1.58	2.19
1,3-Dichloropropane	897	0.497	2.00	7.76	0	1.50	0	n/a	1.42	1.92
Bromodichloromethane	241	0.655	2.00	5.59	0	1.07	0	n/a	0.96	1.62
Bromoforn	929	0.665	2.40	6.58	0	0.91	0	n/a	1.50	2.16
Carbon tetrachloride	387	0.594	2.83	5.95	0	0.001	0	n/a	1.11	1.70
Chlorodibromomethane	585	0.636	2.16	6.09	0	0.99	0	n/a	1.29	1.92
Dibromochloropropane	6910	0.501	2.63*	9.60	0	1.07	0	n/a	2.15	2.66
Tetrachloroethylene	4050	0.516	3.40	6.95	0	0	0	n/a	2.02	2.53
trans-1,2-dichloroethylene	618	0.452	2.09	5.24	0	0.001	0	n/a	1.25	1.70

Solute	K _F (µg/g)	1/n	log D (pH 7)	Polarizability	ARR	Dipole moment	Nr. H-bond	pKa	Log q _a (0.1)	Log q _b (1)
	L/µg)			(Debye C/N)		(Debye)	donor+acceptor groups		(µmol/g)	(µmol/g)
Trichloroethylene	2000	0.482	2.36	6.10	0	0.79	0	n/a	1.72	2.2
gamma-BHC (lindane)	15000	0.433	3.72	8.65	0	2.40	0	n/a	2.35	2.78
1,2-Dichloropropane	313	0.597	1.97*	7.76	0	2.37	0	n/a	1.07	1.67
1,1-Dichloroethane	64.6	0.706	1.79	6.00	0	1.86	0	n/a	0.52	1.22
1,1,2-Trichloroethane	365	0.652	1.89	6.86	0	1.15	0	n/a	1.17	1.82
Chloroform	92.5	0.669	1.97	5.10	0	1.16	0	n/a	0.61	1.28
cis-1,2-dichloroethylene	202	0.587	1.86	5.24	0	1.53	0	n/a	0.90	1.48
Methylene chloride	6.25	0.801	1.25	4.24	0	1.50	0	n/a	-0.39	0.41
Dibromomethane	72.2	0.701	1.70	5.23	0	1.32	0	n/a	0.49	1.19
1,2-Dibromoethane	888	0.471	1.96	5.96	0	0.001	0	n/a	1.27	1.75
1,2-Dichloroethane	129	0.533	1.48	6.00	0	0.001	0	n/a	0.65	1.18
Aliphatic, Hbond d/a										
Methylol	4780	0.290	0.60	14.83	0	3.57	7 (5a+2d)	n/a	1.77	2.06
Methyl ethyl ketone	2530	0.295	0.29	7.50	0	2.81	1 (1a)	n/a	1.80	2.09
Methyl isobutyl ketone	8850	0.279	1.31	11.02	0	2.71	1 (1a)	n/a	2.23	2.50
Chloral hydrate	18900	0.051	0.99	7.77	0	1.36	4 (2a+2d)	n/a	2.12	2.17
Aldicarb	8270	0.402	1.13	16.14	0	1.94	5 (4a+1d)	n/a	2.15	2.55
Ethylene thiourea	716	0.669	-0.66	8.18	0	5.36	4 (2a+2d)	n/a	1.52	2.19
Oxamyl	1740	0.793	-0.47	16.84	0	3.21	7 (6a+1d)	n/a	1.96	2.76
Pichloram	23400	0.180	2.48	13.50	0	0.07	1 (1a)	n/a	2.36	2.54
Chloropicrin	30200	0.155	2.09	6.25	0	2.40	2 (2a)	n/a	2.45	2.61
Hexachlorocyclopentadiene	43000	0.504	5.04	12.43	0	0.68	1 (1a)	n/a	2.92	3.43
Dalapon	4920	0.224	-1.22	7.91	0	0.47	3 (2a+1d)	1.8 (acid)	1.80	2.02
Dichloroacetic Acid	1630	0.462	-1.08	6.15	0	2.07	3 (2a+1d)	1.3 (acid)	1.62	2.08
Endothal	2280	0.329	-0.09	14.08	0	2.82	7 (5a+2d)	3.8 (acid)*	1.51	1.84
Trichloroacetic Acid	11700	0.216	-0.67	7.01	0	1.08	3 (2a+1d)	0.5 (acid)	2.12	2.34
Metribuzin	48700	0.193	0.75	17.93	0	2.04	7 (5a+2d)	7.9 (base)*	2.61	2.80
Isophorone	9750	0.271	1.70	14.78	0	3.88	1 (1a)	n/a	2.16	2.43
1,1,1-Trichloropropanone	74400	0.110	1.12	8.31	0	2.35	1 (1a)	n/a	2.80	2.91
Dichloroacetone nitrile	261000	0.232	0.29	5.48	0	1.91	1 (1a)	n/a	3.62	3.85
Methyl tertiary-butyl ether (MTBE)	218	0.479	0.94	10.02	0	1.37	1 (1a)	n/a	0.85	1.32
Glyphosate	87600	0.119	-6.00	11.39	0	5.16	11 (6a+5d)	0.8 (acid); 9.9 (base)*	2.86	2.98

Table 2: QSAR model equations

MLR equation	n	R ²	Q ²
Aromatic no H-bond d/a			
log qe = 0.525*log D + 0.454*log Ce + 1.22	30	0.84	0.80
Aromatic H-bond d/a			
log qe = 0.140*log D + 0.237*log Ce + 2.53	22	0.81	0.76
Aliphatic no H-bond d/a			
log qe = 0.574*log D + 0.181*polarizability + 0.574*log Ce	48	0.84	0.81
Aliphatic H-bond d/a			
log qe = 0.196*log D + 0.319*log Ce + 2.28	34	0.61	0.55

The model coefficient of determination is 0.61 for the bin with aliphatic solutes with H-bond d/a groups, and between 0.81 and 0.84 for the other bins. Q² is the model R² after internal validation, and is an indication for the predictive power of the model. It is calculated as follows

$$Q^2 = 1 - \frac{PRESS}{TSS}$$

TSS is the total sum of squares. PRESS is the predicted residual sum of squares. Individual residual sum of squares were calculated using “leave-one-out” cross validation. With this method, one solute is omitted from the dataset and a model is constructed with the rest of the dataset. Consequently, log qe values are predicted for the solute which was omitted, and the PRESS is calculated. This is done for every solute in the dataset. The sum of the individual PRESS values is used for the calculation of Q².

All four models produced in this paper meet the statistical criteria for “good models” stated in Eriksson et al. (2003), i.e., Q² > 0.5 and R² - Q² < 0.2. However, even a high Q² does not guarantee predictive power of the models (Gramatica (2007)); external validation is regarded as the most effective way to assess predictive power. In this paper, the available dataset was too limited for such a procedure.

The prediction accuracy of the model can also be assessed (albeit in a less effective way than by external validation) by comparing measured qe values with qe values predicted by the model (Figure 4). This is internal validation, i.e. the dataset used for validation is also used for model construction. The straight line represents the ideal model, where predicted values equal measured values. The maximum deviations from the ideal line, and the average of the absolute deviation are presented in Table 3 for each bin.

Table 3: Deviation of log qe values between predicted and measured values

	Aromatic no H-bond d/a	Aromatic H-bond d/a	Aliphatic no H-bond d/a	Aliphatic H-bond d/a
Max positive deviation	0.28	0.20	0.62	0.43
Max negative deviation	-0.32	-0.20	-0.51	-0.62
Average absolute deviation	0.11	0.06	0.21	0.21

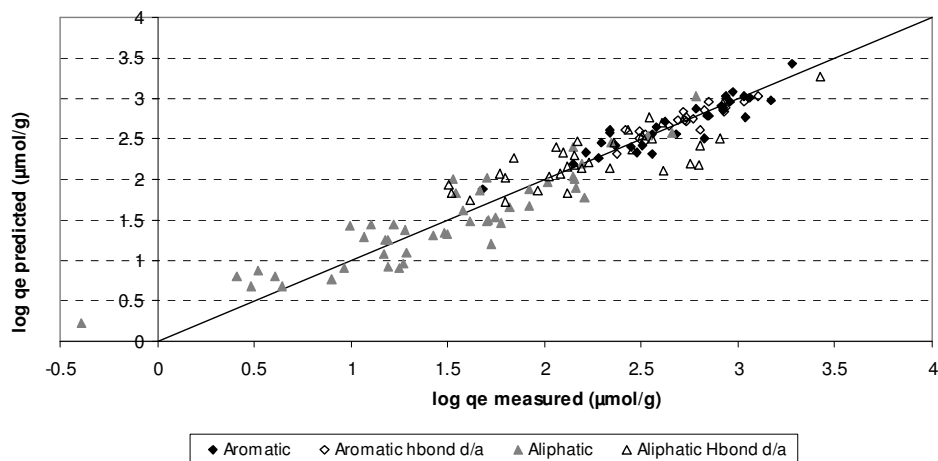


Figure 4: Prediction accuracy of QSAR models

Aliphatic solutes show larger deviations from the ideal line than aromatic solutes. As these are also the solutes which show the lowest removal, and thus the most critical in activated carbon reactor design, further model refinement should focus on increasing prediction accuracy for these groups. The analytical margin of error should also be included in the model accuracy.

6. Potential Model improvements

The proposed QSAR model should be regarded as a tool to better understand adsorption mechanisms and their influence on adsorption capacity. Its main limitation is that it only describes solute removal by one specific carbon type, and that removal is measured in ultrapure water. Carbon characteristics that can be relevant are pore size/volume distribution, pH_{pzc} and hydrophobicity – e.g. expressed as carbon oxygen content or as surface tension. Including water matrix effects will be even more complicated, as model waters never fully represent their natural counterpart, and natural waters usually contain mixtures of natural organic matter (NOM) which are hard to fully characterize. Basic water properties, such as ionic strength, pH and Ca²⁺ content should be measured, and taken into account in a model.

7. Conclusions

The carbon loading can only be predicted accurately after the set of solutes with broad variation in solute properties is subdivided into four bins: aliphatic without H-bond d/a groups, aliphatic with H-bond d/a groups, aromatic without H-bond d/a groups, aromatic with H-bond d/a groups.

Hydrophobic partitioning is relevant for all solutes, as linear relationships were found between log D and carbon loading for each bin.

At lower log D values, carbon loading was higher for solutes which were capable to form H-bonds, and aromatic solutes which could form pi-pi bonds. At a log D of 3.7, the solutes in all bins showed similar removal. This indicates that hydrophobic partitioning is the dominant removal mechanism at that log D value, overruling the influences of pi-pi-interaction and H-bond formation.

London dispersion forces only had dominant influence for the bin containing aliphatic solutes without H-bond d/a groups. As the solutes in this bin are not capable to form H-bonds or pi-pi bonds with the carbon surface, the weaker London dispersion forces – expressed as polarizability – are more dominant.

The influence of the presence or absence of H-bond d/a groups was independent of the amount of H-bond donor or H-bond acceptor groups. As the number of H-bond d/a groups on the carbon surface is limited, a solute can only form a H-bond with a single functional group on the carbon surface. As such, solute carbon loading is independent of the number of solute H-bond d/a groups.

The model(s) predict the carbon loading of most solutes within 0.5 log unit deviation from measured values.

Acknowledgements

This research is based upon work supported by VEWIN, the association of drinking water companies in the Netherlands. Any opinions, findings, conclusions, or recommendations expressed in this publication are those of the authors and do not necessarily reflect the views of the supporting organization.

References

- Bjelopavlic, M., G. Newcombe, R. Hayes (1999) Adsorption of NOM on activated carbon: Effect of surface charge, ionic strength, and pore volume distribution. *Journal of colloid and interface science* 210: 271-280.
- Blum, D. J. W., I. H. Suffet, J. P. Duguet (1994) Quantitative structure-activity relationship using molecular connectivity for the activated carbon adsorption of organic chemicals in water. *Water research* 28(3): 687-699.
- Brasquet, C., P. Le Cloirec (1999) QSAR for organics adsorption onto activated carbon in water: what about the use of neural networks. *Water research* 33(17): 3603-3608.
- Calvet (1989) Adsorption of organic chemicals in soils. *Environmental health perspectives* 83: 145-177.
- Chen, W., L. Duan, D. Zhu (2007) Adsorption of polar and nonpolar organic chemicals to carbon nanotubes. *environmental science and technology* 41(24): 8295-8300.
- Chiou, C. T. (1979) A physical concept of soil-water equilibria for nonionic organic compounds. *Science* 106: 831-832.
- Crittenden, J. C., S. Sanonraj, J. L. Bulloch, D. W. Hand, T. N. Rogers, T. F. Speth, M. Ulmer (1999) Correlation of aqueous-phase adsorption isotherms. *Environmental science and technology* 33: 2926-2933.
- Franz, M., H. A. Arafat, N. G. Pinto (2000) Effect of chemical surface heterogeneity on the adsorption mechanism of dissolved aromatics on activated carbon. *carbon* 38: 1807-1819.
- Gramatica, P. (2007) Principles of QSAR models validation: internal and external. *QSAR & Combinatorial science* 26(5): 694-701.
- Hu, J.-J., T. Aizawa, Y. Magara (1997) Evaluation of adsorbability of pesticides in water on powdered activated carbon using octanol-water partitioning coefficient. *water science and technology* 35(7): 219-226.
- Iriarte-Velasco, U., J. I. Alvarez-Uriarte, N. Chimeno-Alanis, J. R. Gonzalez-Velasco (2008) Natural organic matter adsorption onto granular activated carbons: Implications in the molecular weight and disinfection byproducts formation. *Industrial & engineering chemistry research* 47: 7868-7876.
- Kruhlak, N. L., J. F. Contrera, R. D. Benz, E. J. Matthews (2007) Progress in QSAR toxicity screening of pharmaceutical impurities and other FDA regulated products. *Adv. Drug Delivery Rev.* 59: 43-55.
- Lei, H., S. A. Snyder (2007) 3D QSPR models for the removal of trace organic contaminants by ozone and free chlorine. *Water research* 41: 4051-4060.

- Li, L., P. A. Quinlivan, D. R. U. Knappe (2002) Effects of activated carbon surface chemistry and pore structure on the adsorption of organic contaminants from aqueous solution. *carbon* 40: 2085.
- Li, L., P. A. Quinlivan, D. R. U. Knappe (2005) Predicting adsorption isotherms for aqueous organic micropollutants from activated carbon and pollutant properties. *Environ. Sci. Technol.* 39(9): 3393-3400.
- Luehrs, D. C., J. P. Hickey, P. E. Nilsen, K. A. Godbole, T. N. Rogers (1996) Linear solvation energy relationship of the limiting partition coefficient of organic solutes between water and activated carbon. *Environmental science and technology* 30: 143-152.
- Magnuson, M. L., T. F. Speth (2005) Quantitative structure-property relationships for enhancing predictions of synthetic organic chemical removal from drinking water by granular activated carbon. *Environmental science and technology* 39: 7706-7711.
- McElroy, J. A. (2005). Adsorption of substituted aromatic compounds by activated carbon: a mechanistic approach to quantitative structure activity relationships, University of Florida. Msc.: 71.
- Moreno-Castilla, C. (2004) Adsorption of organic molecules from aqueous solutions on carbon materials. *carbon* 42: 83-94.
- Nguyen, T. H., K.-U. Goss, W. P. Ball (2005) Polyparameter linear free energy relationships for estimating the equilibrium partition of organic compounds between water and the natural organic matter in soils and sediments. *Environ. Sci. Technol.* 39(4): 913-924.
- Pendleton, P., S. H. Wong, R. Schumann, G. Levay, R. Denoyel, J. Rouquerol (1997) Properties of activated carbon controlling 2-methylisoborneol adsorption. *carbon* 35: 1141.
- Quinlivan, P. A., L. Li, D. R. U. Knappe (2005) Effects of activated carbon characteristics on the simultaneous adsorption of aqueous organic micropollutants and natural organic matter. *Water research* 39: 1663-1673.
- Schwarzenbach, R. P., B. I. Escher, K. Fenner, T. B. Hofstetter, C. A. Johnson, U. Von Gunten, B. Wehrli (2006) The challenge of micropollutants in aquatic systems. *Science* 313: 1072-1077.
- Schwarzenbach, R. P., P. M. Geschwend, D. M. Imboden, Eds. (2003). *Environmental organic chemistry*, John Wiley & Sons.
- Shih, Y.-H., P. M. Gschwend (2009) Evaluating activated carbon water sorption coefficients of organic compounds using a linear solvation energy relationship approach and sorbate chemical activities. *Environ. Sci. Technol.* 43(3): 851-857.
- Southworth, G. R., J. L. Keller (1986) Hydrophobic sorption of polar organics by low organic carbon soils. *Water, air and soil pollution* 28: 239-248.
- Speth, T. F., R.J. Miltner (1990) Technical note: Adsorption capacity of GAC for synthetic organics. *Journal of AWWA* 82(2): 72-75.
- Speth, T. F., R.J. Miltner (1998) technical note: adsorption capacity of GAC for synthetic organics. *Journal of AWWA* 90(4): 171-174.
- Strelko, V., D. J. Malik (2002) Characterization and metal sorptive properties of oxidized active carbon. *Journal of colloid and interface science* 250: 213-220.
- Verliefde, A. R. D., E. R. Cornelissen, S. G. J. Heijman, E. M. V. Hoek, G. L. Amy, B. van der Bruggen, J. C. van Dijk (2009) Influence of solute-membrane affinity on rejection of uncharged organic solutes by nanofiltration membranes. *Environmental science and technology* 43: 2400-2406.
- Villacanas, F., M. F. R. Pereira, J. J. M. Orfao, J. L. Figueiredo (2005) Adsorption of simple aromatic compounds on activated carbons. *journal of colloid and interface science* 293: 128-136.

- Westerhoff, P., Y. Yoon, S. Snyder, E. Wert (2005) Fate of endocrine-disruptor, pharmaceutical and personal care product chemicals during simulated drinking water treatment processes. *Environmental science and technology* 39: 6649-6663.
- Xu, Y.-J., H. Gao (2003) Dimension related distance and its application in QSAR/QSPR model error estimation. *QSAR & Combinatorial science* 22(4): 422-429.
- Yangali-Quintanilla, V., T.-U. Kim, M. Kennedy, G. L. Amy (2008) Modeling of RO/NF membrane rejections of PhACs and organic compounds: a statistical analysis. *Drinking water engineering and science* 1: 7-15.
- Zwiener, C. (2007) Occurrence and analysis of pharmaceuticals and their transformation products in drinking water treatment. *anal. bioanal. chem.* 287: 1159-1162.

Supporting information

Chapter 2

A mechanistic approach to determine equilibrium adsorption of organic micropollutants onto activated carbon

D.J. de Ridder¹*, L. Villacorte²), A.R.D. Verliefde¹) ³), S.G.J. Heijman¹), G. Amy¹) ²), J.C. van Dijk¹)

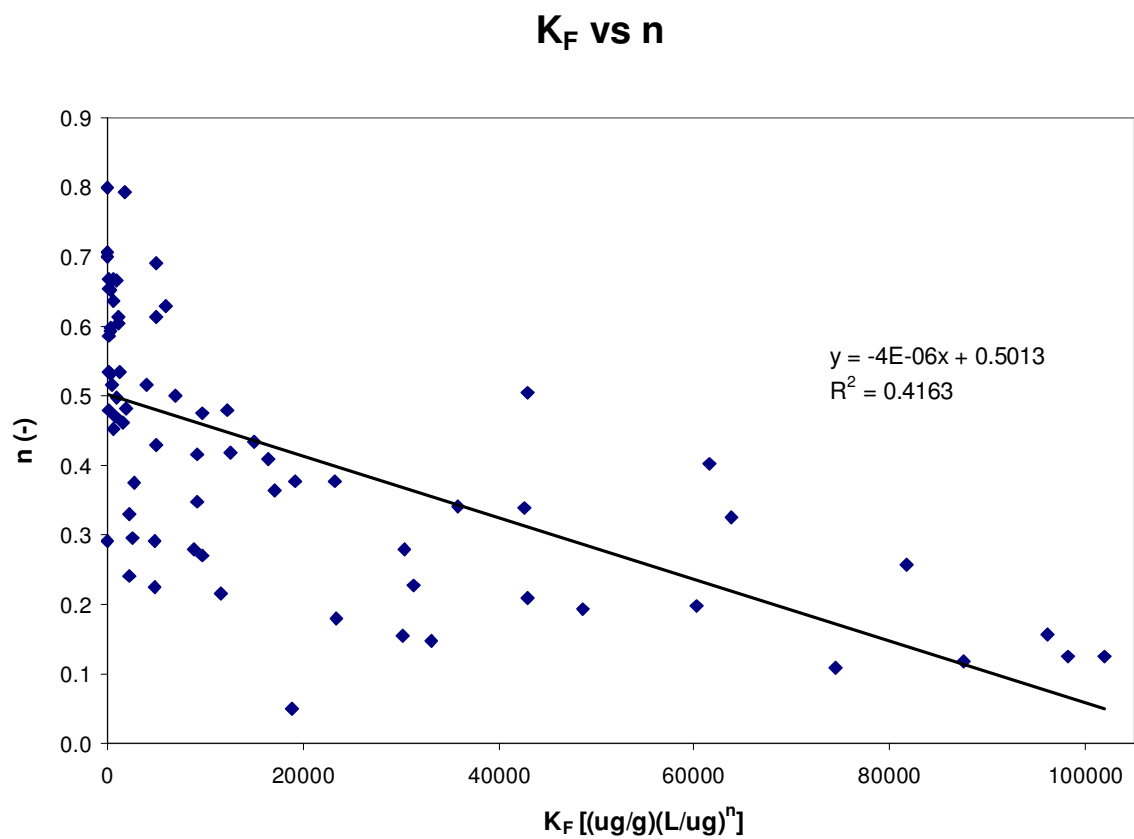


Figure S.1: Relation between the Freundlich parameters K_F and n

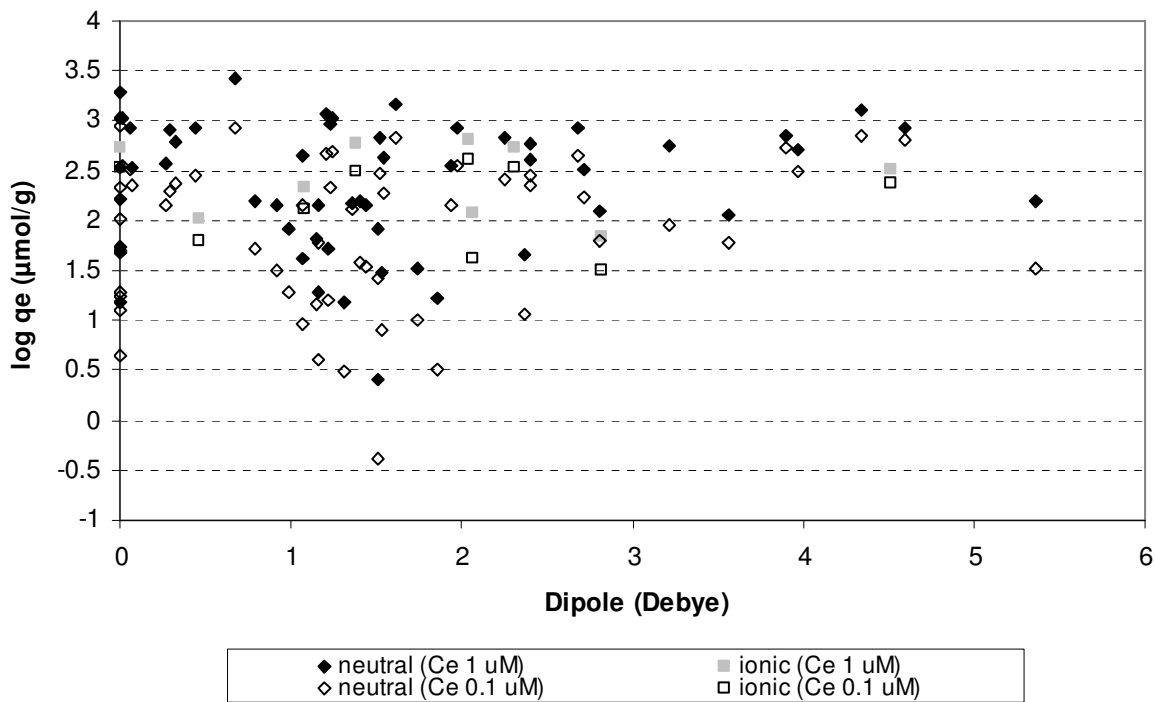


Figure S.2: Relation between dipole moment and log qe for neutral and ionic solutes at Ce 1 uM and 0.1 uM

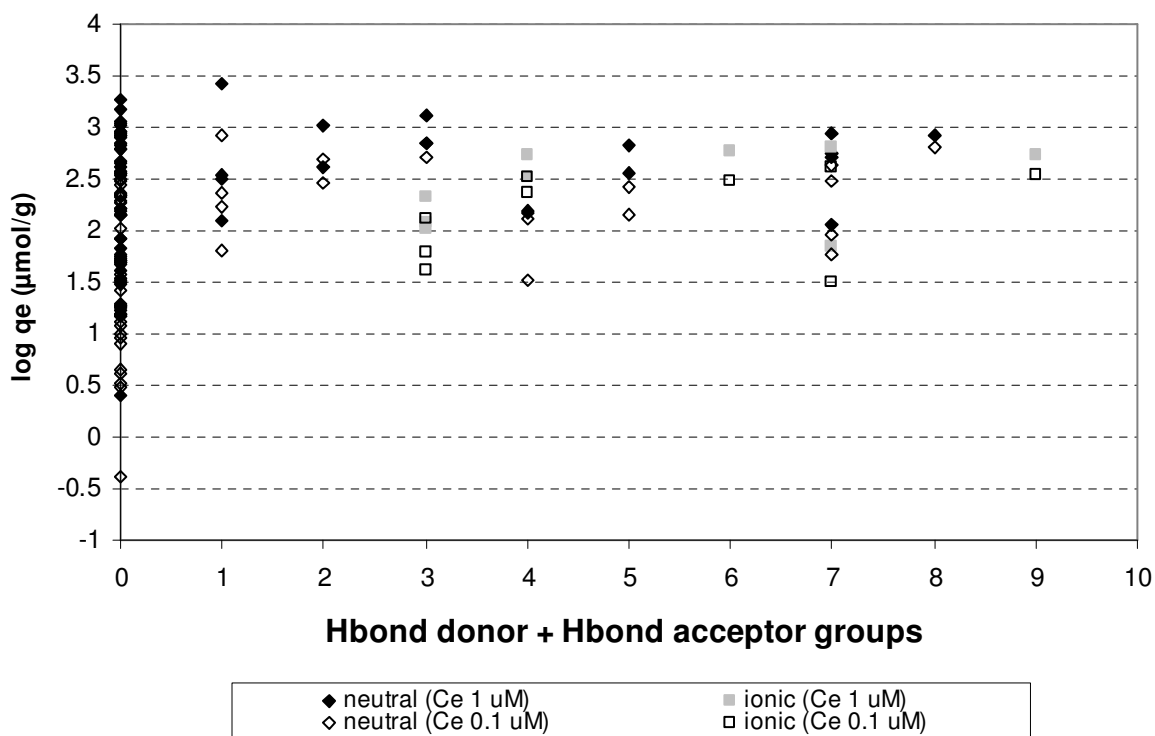


Figure S.3: Relation between total number of H bond donor and acceptor groups and log qe for neutral and ionic solutes at Ce 1 uM and 0.1 uM

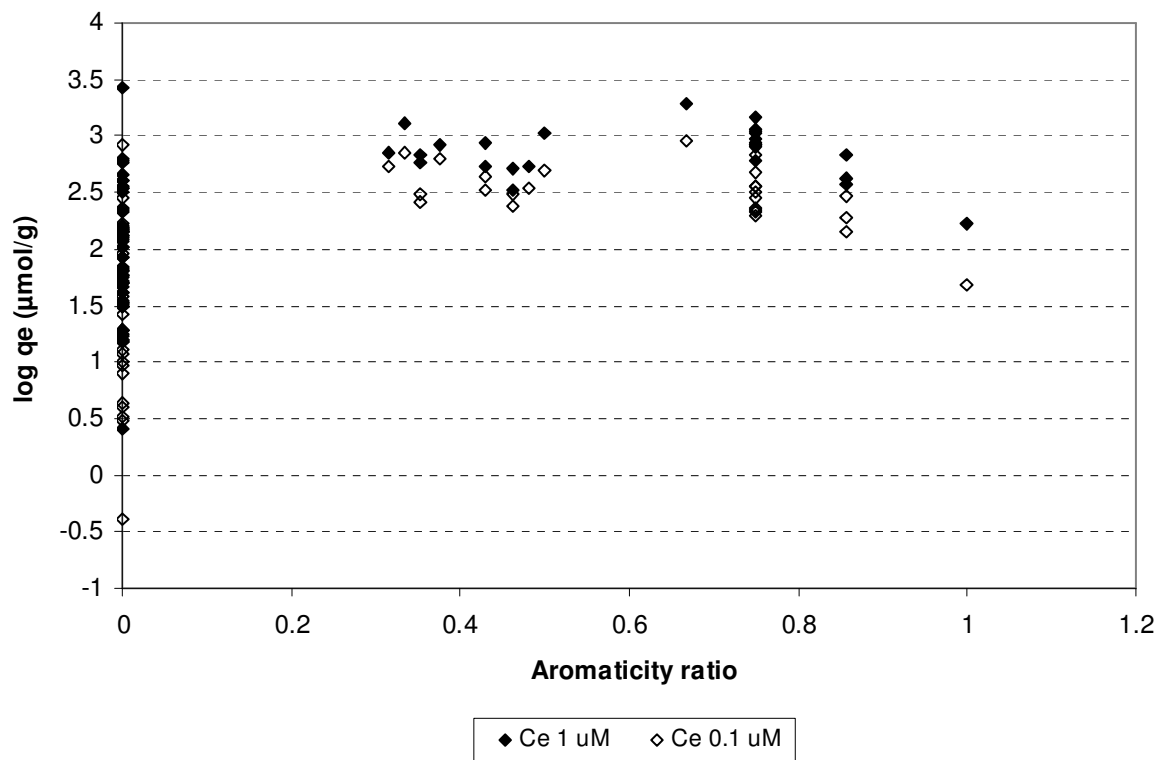


Figure S.4: Relation between aromaticity ratio and $\log q_e$ for neutral and ionic solutes at Ce 1 μM and 0.1 μM

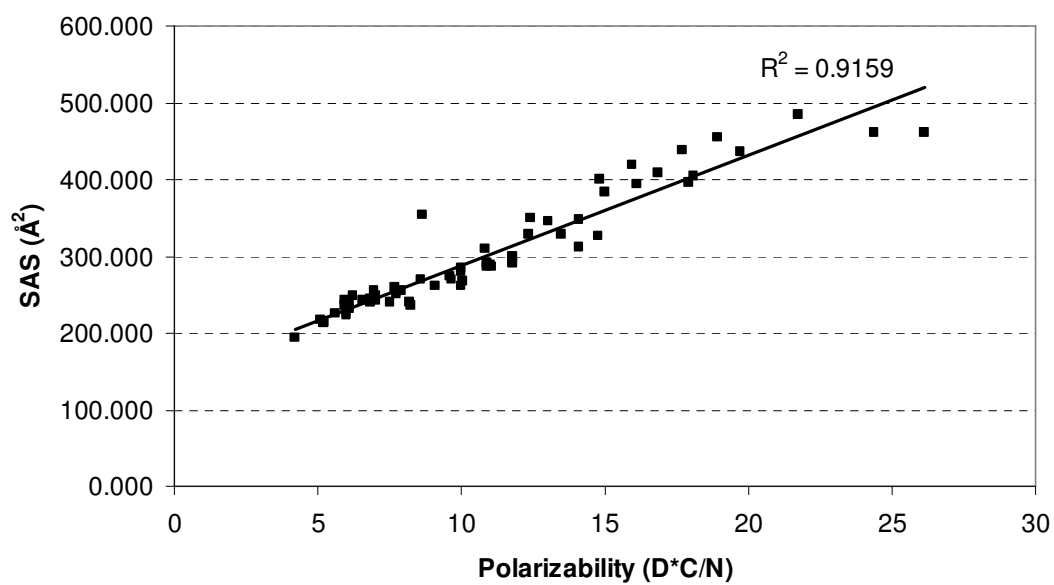


Figure S.5: Relation between polarizability and solvent (water) accessible surface

Aromatic Hbond d/a

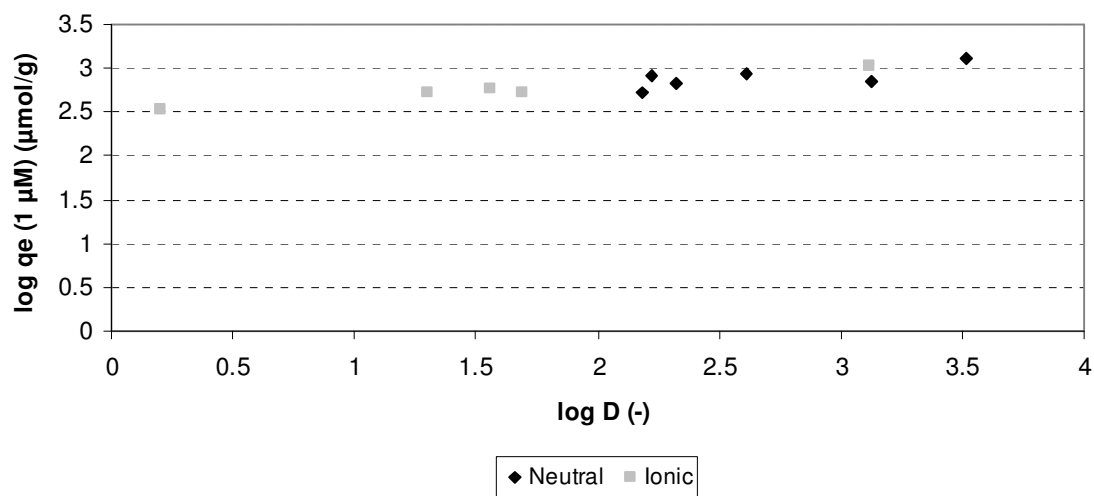


Figure S.6: Effect solute charge on the relation between $\log D$ and $\log q_e$ (1 μM)

Aromatic Hbond d/a

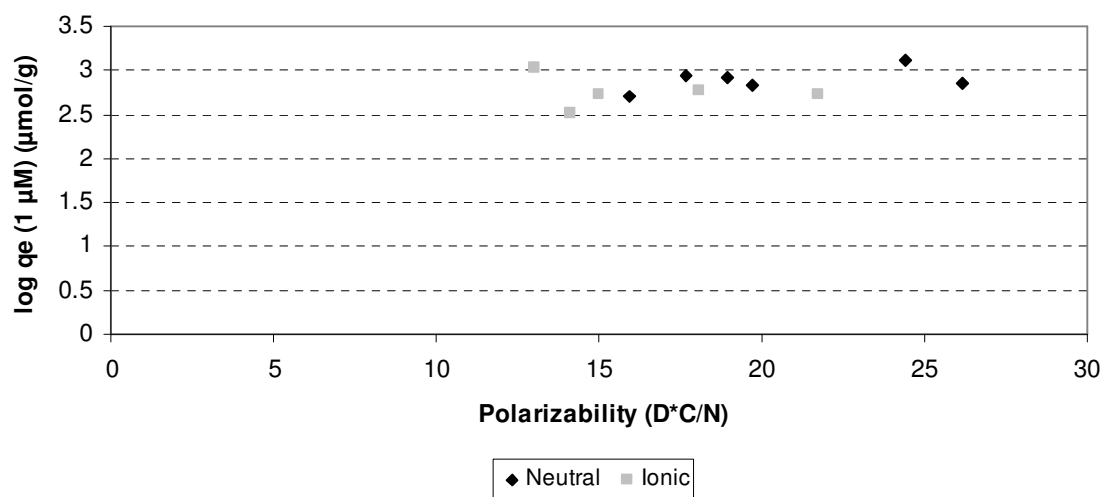


Figure S.7: Effect solute charge on the relation between polarizability and $\log q_e$ (1 μM)

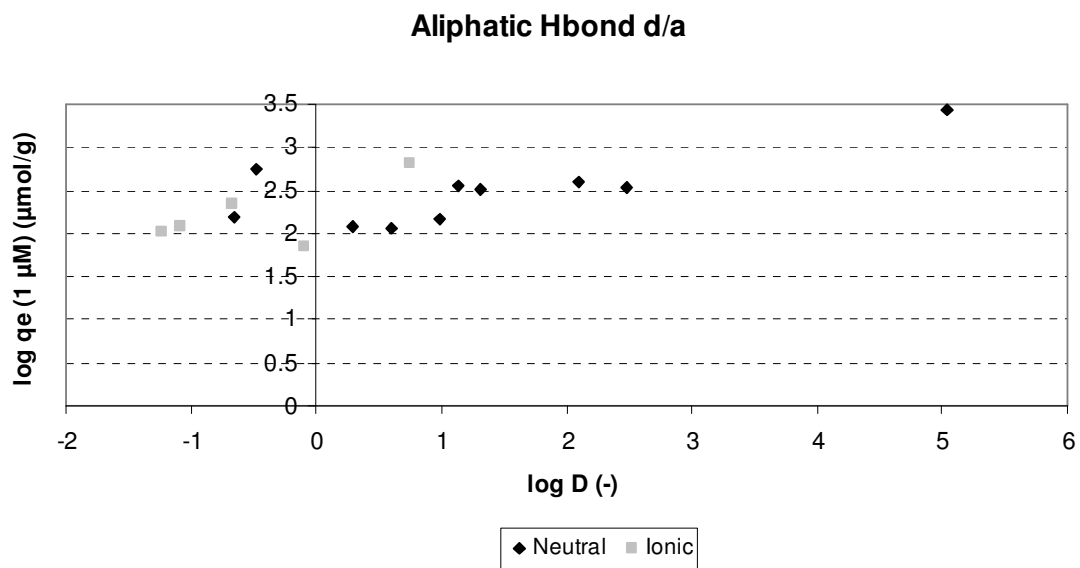


Figure S.8: Effect solute charge on the relation between $\log D$ and $\log q_e$ ($1 \mu\text{M}$)

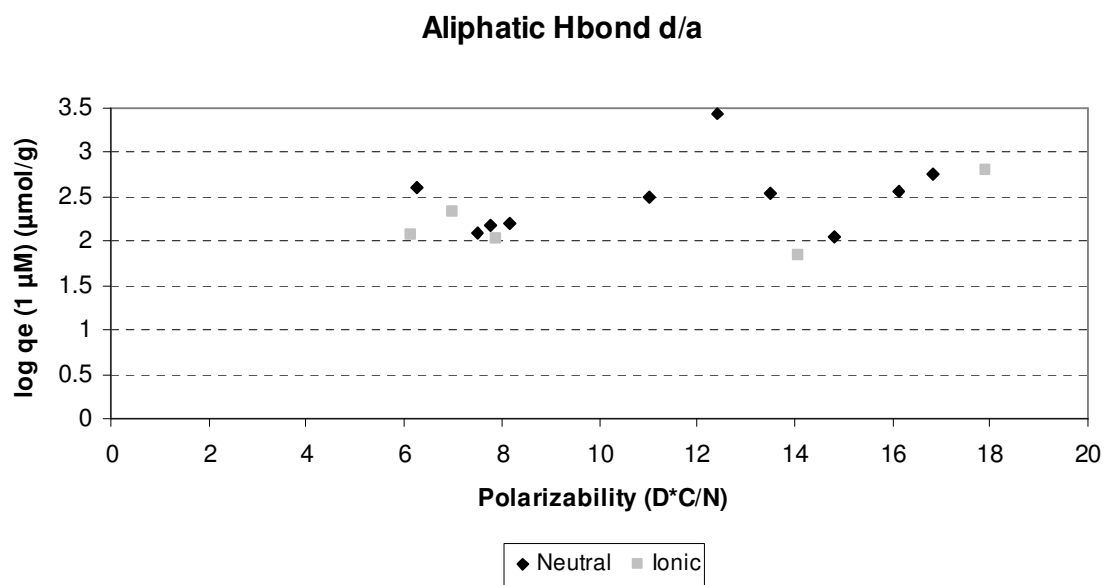


Figure S.9: Effect solute charge on the relation between polarizability and $\log q_e$ ($1 \mu\text{M}$)

Aromatic Hbond d/a

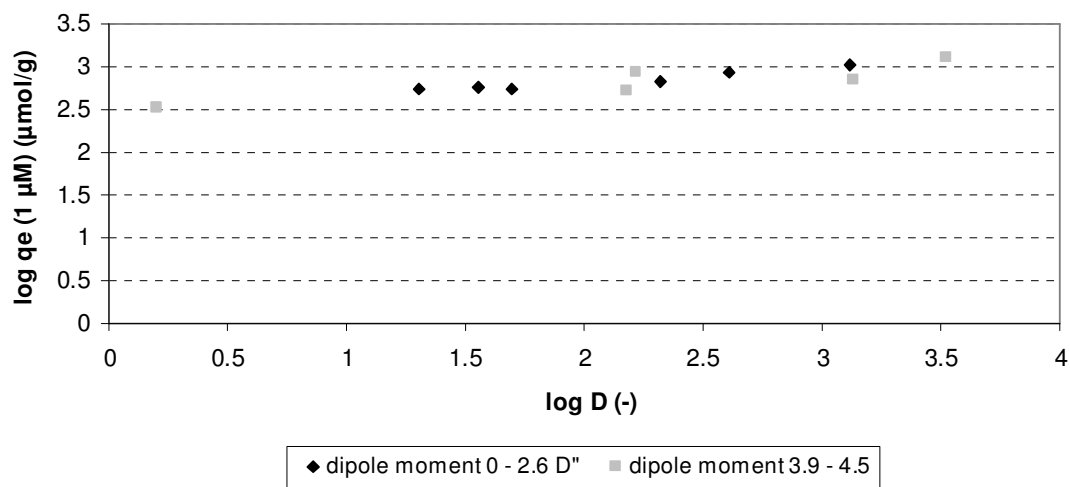


Figure S.10: Effect solute dipole moment on the relation between $\log D$ and $\log q_e$ (1 μM)

Aromatic Hbond d/a

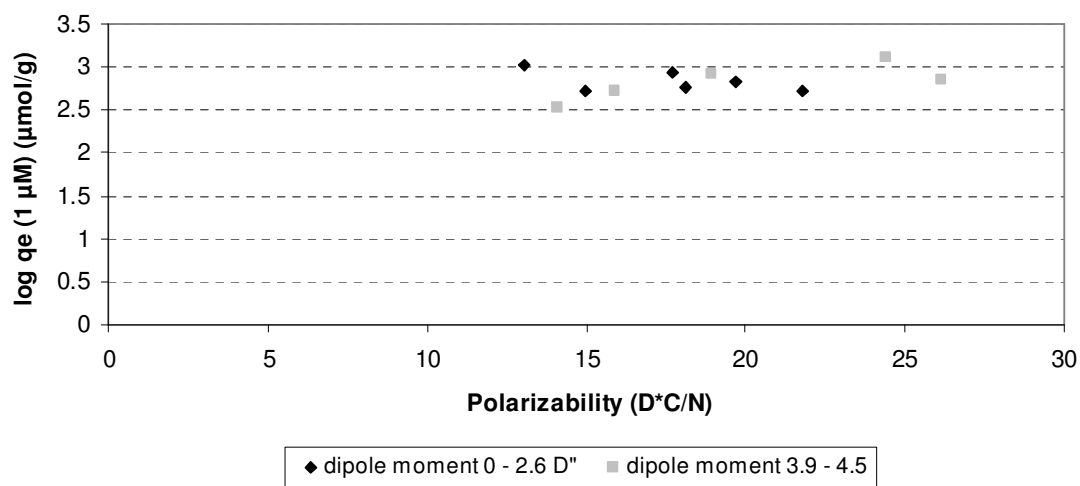


Figure S.11: Effect solute dipole moment on the relation between polarizability and $\log q_e$ (1 μM)

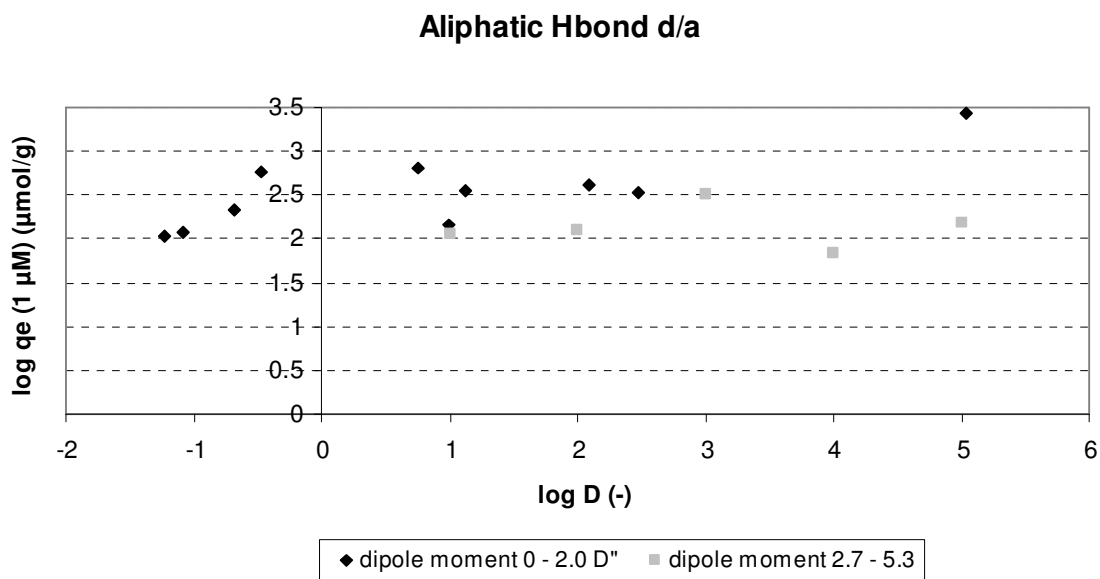


Figure S.12: Effect solute dipole moment on the relation between $\log D$ and $\log q_e$ ($1 \mu M$)

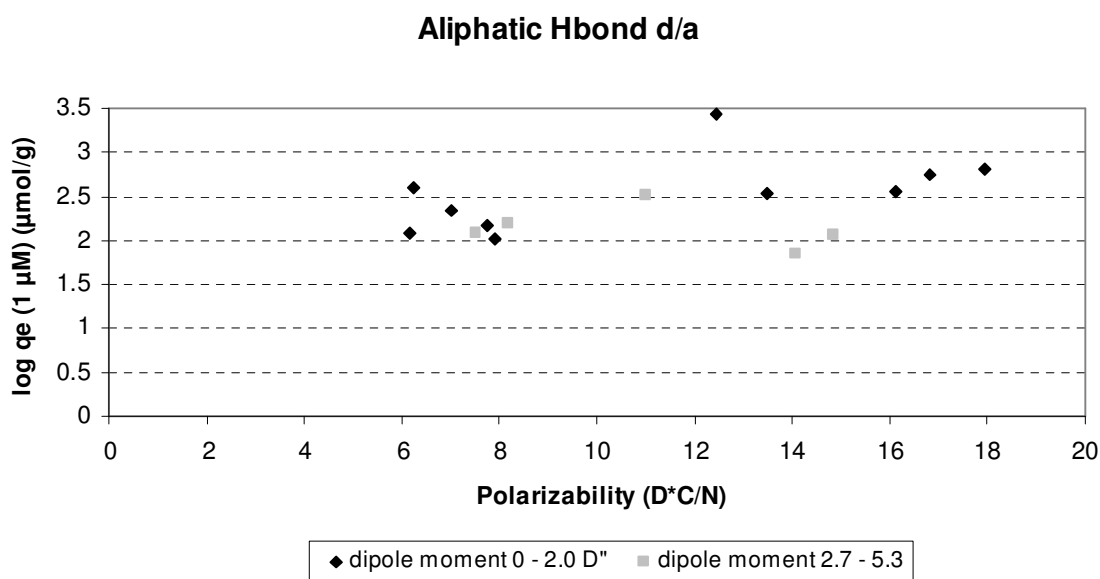


Figure S.13: Effect solute dipole moment on the relation between polarizability and $\log q_e$ ($1 \mu M$)

Chapter 3

A thermodynamic approach to assess organic solute adsorption onto activated carbon in water

David J. de Riddera *, Arne R.D. Verliefde^{a,b}, Bas G.J. Heijmana, Simon Gelinc, Manuel F.R. Pereirad, Raquel P. Rochad, José L. Figueiredod, Gary L. Amya,e, Hans C. van Dijkstra

a Delft University of Technology, P.O. Box 5048, 2600 GA Delft, The Netherlands

b Ghent University, Coupure Links 653, B-9000 Gent, Belgium

c École des Ponts Paristech, 6-8 Avenue Blaise Pascal, 77455 Marne-la-Vallée Cedex 2, France

d Laboratório de Catálise e Materiais, Laboratório Associado LSRE/LCM, Faculdade de Engenharia, Universidade do Porto, 4200-465 Porto, Portugal

e King Abdullah University of Science and Technology, Thuwal, Saudi Arabia

Carbon 50 (2012) 3774-3781

Abstract

In this paper, the hydrophobicity of 13 activated carbons is determined by various methods; water vapour adsorption, immersion calorimetry, and contact angle measurements. The quantity and type of oxygen-containing groups on the activated carbon were measured and related to the methods used to measure hydrophobicity. It was found that the water-activated carbon adsorption strength (based on immersion calorimetry, contact angles) depended on both type and quantity of oxygen-containing groups, while water vapour adsorption depended only on their quantity. Activated carbon hydrophobicity measurements alone could not be related to 1-hexanol and 1,3-dichloropropene adsorption. However, a relationship was found between work of adhesion and adsorption of these solutes. The work of adhesion depends not only on activated carbon-water interaction (carbon hydrophobicity), but also on solute-water (solute hydrophobicity) and activated carbon-solute interactions. Our research shows that the work of adhesion can explain solute adsorption and includes the effect of hydrogen bond formation between solute and activated carbon.

1. Introduction

In drinking water treatment, one of the most frequently used techniques to remove organic solutes is adsorption onto granular or powdered activated carbon. Among the factors influencing the efficacy of this process, hydrophobic interaction can be an important adsorption mechanism and this depends on the hydrophobicity of both the solute and the activated carbon surface [1, 2]. Theoretically, the energy (or work) of adhesion of two solids in water is expressed by the following equation [3]:

$$W_{scw} = W_{sc} + W_{ww} - W_{sw} - W_{cw} \quad (1)$$

Here, W_{ij} (mJ/m^2) is the work required per unit area to separate two phases i and j and subscripts c , s , and w refer to activated carbon, solute and water, respectively. Activated carbon hydrophobicity is included in W_{cw} , solute hydrophobicity in W_{sw} , and interaction between solute and activated carbon in W_{sc} .

In recent predictive models, the total oxygen content of activated carbon is used as a measure of hydrophobicity for (modified) activated carbons [4-6]. Even though a significant influence of carbon oxygen content on organic solute adsorption appears to exist, care should still be taken when using oxygen content as a model parameter to represent activated carbon surface characteristics in organic adsorption models;

Carbon hydrophobicity can be related to the quantity of oxygen-containing functional groups and basic sites. Basic sites can be nitrogen-containing functional groups and electron-rich

areas on the basal planes, both of which are not included when only using oxygen content to describe carbon surface properties [7, 8].

The different types of oxygen-containing functional groups on the carbon surface have different influences on carbon hydrophobicity [9].

Alternative methods to measure activated carbon hydrophobicity are contact angle measurements, immersion calorimetry, and water vapour uptake [7, 10, 11]. In contrast to a quantification of oxygen-containing functional groups, these methods are non-specific and consequently also include factors that affect activated carbon hydrophobicity that are omitted when total oxygen content is used.

The goal of this paper is to determine the most suitable parameter out of the measurements described above to describe activated carbon hydrophobicity, and use it to explain the efficacy of solute adsorption.

Therefore, in this paper, the hydrophobicity of a broad set of activated carbons is determined with the methods discussed above. The adsorption efficacy of two probe organic solutes with different modes of adsorption onto the carbons was investigated; 1-hexanol and 1,3-dichloropropene (1,3-DCP). 1-Hexanol and 1,3-DCP have similar sizes (molecular weight 102 and 111 g/mol, respectively) and solute hydrophobicities (values for octanol-water partitioning coefficient ($\log K_{ow}$) 2.03 and 2.04, respectively). However, 1-hexanol can form Hydrogen-bonds with oxygen-containing functional groups on the activated carbon surface, while 1,3-DCP cannot. As such, hydrophobic interaction is similar for 1-hexanol and 1,3-DCP (based on their $\log K_{ow}$ values), but 1-hexanol has an additional mechanism to adsorb onto the activated carbon. Thus we expect that 1-hexanol will be removed more effectively than 1,3-DCP, which would be in line with our previous findings [12].

2. Materials and methods

The hydrophobicity of 13 commercial carbons (see Table 1) was investigated. These activated carbons vary in oxygen content and oxygen-containing functional group composition. All granular activated carbons were ground to powder with a disk mill (HSM100, Herzog). Carbon hydrophobicity was measured using three different methods: the capillary rise method to determine the activated carbon-water contact angle, immersion calorimetry, and water vapour uptake. The types of functional groups on the carbon surface were analysed with temperature programmed desorption.

The solutes, 1-hexanol (98%) and 1,3-dichloropropene (90%, cis+trans), were obtained from Sigma-Aldrich.

2.1 Capillary rise

A sigma 701 tensiometer (Technex) and glass column with a porous bottom (Technex, cat. Nr. T112) were used in the capillary rise experiments. Before each measurement, the glass column was rinsed with acetone and demineralised water and both the column and activated carbon powder were dried for 30 minutes at 100 °C. After drying, the height of the glass column was extended with a tight fitting polyethylene tube, and both the column and the tube were filled with carbon powder. The carbon powder was compacted by centrifuge (Heraeus labofuge 400; Thermo scientific) for 5 minutes at 1000 rpm (134 G).

The porous bottom of the column was submerged in either hexane or demineralised water, and the mass (increase) of the column was recorded in 10 s intervals. For each commercial carbon, both hexane and water uptake was measured at least twice.

Water-carbon-air contact angles were calculated from liquid uptake rates using the Washburn equation [13]:

$$\frac{m^2}{t} = \frac{c\rho^2\gamma_L \cos\theta}{\eta} \quad (2)$$

With the mass (m , in g), density (ρ , in g/m^3), liquid surface tension (γ_L , in mJ/m^2), the water-carbon-air contact angle (θ , in $^\circ$) and viscosity (η , in Pa s). Parameter c (in m^5) is a factor describing the geometry of the carbon powder bed, and includes capillary radius (r , in m), tortuosity (τ , unitless) and number of capillaries (n).

$$c = \frac{1}{2}\pi^2(\tau r)^5 n^2 \quad (3)$$

Hexane can be used to determine c ; as hexane is a completely wetting liquid, its contact angle is known ($\theta=0$) and c can be calculated from the hexane uptake rate for each carbon. This c is used when determining the water-carbon contact angle from the water uptake rate.

2.2 Immersion Calorimetry

A solution calorimeter (model 6755, Parr) and calorimetric thermometer (model 6772, Parr) were used in the calorimetry experiments. A closed glass container filled with 0.5 g activated carbon powder was submerged in 100 ml, 1-hexanol, 1,3-DCP or demineralised water, in order to obtain the W_{sc} of both 1-hexanol and 1,3-DCP and to obtain the W_{cw} . The container was continuously rotated to provide mixing. When the system was in equilibrium (i.e. the heat increase due to mixing was constant), the activated carbon powder was released from the glass container and the additional heat produced upon immersion of the carbon was measured. The measured heat increase was corrected for the heat capacity of water (4.19 J/g K), 1-hexanol (2.33 J/g K), or 1,3-DCP (0.80 J/g K), respectively.

2.3 Water vapour uptake

The activated carbon samples were dried for 30 hours at 105 $^\circ\text{C}$. After drying, 1.0 g of each carbon was weighed and placed in a 5 ml polystyrene cup (microbeaker, Fisher Scientific). The carbon samples and an empty cup (reference) were placed in a moisture conditioned room, at 100% humidity and 19 $^\circ\text{C}$, for 96 days and were weighed weekly.

2.4 Temperature programmed desorption

Temperature-programmed desorption (TPD) spectra were obtained with an AMI-200 catalyst characterisation apparatus (Altamira Instruments) connected to a Dycor Dymaxion mass spectrometer. The carbon sample (0.1 g) was placed in a U-shaped quartz tube located inside an electrical furnace and heated to 1100 $^\circ\text{C}$ at 5 $^\circ\text{C}/\text{min}$, using a constant helium flow of 25 cm^3/min . CO and CO₂ were measured by mass spectroscopy. For quantification of the amount of CO and CO₂ released, calibration of these gases was carried out at the end of each analysis. The amount of each surface group was obtained by deconvolution of the CO and CO₂ TPD spectra, based on previously discussed assumptions [14, 15].

2.5 1-Hexanol and 1,3-DCP adsorption isotherms

Adsorption isotherms were obtained in demineralized water containing 1-hexanol or 1,3-DCP, respectively, with activated carbon doses varying between 100 and 750 mg/l. All samples were mixed using magnetic stirrers and equilibrated for 24 hours at room temperature (\approx 18 $^\circ\text{C}$). Sample bottles were completely filled in order to minimize 1-hexanol or 1,3-DCP losses due to vaporization. The initial concentration of both solutes was 45-50 mg/l. With each isotherm series, a blank sample (0 mg/l carbon dose) was included to account for errors in stock solution dosing or vaporization losses. A blank sample of the demineralized water

was added to quantify the background level of total-C. Also, a blank sample of activated carbon (750 mg/l carbon dose, no 1-hexanol/1,3-DCP) was added to account for uptake or release of CO₂ or other C-containing contaminants by the activated carbon.

1-Hexanol and 1,3-DCP concentrations were measured by total-C analysis (TOC-VCPH, Shimadzu). All samples were acidified to pH 4 to strip off HCO₃⁻ and thus limit the quantity of background C in the TOC analysis.

3. Results and discussion

3.1 Evaluating analysis methods for hydrophobicity

The results obtained from the methods to define activated carbon hydrophobicity are included in Table 1. Results from temperature programmed desorption indicate that for almost all carbon types, functional groups released as CO (such as phenol, carbonyl, quinone) are typically present at higher concentrations than functional groups released as CO₂ (such as carboxylic acid and lactone). This is also schematically illustrated in Figure S1 in the supporting information. The coconut-based carbon contains a relative large quantity of carboxylic acid functional groups, while the peat-based carbons, SA Super and W35, contain high quantities of phenol functional groups and the peat-based ROW contains a large quantity of lactone functional groups. With the exception of SN4 and CS30, the coal-based and re-agglomerated-coal-based carbons had rather similar functional group distributions. Because the main differences in functional group distributions were related to the activated carbon base material, the carbons were classified by base material (i.e., Coal, Re-agglomerated coal (pulverized and “glued” into a granule), Peat, Coconut) when measuring and assessing the influence of activated carbon hydrophobicity.

Table 1: Activated carbon characteristics
Error in $\Delta H_{imm} \pm 2.0 \text{ mJ/m}^2$; Error in $\theta \text{ water} \pm 1.5^\circ$; Error in H_2O vapour uptake $\pm 0.06 \text{ mg/m}^2$

Activated Carbon	Base material	BET surface (m ² /g)	Ash content (mass-%)	CO (μmol/g)	CO ₂ (μmol/g)	O surface density (μmol/m ²)	ΔH_{imm} in water (mJ/m ²)	θ water (°)	H ₂ O vapour uptake (mg/m ²)
SN4	Coal	1344	7	379	344	0.79	24.2	55.5	0.53
UC830	B coal	900	1	387	66	0.57	26.6	44.9	0.45
CS30	B coal	900	14	654	70	0.88	30.2	64.5	0.50
NoRise	Coal	900		667	324	0.84	28.8	58.6	0.43
HD4000	L Coal	628	23	723	226	1.87	40.3	55.1	1.20
F400	B coal, RA	972	8	684	108	0.92	30.5	62.5	0.61
F200	B coal, RA	850	7	542	155	1.00	27.8	68.0	0.46
Centaur HSL	B coal, RA	909	7	765	178	1.23	39.7	55.0	0.58
F600	B coal, RA	847	6	854	273	1.65	26.9	62.7	0.38
SA Super	Peat	1150	10	776	397	1.36	24.3	75.6	0.72
ROW 0.8 supra	Peat	1140	7	619	561	1.53	31.7	74.7	0.79
W35	Peat	850	10	1027	736	2.94	29.6	65.7	0.76
AC1230C	Coconut	932	2	525	530	1.7	26.5	83.6	0.90

B: Bituminous
L: Lignite
RA: Re-Agglomerated

When the measured quantity of oxygen-containing groups (oxygen surface density) was plotted against measured water vapour uptake, a positive linear relationship was found (Figure 1). This indicates that the specific type of functional groups is irrelevant for the amount of water molecules adsorbed, as water uptake can be related to the general sum parameter of oxygen surface density. A similar conclusion was also drawn from previous molecular modelling studies [16].

One re-agglomerated coal based carbon (F600) and one peat based carbon (W35) showed somewhat lower water uptake than expected based on their surface oxygen content (i.e., they are relatively hydrophobic compared to the other carbons). As the ash content of these carbons (7 and 10%, respectively) was comparable with the other activated carbons, it can not explain this observation. A possible explanation might be found in the distribution of the oxygen-containing groups across the surface, combined with the pore geometry (pore size and connectivity). It is well known from the literature that water molecules associate to form clusters around oxygen-containing functional groups, and it is proposed that these clusters may hinder pore entrance [4, 17, 18]. If F600 and W35 would have a relative high concentration of oxygen-containing functional groups at pore entrances, this would limit access of water to the pore internals as (i) water clusters block the entrance and (ii) the pore internal is relatively hydrophobic. Poor pore connectivity may further enhance the effect of pore blockage by water clusters. As a consequence, part of the BET surface of F600 and W35 might not be wetted, resulting in lower water vapour uptake per surface area. However, experimental determination of the distribution of oxygen-containing functional groups is extremely difficult.

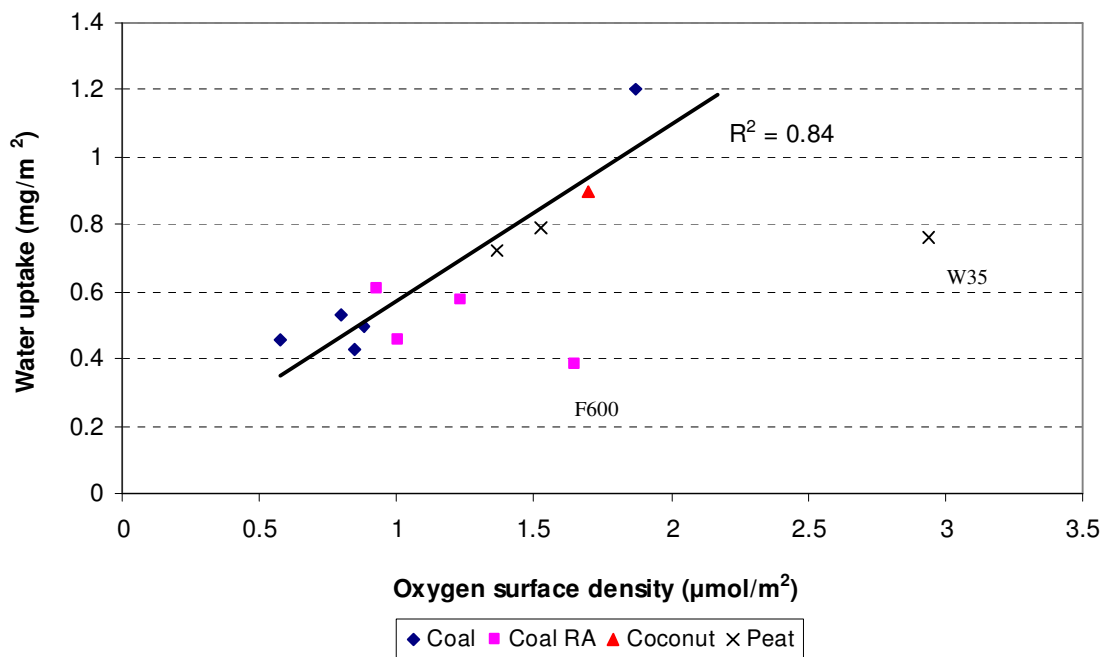


Figure 1: Activated carbon O content vs water vapour uptake. F600 and W35 are not included in the correlation.

In contrast to the clear relationship between water vapour uptake and carbon oxygen surface density, no clear relationships were found between heat of water immersion and carbon oxygen surface density (Supporting information; S2). Also the relationship between water-carbon contact angle and carbon oxygen surface density is poor, and in contrast to the expectations appears to be positive (S3). This would be unrealistic, as that would imply that carbons with high oxygen surface density are more hydrophobic. These findings suggest that while the amount of water vapour adsorbed is independent of the type of oxygen-containing

functional groups, the interaction energy of the adsorbed water molecules (i.e., the bonding strength) is not. As the work of adhesion according to equation (1) is calculated from interaction energies of the different phases, this would imply that (single batch) water vapour uptake and oxygen surface density are not accurate for estimating W_{cw} .

When water is bonding with initially dry activated carbon, heat is released. The quantity of heat released depends on the bonding strength (higher bonding strength releases more heat) and the total wetted surface. The dependency of heat of immersion on the type of oxygen-containing functional groups has already been shown before: Rodriguez-Reinoso and co-workers, and Barton and co-workers showed that heat of immersion was positively related to the quantity of functional groups that are released as CO during temperature programmed desorption [9, 19]. However, no explanation was provided by these authors as to why specifically CO-releasing functional groups (CO-RFG) have high interaction energy with water. A possible explanation is that the hydrogen bond acceptor position of carbonyl functional groups can be easily accessed by water molecules, while the hydrogen bond acceptor and hydrogen bond donor positions of carboxylic functional groups are not, resulting in suboptimal use of hydrogen bond donor/acceptor positions due to steric hindrance.

A similar positive correlation as observed by Rodriguez-Reinoso et al. and Barton et al. between heat of immersion and CO-RFG was observed in this study (Figure 2). The slope of the correlation found in this study (19.7 mJ/ μmol CO-RFG) approximates the slope found by Rodriguez-Reinoso and co-workers (15 mJ/ μmol CO-RFG) and Barton and co-workers (17.2 mJ/ μmol CO-RFG).

The activated carbons F600 and W35 have a relatively lower heat of immersion in water (i.e. they are relatively “hydrophobic” compared to other carbons) and do not fit the trend exactly. These activated carbons were relatively “hydrophobic” in the water vapour experiments as well, and the same explanation applies for this behaviour. Centaur HSL activated carbon, on the other hand, is relatively hydrophilic in the relation between heat of immersion and CO-releasing functional groups. Centaur HSL is advertised as a catalytically active carbon, however, the exact modifications to achieve this are patented, and it is possible that these enhance water-carbon interaction. Centaur HSL is included in the calculated coefficient of determination in Figure 2, F600 and W35 are excluded.

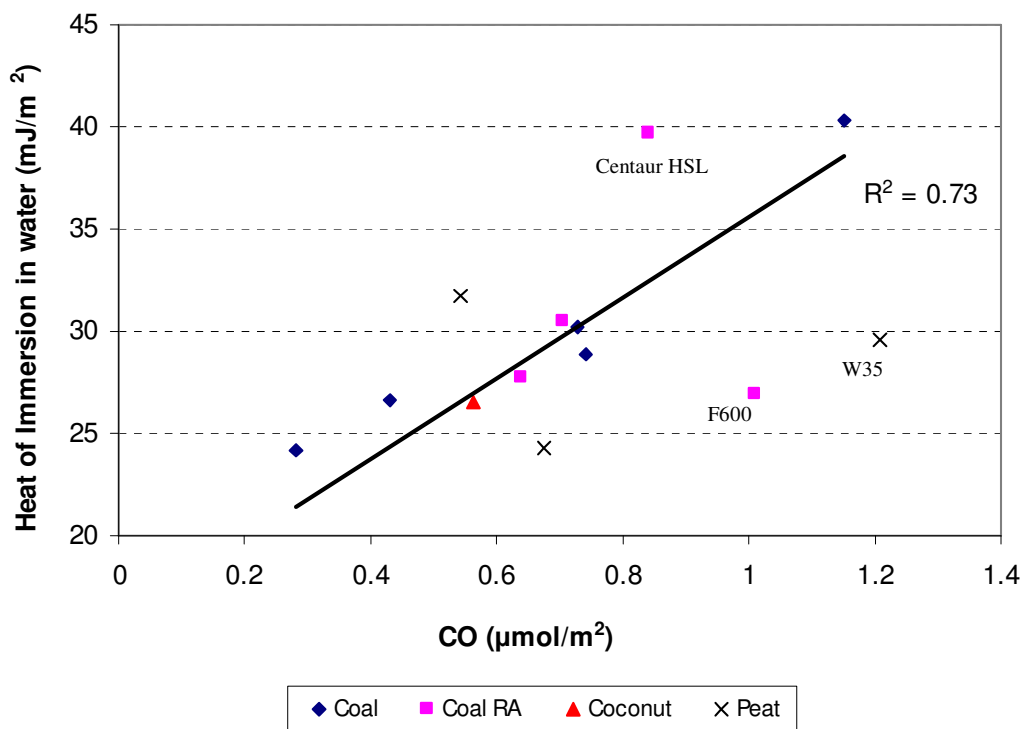


Figure 2: Heat of Immersion in water vs CO-RFG density. F600 and W35 are not included in the correlation, and Centaur HSL is included.

When comparing contact angle measurements with the density of CO-releasing functional groups, a negative linear relationship is found for most carbons (middle part of Figure 3). It was found that the carbons with a CO-RFG density larger than $1.0 \mu\text{mol}/\text{m}^2$ yielded higher contact angles than expected (i.e. are relatively hydrophobic). However activated carbons with a CO-RFG density $< 0.5 \mu\text{mol}/\text{m}^2$ yielded lower contact angles than expected (i.e., are relatively more hydrophilic compared to the other carbons).

This deviates from the findings of immersion calorimetry, and can possibly be explained by the nature of the characterisation method; contact angles are measured by the capillary rise of water through a packed bed of pulverised activated carbon, which is expected to mainly depend on the characteristics of the external activated carbon surface, rather than the total pore surface as is the case for immersion calorimetry.

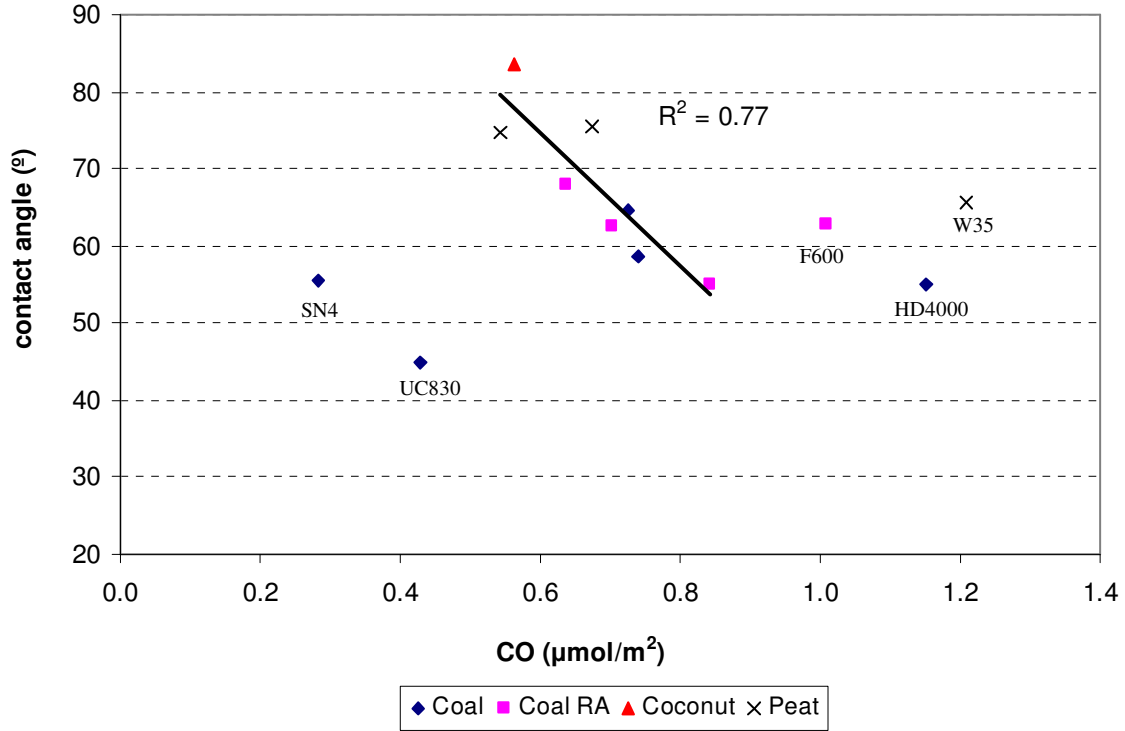


Figure 3: Contact angle vs CO-RFG density. SN4, UC830, F600, W35, HD4000 are not included in the correlation.

3.2 Influence of hydrophobicity on 1-hexanol and 1,3-dichloropropene adsorption

According to equation (1), activated carbon hydrophobicity (or W_{cw}) is only one of the interactions that determine the work of adhesion in a solute-carbon-water system. As such, it should not be directly related to solute adsorption, as such an approach would neglect solute-carbon and solute-water interactions. Indeed, in this study, no correlation was found between equilibrium loading of 1-hexanol or 1,3-DCP and contact angle, heat of immersion of carbon in water, water vapour uptake or carbon oxygen content.

In this study, it was hypothesized that the measured heat of immersion of the carbon in water could be used to define W_{cw} . Similarly, the measured heat of immersion of the carbon in 1-hexanol and 1,3-DCP was used to define W_{sc} . In doing so, only the influence of enthalpy is included in W_{sc} and the calculated work of adhesion W_{scw} . It is assumed that the influence of entropy per unit of contact surface area is similar for both solutes and for the different carbons. As the entropy is unknown, W_{scw} can only be used in a relative way.

The solute-water interfacial tension of 1,3-DCP was calculated using equation (4), which applies only for van der Waals interaction [3, 20]:

$$\gamma_{ij} = \gamma_i + \gamma_j - 2\sqrt{\gamma_i\gamma_j} \quad [4]$$

Where γ is the interfacial tension, and the subscripts i and j denote the water and 1,3-DCP phase. The work of adhesion in a binary system can be calculated by:

$$W_{ij} = \gamma_i + \gamma_j - \gamma_{ij} \quad [5]$$

Values for the 1-hexanol-water interfacial tension and (binary) work of 1-hexanol/water adhesion (W_{sw}) were obtained from Freitas and co-workers [21]. The values of the interfacial tension and binary work of adhesion of 1-hexanol, 1,3-DCP and water can be found in the supporting information (S4).

The adsorption isotherms of 1-hexanol and 1,3-DCP are included in the supporting information (S5, S6), and the activated carbon loading at the same equilibrium concentration was determined. The carbon loading at an equilibrium concentration of 0.3 mmol/L is selected as a basis of comparison, as it is included within the measured range for both 1-hexanol and 1,3-DCP. When this equilibrium concentration did not fall within the measured range for a specific carbon type, the linearized Freundlich isotherm was extrapolated to an equilibrium concentration of 0.3 mmol/L. For all activated carbons, the values for carbon loading for both solutes at this equilibrium concentration, and the enthalpy of immersion in water, 1-hexanol and 1,3-DCP, are included in the supporting information (S7).

The set of activated carbons was extended with two wood-based carbons; CN1 and CG1. These activated carbons were activated by phosphoric acid, while the other carbons in this paper were activated by steam. These were added as “highly hydrophilic” extremes. Previous authors found that a commercial acid-activated wood-based activated carbon had an oxygen content that was 3-5 times higher than other commercial activated carbons used [6], and we found a significantly higher interaction with water than the other carbons, with an enthalpy of immersion of 43.39 for CN1 and 41.77 mJ/m² for CG1.

When comparing the enthalpy of immersion of activated carbon in 1-hexanol or 1,3-DCP (W_{sc}) with the carbon loading of these solutes at an equilibrium concentration 0.3 mmol/L in Figure 4, it is observed that 1-hexanol has a stronger interaction energy with, and thus affinity for, the activated carbon surface than 1,3-DCP. This is in line with our previous findings [12]: aliphatic and aromatic solutes with hydrogen bond donor/acceptor groups showed higher adsorption than solutes of similar hydrophobicity (similar octanol-water partitioning coefficient) but without these groups. Both solutes are capable of van der Waals interaction with the activated carbon surface, but only solutes with hydrogen bond donor/acceptor groups can additionally form hydrogen bonds, which are typically stronger than van der Waals bonds. This results in higher adhesion energy and consequently higher adsorption than for solutes without hydrogen bond donor/acceptor groups but with a similar octanol-water partitioning coefficient.

There is no correlation between W_{sc} for 1,3-DCP, while a better correlation is found for 1-hexanol ($R^2=0.58$). This indicates that the stronger, specific interaction between 1-hexanol and activated carbon may contribute significantly to 1-hexanol adsorption in a 3-phase system (hexanol, activated carbon, water). This is not the case for 1,3-DCP.

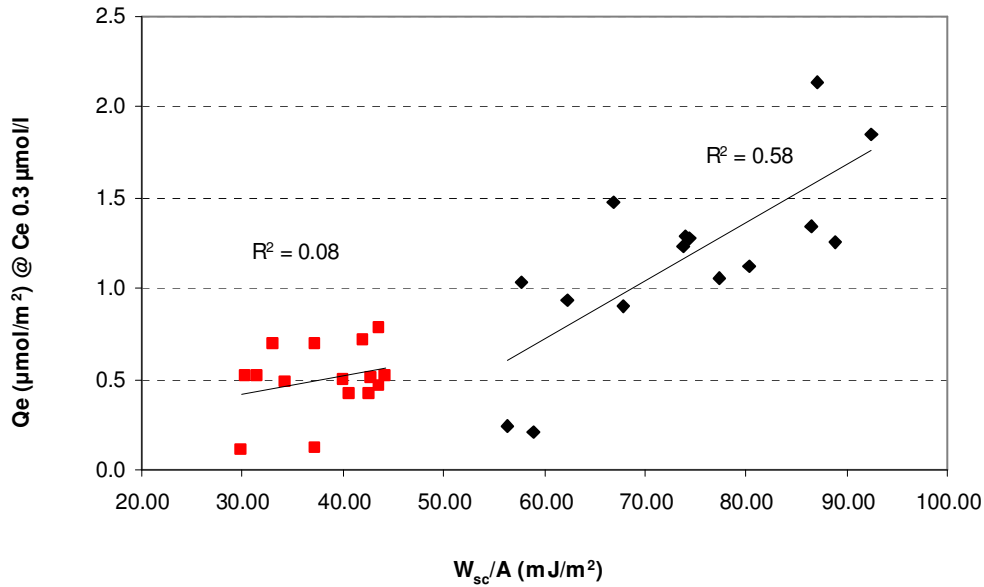


Figure 4: Relationship between activated carbon loading of 1-hexanol (diamonds) and 1,3-dichloropropene (squares), and the binary work of adhesion between activated carbon and solute.

When comparing the enthalpy of immersion of activated carbon in water (W_{cw}) with the carbon loading of 1-hexanol and 1,3-DCP in Figure 5, a weak negative correlation is found for both solutes ($R^2=0.40$ and 0.42 , respectively). While a negative correlation is indeed expected [5, 6], W_{cw} alone is insufficient to explain 1-hexanol and 1,3-DCP adsorption in a 3-phase system.

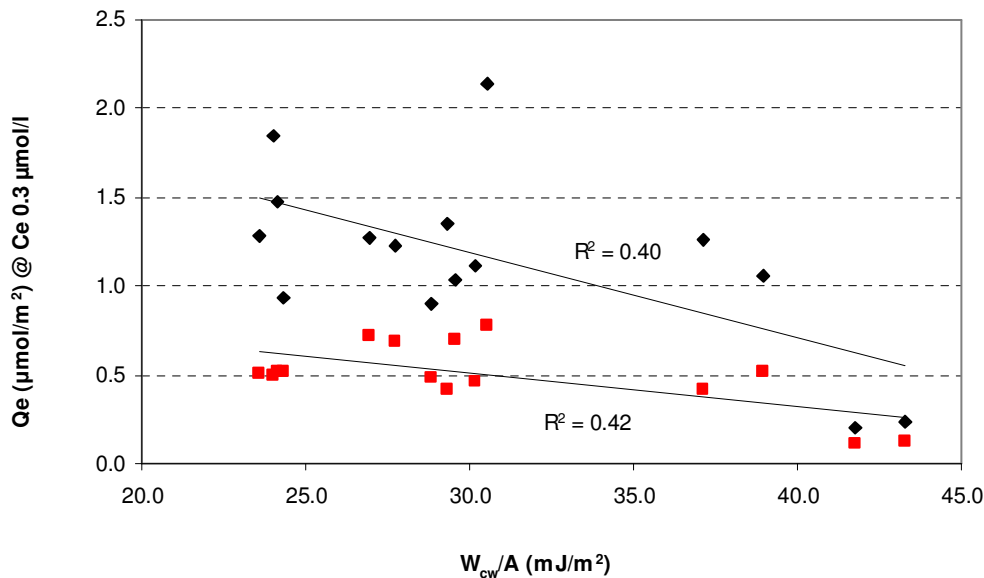


Figure 5: Relationship between activated carbon loading of 1-hexanol (diamonds) and 1,3-dichloropropene (squares), and the binary work of adhesion between activated carbon and water.

In Figure 6, the work of adhesion in a 3-phase system, as calculated with equation (1), is compared to the carbon loadings of 1-hexanol and 1,3-DCP. It is found that the activated carbon loading increases with increasing work of adhesion. The results of 1-hexanol and

1,3-DCP overlap, indicating that both van der Waals interactions and hydrogen bond interactions are measured and accounted for by the calculated work of adhesion. When extrapolating 1-hexanol and 1,3-DCP carbon loadings to equilibrium concentrations of 0.2 mmol/L and 0.4 mmol/L, similar linear relationships are found as in Figure 6, with a coefficient of determination of 0.83 and 0.78, respectively (supporting information; S8 and S9). Extrapolation of 1,3-DCP carbon loading onto ROW 0.8 supra and AC1230C to these equilibrium concentrations was inaccurate, as the Freundlich 1/n of their linearized isotherm was 1.6 and 2.0, respectively. These activated carbons are highlighted in the supporting information, but included in the correlation. CN1 and CG1 activated carbon reached a plateau value for 1,3-DCP carbon loading. This plateau value is used for all equilibrium concentrations.

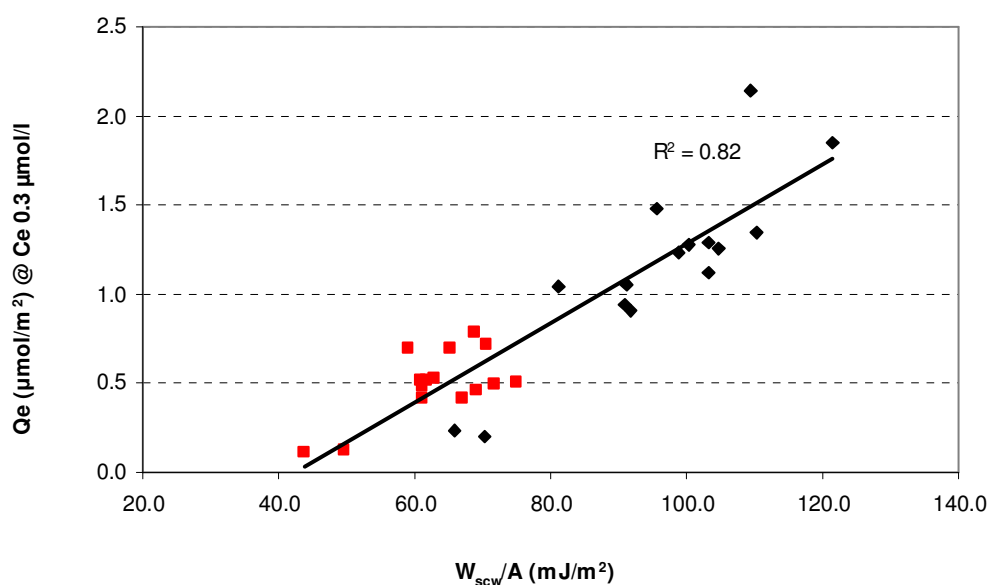


Figure 6: Relationship between activated carbon loading of 1-hexanol (diamonds) and 1,3-dichloropropene (squares), and the 3-phase work of adhesion.

4. Conclusions

- While the amount of water (as determined from water vapour uptake) adsorbed on activated carbon is independent of the type of oxygen-containing functional groups, the interaction energy of the adsorbed water molecules (as determined from immersion calorimetry and contact angle measurements) is not.
- Immersion calorimetry can be used to determine carbon-water and carbon-solute interactions, provided that the solutes are liquids.
- Carbon-water, Carbon-solute and solute-water interactions alone are insufficient to explain solute adsorption. The work of adhesion, which includes all these interactions, can explain the adsorption of 1-hexanol and 1,3-dichloropropene well ($R^2=0.78-0.84$).
- While 1-hexanol and 1,3-dichloropropene have a similar size and hydrophobicity (based on octanol-water partitioning coefficient), 1-hexanol removal is higher. This can be explained by the stronger interaction between 1-hexanol and activated carbon due to hydrogen bond formation.

Acknowledgements

The authors wish to express their gratitude to Ellen Meijvogel (Delft University of Technology) for her support with the contact angle measurements. This research was partially financed by VEWIN, the association of drinking water companies in the Netherlands, and by FCT and FEDER under Program COMPETE, project FCOMP-01-0124-FEDER-022706 (Ref. FCT Pest-C/EQB/LA0020/2011).

References

- [1] Pendleton P, Wong SH, Schumann R, Levay G, Denoyel R, Rouquerol J. Properties of activated carbon controlling 2-methylisoborneol adsorption. *Carbon*. 1997;35:1141-9.
- [2] Quinlivan PA, Li L, Knappe DRU. Effects of activated carbon characteristics on the simultaneous adsorption of aqueous organic micropollutants and natural organic matter. *Water Res*. 2005;39:1663-73.
- [3] Israelachvili JN, editor. *Intermolecular and surface forces*. 2nd ed: Academic Press; 1992.
- [4] Li L, Quinlivan PA, Knappe DRU. Predicting adsorption isotherms for aqueous organic micropollutants from activated carbon and pollutant properties. *Env. Sci. Technol*. 2005;39:3393-400.
- [5] Pendleton P, Wu SH, Badalyan A. Activated carbon oxygen content influence on water and surfactant adsorption. *J. Colloid Interf. Sci*. 2002;246:235-40.
- [6] Li L, P.A. Quinlivan, D.R.U. Knappe. Effects of activated carbon surface chemistry and pore structure on the adsorption of organic contaminants from aqueous solution. *Carbon*. 2002;40:2085.
- [7] Stoeckli F, Moreno-Castilla C, Carrasco-Marin F, Lopez-Ramon MV. Distribution of surface oxygen complexes on activated carbons from immersion calorimetry, titration and temperature-programmed desorption techniques. *Carbon*. 2001;39:2231-7.
- [8] Lopez-Ramon MV, Stoeckli F, Moreno-Castilla C, Carrasco-Marin F. Specific and non-specific interactions of water molecules with carbon surfaces from immersion calorimetry. *Carbon*. 2000;38:825-9.
- [9] Rodriguez-Reinoso F, Molina-Sabio M, Gonzalez MT. Effect of oxygen surface groups on the immersion enthalpy of activated carbons in liquids of different polarity. *Langmuir*. 1997;13:2354-8.
- [10] Olson DH, Haag WO, Borghard WS. Use of water as a probe of zeolitic properties: interaction of water with HSZM-5. *Micropor. Mesopor. Mat*. 2000;35-36:435-46.
- [11] Galet L, Patry S, Dodds J. Determination of the wettability of powders by the Washburn capillary rise method with bed preparation by a centrifugal packing technique. *J. Colloid Interf. Sci*. 2010;346(2):470-5.
- [12] de Ridder DJ, Villacorte L, Verliefde ARD, Verberk JQJC, Heijman SGJ, Amy GL, et al. Modeling equilibrium adsorption of organic micropollutants onto activated carbon. *Water Res*. 2010;44:3077-86.
- [13] Michel J-C, Riviere L-M, Bellon-Fontaine M-N. Measurement of the wettability of organic materials in relation to water content by the capillary rise method. *Eur. J. Soil Sci*. 2001;52:459-67.
- [14] Figueiredo JL, Pereira MFR, Freitas MMA, Orfao JJM. Modification of the surface chemistry of activated carbons. *Carbon*. 1999;37:1379-89.
- [15] Figueiredo JL, Pereira MFR, Freitas MMA, Orfao JJM. Characterisation of active sites on carbon catalysts. *Ind. Eng. Chem. Res*. 2007;46:4110-5.
- [16] Jorge M, Schumacher C, Seaton NA. Simulation study of the effect of the chemical heterogeneity of activated carbon on water adsorption. *Langmuir*. 2002;18:9296-306.

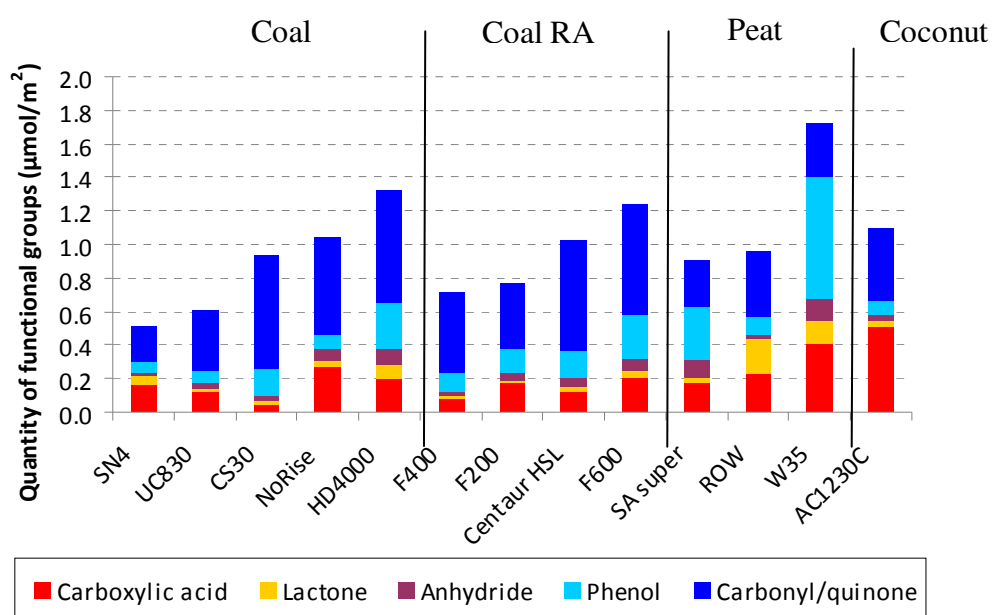
- [17] Brennan JK, Thomson KT, Gubbins KE. Adsorption of water in activated carbons: effects of pore blocking and connectivity. *Langmuir*. 2002;18:5438-47.
- [18] Kato Y, Machida M, Tatsumoto H. Inhibition of nitrobenzene adsorption by water cluster formation at acidic oxygen functional groups on activated carbon. *J. Colloid Interf. Sci.* 2008;322(2):394-8.
- [19] Barton SS, Evans MJB, Harrison BH. Surface studies on carbon: Water adsorption on Polyvinylidene Chloride carbon. *J. Colloid Interf. Sci.* 1972;45(3).
- [20] van Oss CJ. *Interfacial forces in aqueous media*. 2nd ed.: CRC Press; 2006.
- [21] Freitas AA, Quina FH, Carroll FA. Estimation of water-organic interfacial tensions. A linear free energy relationship analysis of interfacial adhesion. *J. Phys. Chem. B.* 1997;101:7488-93.

Supporting information

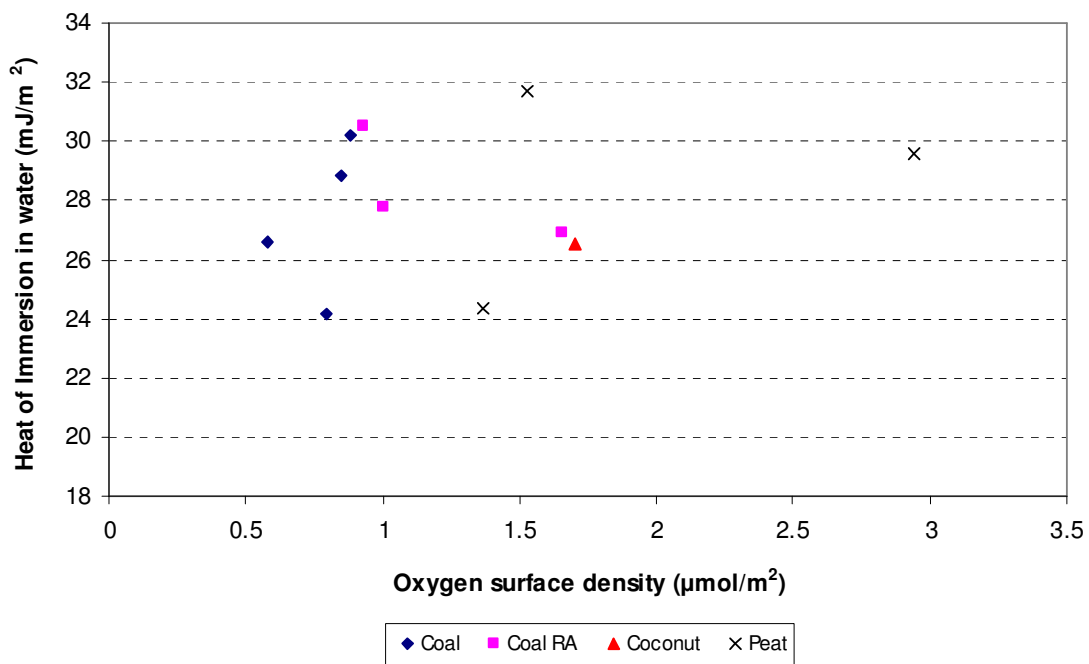
Chapter 3

A thermodynamic approach to assess organic solute adsorption onto activated carbon in water

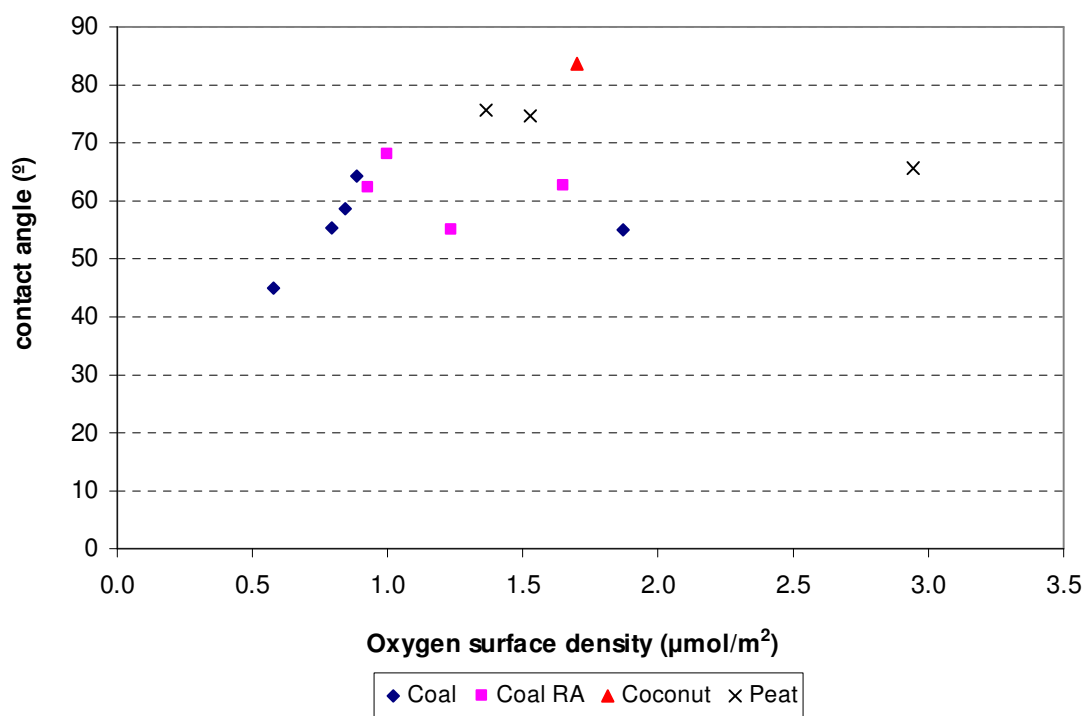
David J. de Riddera *, Arne R.D. Verliefde^{a,b}, Bas G.J. Heijmana, Simon Gelinc, Manuel F.R. Pereirad, Raquel P. Rochad, José L. Figueiredod, Gary L. Amya^e, Hans C. van Dijk



S1: Functional group quantities, as determined by TPD



S2: Activated carbon oxygen surface density vs H_{ol} in water

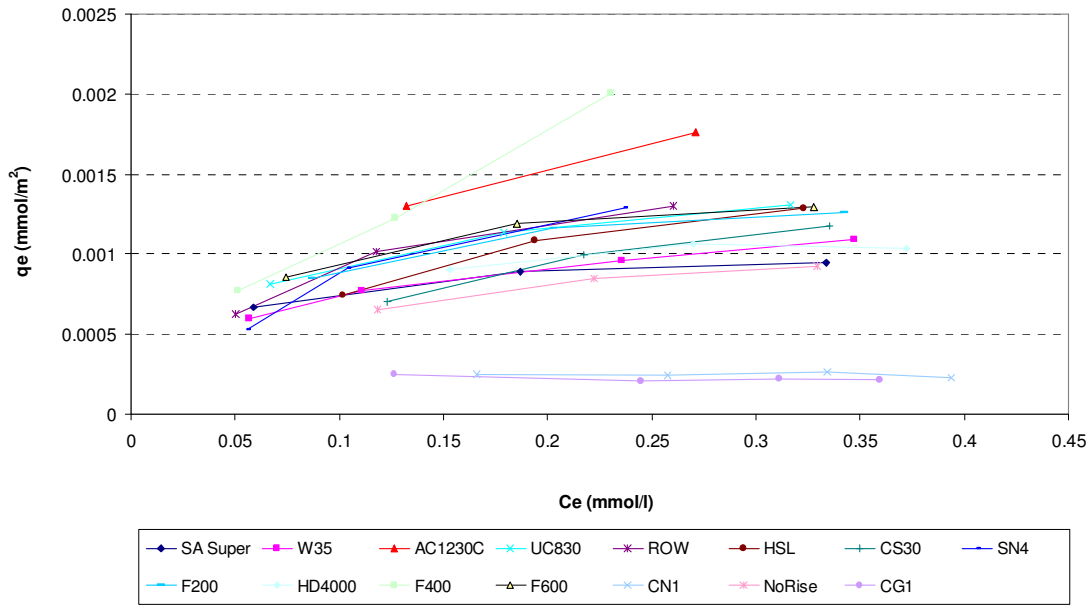


S3: Activated carbon oxygen surface density vs water contact angle

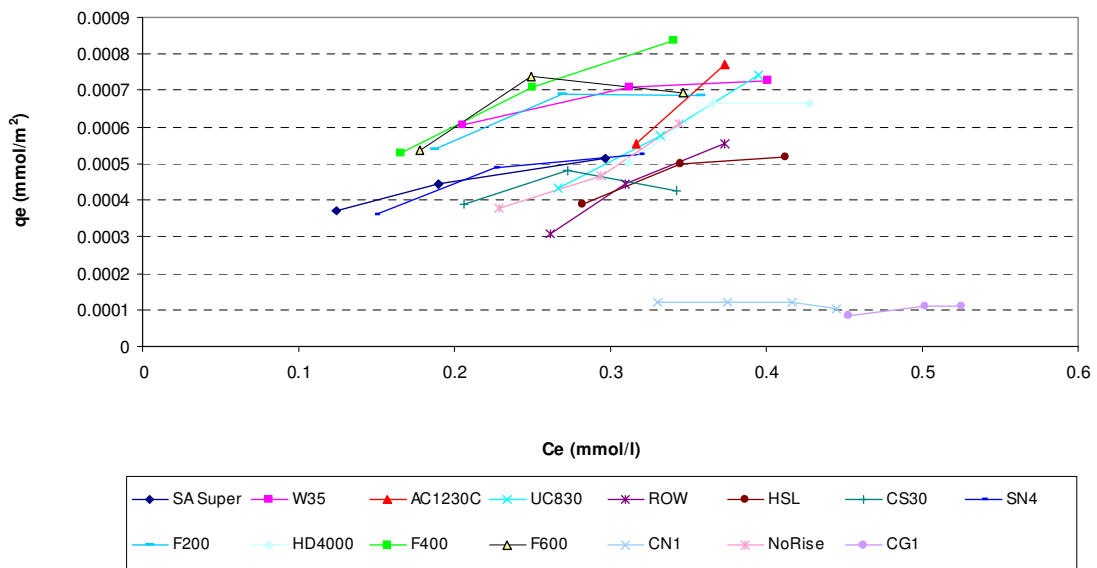
S4: Interfacial tensions and binary work of adhesion for 1,3-dichloropropene, 1-hexanol and water

	1,3-DCP	1-hexanol	Water
γ_i (mJ/m ²)	27.1		71.99
γ_{ij} with water (mJ/m ²)	10.7	6.7 1)	
W_{sw} (mJ/m ²)	88.3	91.8 1)	144

1) Obtained from Freitas et al. 21



S5: Hexanol equilibrium adsorption isotherms, measured at room temperature

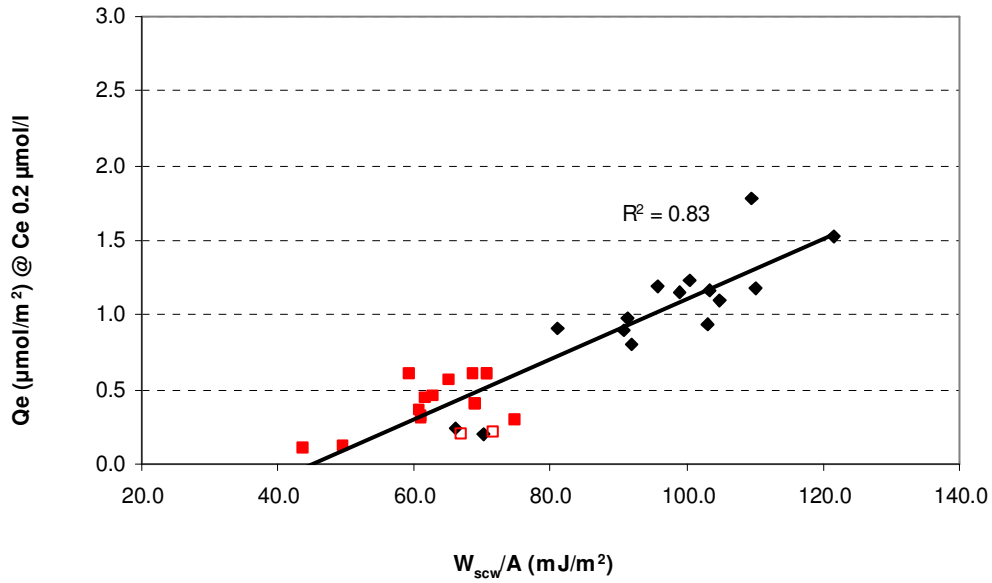


S6: 1,3-Dichloropropene equilibrium adsorption isotherms, measured at room temperature

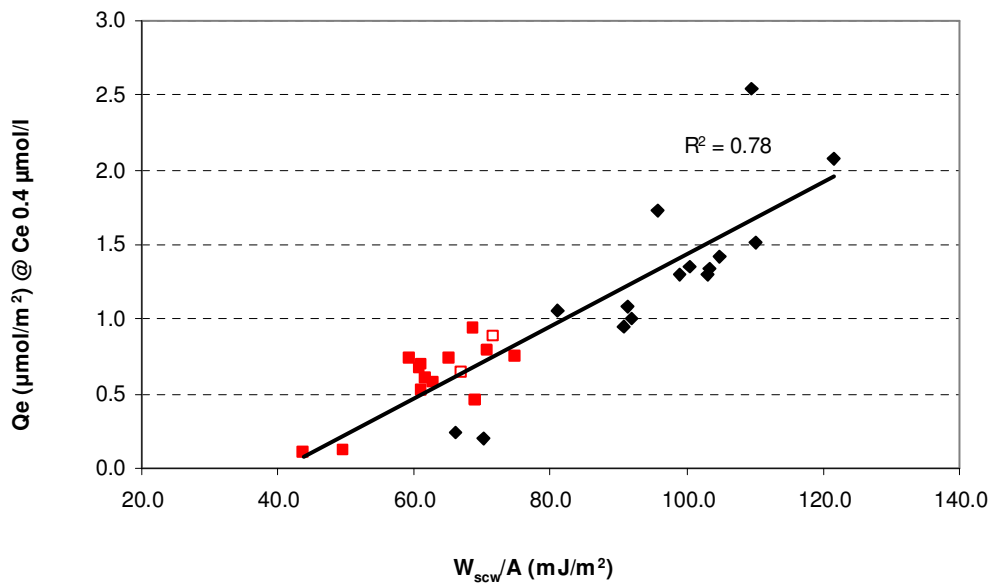
S7: Results calorimetric experiments and adsorption isotherms hexanol and 1,3-DCP. Error in ΔH_{imm} ± 2.0 mJ/m²

Carbon	ΔH_{imm} in water (mJ/m ²)	ΔH_{imm} in hexanol (mJ/m ²)	ΔH_{imm} in 1,3- DCP (mJ/m ²)	Hexanol qe ($\mu\text{mol}/\text{m}^2$) @ Ce 0.3 mmol/L	1,3-DCP qe ($\mu\text{mol}/\text{m}^2$) @ Ce 0.3 mmol/L
SN4	24.15	66.86	30.23	1.50*	0.52
UC830	26.60	73.90	42.92	1.28	0.51
CS30	30.19	80.33	43.63	1.12	0.46
NoRise	28.85	67.75	34.29	0.90	0.49
HD4000	40.30	77.30	44.18	1.05	0.51*
F400	30.52	87.00	43.59	2.18*	0.78
F200	27.76	73.72	37.35	1.22	0.69
Centaur HSL	39.70	88.90	42.67	1.25	0.42
F600	26.92	74.40	41.96	1.27	0.72
SA Super	24.33	62.20	31.49	0.93	0.52*
W35	29.59	57.74	33.18	1.04	0.70
ROW 0.8	31.70	86.50	40.71	1.38*	0.42
supra					
AC1230C	26.50	92.50	40.06	1.83*	0.50*
CN1	43.29	56.30	37.28	0.24	0.12*
CG1	41.77	59.00	29.94	0.20	0.11*

*extrapolated to Ce=0.3 mmol/L



S8: Relationship between work of adhesion per unit area and activated carbon loading of hexanol (diamonds) and 1,3-dichloropropene (squares) at $C_e = 0.2 \text{ mmol}/\text{L}$. Open squares: ROW and AC1230C activated carbon.



S9: Relationship between work of adhesion per unit area and activated carbon loading of hexanol (diamonds) and 1,3-dichloropropene (squares) at $C_e = 0.4 \text{ mmol}/\text{L}$. Open squares: ROW and AC1230C activated carbon.

Chapter 4

Relation between interfacial energy and adsorption of organic micropollutants onto activated carbon

D.J. de Ridder a, *, A.R.D. Verliefde a,b, K. Schoutteten b, S.G.J. Heijman a, I. Beurroies c, R. Denoyel c, G.L. Amy a,d, J.C. van Dijk a

a Delft University of Technology, P.O. Box 5048, 2600 GA Delft, The Netherlands

b Ghent University, Coupure Links 653, B-9000 Gent, Belgium

c Université de Provence, Madirel, UMR CNRS, Centre de St. Jérôme, F-13397 Marseille Cedex 20, France

d King Abdullah University of Science and Technology, Thuwal, Saudi Arabia

accepted in Carbon

Abstract

The adsorption efficacy of sixteen pharmaceuticals on six different activated carbons is correlated to the thermodynamic work of adhesion, which was derived following the surface tension component approach. Immersion calorimetry was used to determine the surface tension components of activated carbon, while contact angle measurements on compressed plates were used to determine these for solutes. We found that the acid-base surface tension components of activated carbon correlated to the activated carbon oxygen content. Solute-water interaction correlated well to their solubility, although four solutes deviated from the trend. In the interaction between solute and activated carbon, van der Waals interactions were dominant and explained 65-94% of the total interaction energy, depending on the hydrophobicity of the activated carbon and solute. A reasonable relationship ($r^2 > 0.70$) was found between the calculated work of adhesion and the experimentally determined activated carbon loading.

1. Introduction

The efficacy of activated carbon to remove solutes from water is often attributed to the hydrophobicity of the solutes and the activated carbon. Hydrophobicity of solutes is often expressed as the octanol-water partitioning coefficient ($\log K_{ow}$). The hydrophobicity of the activated carbon surface, when expressed as carbon oxygen content, has shown to have a profound impact on adsorption as well [1-3]. According to thermodynamics, however, adsorption onto activated carbon is broader than hydrophobic interactions. In fact, adsorption energy depends on solute-water interactions, carbon-water interactions, solute-carbon interactions and water cohesion [4]:

$$W_{scw} = W_{sc} + W_{ww} - W_{sw} - W_{cw} \quad (1)$$

Here, W_{ij} (mJ/m^2) is the work required per unit area to separate two phases i and j and subscripts c , s , and w refer to activated carbon, solute and water, respectively. W_{scw} is the work of adhesion of the solute to activated carbon in water, i.e., an absolute measure of the adsorption energy of the solute onto the activated carbon in a water phase. Activated carbon hydrophobicity is included in W_{cw} , solute hydrophobicity in W_{sw} , and solute-carbon interfacial interaction in W_{sc} .

Van Oss, Chaudhury and Good [5] refined this basic thermodynamic equation (Equation (1)) by introducing surface tension components. In their theory, it was postulated that any interaction between different species depends on apolar (Lifshitz-van der Waals) interactions and acid-base interactions (amongst which hydrogen bond interactions), which can be

described as a mathematical equation between the surface tensions of the different species. As such, the surface tension of water, solutes and solids was divided into an apolar (γ^{LW}), electron-acceptor (γ^+) and electron-donor (γ^-) component. The work of adhesion between two phases could then be calculated as [6, 7]:

$$W_{SL} = -\Delta G_{SL} = 2 \left[\sqrt{\gamma_S^{LW} \gamma_L^{LW}} + \sqrt{\gamma_S^+ \gamma_L^-} + \sqrt{\gamma_S^- \gamma_L^+} \right] \quad (2)$$

Where subscript S represents a solid, and subscript L represents a liquid. The surface tension components of the solid (i.e. activated carbon or a solute) can be determined by measuring ΔG_{SL} between the solid and at least three liquids with known surface tension components. ΔG_{SL} is related to the contact angle found between the two phases [7]:

$$-\Delta G_{SL} = \gamma_L (1 + \cos \theta) \quad (3)$$

Alternatively, ΔG_{SL} can be determined with immersion calorimetry [8, 9].

$$-\Delta G_{SL} = -\frac{1}{k} \Delta H_{imm} + \gamma_L \quad (4)$$

Where

$$k = 1 - \frac{T \Delta S_{imm}}{\Delta H_{imm}} \quad (5)$$

For the interaction between various minerals (quartz, talc, chlorite, kaolinite) and liquids (heptane, benzene, water), Médout-Marère and co-workers [9] found that $1/k$ varied inbetween 0.4-0.53 at ambient temperature (27 °C). In their work, ΔG_{SL} was calculated from vapor adsorption isotherms, and ΔH_{imm} was obtained from immersion calorimetry.

For various (modified) activated carbons, $1/k$ varied inbetween 0.36-0.59 for benzene and methylethylketone, with for both an average value of 0.45 [10]. Médout-Marère and co-workers postulate that a value for $1/k$ of 0.4 is a reasonable assumption when calculating ΔG_{SL} from the enthalpy of immersion, while Douillard and coworkers assume a value of 0.5. In our work, we use a value for $1/k$ of 0.45, as this value is based on experiments where activated carbon is used rather than minerals. This is a first approximation of the contribution ratio of enthalpy and entropy, and in future work, it is recommended to confirm this experimentally.

When rewriting Equation (1) using Equation (2) for solute-water, solute-carbon, carbon-water and water-water interactions, the 3-phase work of adhesion, or free energy can be expressed in surface tension components [6, 11].

$$W_{SCW} = -\Delta G_{SCW} = -2 \left[\begin{aligned} &\sqrt{\gamma_C^{LW} \gamma_W^{LW}} + \sqrt{\gamma_S^{LW} \gamma_W^{LW}} - \sqrt{\gamma_C^{LW} \gamma_S^{LW}} - \gamma_W^{LW} + \sqrt{\gamma_W^+} \left(\sqrt{\gamma_C^-} + \sqrt{\gamma_S^-} - \sqrt{\gamma_W^-} \right) \\ &+ \sqrt{\gamma_W^-} \left(\sqrt{\gamma_C^+} + \sqrt{\gamma_S^+} - \sqrt{\gamma_W^+} \right) - \sqrt{\gamma_C^+ \gamma_S^-} - \sqrt{\gamma_C^- \gamma_S^+} \end{aligned} \right] \quad (6)$$

With subscript C representing activated carbon, W representing water and S representing the solute. Equation (6) has been used by various authors to explain physical-chemical processes, such as protein adsorption onto polymers [6], adhesion of biofilms to carrier materials [12-14], explaining interaction between organic micropollutants and polymeric membranes [15], separation of minerals by flotation and selective flocculation [7], and proposed to be useful for oil recovery [8, 9]. No literature was found where adsorption of organic micropollutants onto activated carbon was explained using this approach. In our previous work, we used immersion calorimetry to directly determine W_{sc} and W_{cw} of Equation (1), while obtaining W_{ww} and W_{sw} from literature and explained adsorption of hexanol and 1,3-dichloropropene on

a wide range of activated carbons [16]. The resulting W_{scw} could be related to the activated carbon loading of the two solutes onto the different activated carbons, indicating that this thermodynamic approach can explain adsorption.

A major limitation of this method is that determination of W_{sc} with immersion calorimetry requires the use of liquid solutes, while most organic micropollutants which are relevant for water treatment are solid at room temperature. Furthermore, W_{sc} has to be determined experimentally for each activated carbon/solute combination. In this work, we investigate if an approach with surface tension components (Equation (6)) is fruitful to explain adsorption of organic micropollutants onto activated carbon. Here, W_{sc} can be (indirectly) calculated from surface tension components, which are determined using independent methods for activated carbon (immersion calorimetry) and (solid) solutes (contact angle measurements). When the surface tension components of individual solutes are known, W_{sc} can be calculated for all activated carbons for which the surface tension components were determined previously. The influence of solute charge is investigated explicitly, as it is not included in the surface tension components approach.

2. Materials and methods

2.1 Activated carbons

Six commercial activated carbon types were used: HD4000, ROW 0.8 Supra, CN1 were obtained from Norit Nederland BV (Amersfoort, The Netherlands), AC1230C, UC830 were obtained from Siemens Water Technologies (Warrendale, USA), and Centaur HSL was obtained from Chemviron Carbon (Feluy, Belgium).

The pore size distributions (as calculated by the Non-local Density Functional Theory) and specific surface areas (as calculated with the theory of Brunauer, Emmett and Teller (BET)) were determined by N_2 adsorption at $-196\text{ }^\circ\text{C}$. The adsorption and desorption measurements were executed on a Micromeritics ASAP 2010 gas adsorption analyzer equipped with additional 1 mmHg and 10 mmHg pressure transducers in order to achieve high resolution in the low pressure range ($p/p_0=0.01$). This allows for a more accurate analysis of the micropores as compared to conventional N_2 adsorption measurements (with typically $p/p_0=0.05$ as lowest relative pressure). Prior to the adsorption measurement, the samples were in-situ degassed at $300\text{ }^\circ\text{C}$ during 16 hours. The free space volume of the sample cell was determined in a separate measurement, in order to avoid helium entrapment which adversely affects adsorption in the low pressure range. These experiments were executed by Delft Solids Solutions BV (Delft, The Netherlands).

The pH-point of zero charge measurements were done following the “pH drift” procedure, as described in reference [17]. The oxygen surface density of activated carbon was calculated from the sum of CO and CO_2 released during Temperature Programmed Desorption (TPD). Here, activated carbon is first heated at $80\text{ }^\circ\text{C}$ for three hours. Then, 80 mg of activated carbon is weighed and mixed with 200 mg of SiC to improve heat transfer during TPD. Remaining water vapour is expelled under helium flow at room temperature, typically for 1.5 hours, until no release of H_2O is detected by the mass spectrometer. Subsequently, the temperature is increased with $10\text{ }^\circ\text{C}/\text{min}$ to $1000\text{ }^\circ\text{C}$, and kept at this temperature for 5 minutes. The amount of CO and CO_2 that is released is continuously monitored by the mass spectrometer. $CaCO_3$ and $CaC_2O_4 \cdot H_2O$ are used as standards to calibrate the CO, CO_2 and H_2O output signals.

For measuring the enthalpy of immersion a method similar as described in [18] was used; prior to analysis, the activated carbons (about 0.1-0.2 g) were placed in a glass ampoule and outgassed under $1 \cdot 10^{-2}$ mbar and at a temperature of $105\text{ }^\circ\text{C}$, during 12 hours. Thereafter, the ampoule was sealed and placed in a calorimetric cell containing 7 ml of water, cyclohexane or

ethylene glycol, respectively. After equilibrium was reached, the ampoule was broken and the heat upon immersion of the carbon into the liquid was recorded. A blank experiment with an empty ampoule was carried out, to account for the contribution of breaking the ampoule and vaporization of the liquid to the enthalpy.

2.2 Chemicals and pharmaceuticals

All liquids and pharmaceuticals were obtained from Sigma-Aldrich Chemie BV (Zwijndrecht, The Netherlands). The liquids had a purity >99%, and the water used was demineralized tap water, after treatment with ion exchange and reverse osmosis. The total organic carbon concentration of this water was <0.2 mg/l.

Contact angle measurements of the respective liquids (see Table 1) on the pharmaceuticals were obtained by the sessile drop technique onto a plate of pharmaceutical. The pharmaceuticals were pressed into a plate with a hydraulic press (Carver manual laboratory press, model B) at a pressure of 1347 bar for 30 minutes. Sessile drop contact angle measurements were carried out with water, glycerol and diiodomethane using a goniometer (Krüss, model DSA10-MK2. Analysis software: Drop Shape Analysis v1.80.0.2). For each of the liquids, a new pharmaceutical plate was used, and contact angles were measured at least in triplicate to minimize errors. The properties of the liquids used are shown in Table 1, while the properties of the pharmaceuticals are shown in Table 2.

Table 1: Properties liquids used for contact angle measurements and immersion calorimetry. Source: references [6, 19]

Liquid	Stokes diameter (Å)	MW (g/mol)	γ (mJ/m ²)	γ^{LW} (mJ/m ²)	γ^{AB} (mJ/m ²)	γ^+ (mJ/m ²)	γ^- (mJ/m ²)
Water	1.5	18	72.8	21.8	51	25.5	25.5
Cyclohexane	3.01	84.16	25.24	25.24	0	0	0
Ethylene glycol	2.44	62.07	48	29	19	1.9	47
Glycerol	2.82	92.09	64	34	30	3.92	57.4
Diiodomethane	2.78	267.83	50.8	50.8	0	0	0

Table 2: Pharmaceutical properties. Sources: Chemspider (www.chemspider.com)(pKa), ChemID (www.chem.sis.nlm.nih.gov/chemidplus) (MW, solubility), Hyperchem release 7.5 (Molecular surface), ADME (ACD labs)(log D), Drugbank (www.drugbank.ca)(solubility)

Name	pKa (charge)	MW (g/mol)	Molecular surface (Å ²)	Log D (pH 6)	Solubility at 25°C (mg/l)
Atenolol	9.43 (+)	266	527	-2.25	13,300
	9.49 (+)	257	572	-0.87	16,900
Metoprolol					(drugbank)
Lidocaine	8.0 (+)	234	436	1.13	4,100
Lincomycin hydrochloride	7.7 (+)	407	578	-2.20	2,930 (drugbank, predicted)
Trimethoprim	7.12 (+)	290	519	0.47	400
Hydrochlorothiazid	7.9 (+)	298	374	-0.73	722
e					
Theophylline	8.8 (0)	180	339	-1.57	7,360
Paracetamol	9.38 (0)	151	334	0.90	14,000
Cyclophosphamide	n/a (0)	261	422	-0.16	40,000
Carbamazepine	n/a (0)	236	426	2.26	17.7 (drugbank)
Sulfamethoxazole	5.7 (0)	253	435	0.70	610
Gemfibrozil	4.45 (-)	250	515	2.80	27.8 (drugbank, predicted)
Naproxen	4.3 (-)	230	442	1.17	15.9
Ketoprofen	4.45 (-)	254	483	1.53	51.0
Ibuprofen	4.3 (-)	206	434	2.69	21.0
Clofibric acid	4 (-)	214	392	0.45	583 (EST)

2.3 Adsorption isotherms

Batch adsorption experiments were carried out in demineralized water (pH 6), with an initial pharmaceutical concentration of 5 µg/l, and activated carbon doses varying between 0-20 mg/l. Pharmaceuticals were dosed simultaneously as a mixture. No competition was expected in this low concentration range. The samples were stirred during adsorption using a magnetic stirrer. After 72 h of equilibration, the samples were filtrated over a 0.45 µm glassfiber filter, concentrated on Oasis HLB 6cc/200mg SPE cartridges, eluated with methanol and analysed with UPLC/MS/MS (Ultrahigh Performance Liquid chromatography, tandem Mass Spectroscopy).

3. Results and discussion

The results of the activated carbon characterisation are presented in Table 3. UC830 and HD4000 had significantly less equivalent BET surface area than the other carbons, although care should be taken that this surface does not necessarily represent the actually accessible surface for solutes [20]. Pore size distributions are qualitatively similar for the 6 activated carbons, with peak quantities of pores between 0.8-1.5 nm and 2-3 nm (Supporting information; S1-S3). CN1 and HD4000 had a significantly larger amount of pores in the range 3-20 nm than the other activated carbons. The smallest pore size that could be measured in the pore size distribution was 0.55 nm. With the exception of Lincomycine, all pharmaceuticals have a stokes diameter under 0.51 nm [21], indicating that the activated carbon surfaces presented in Table 3 are completely accessible. For Lincomycine, the accessible carbon surface (pores > 0.6 nm) reduces to 777 m²/g (UC830), 333 m²/g (HD4000), 1082 m²/g

(ROW), 1003 m²/g (HSL), 954 m²/g (CN1) and 832 m²/g (AC1230C). Complete adsorption of all 16 solutes corresponds to a monolayer of 0.45 m². In the most critical case (HD4000, at the lowest carbon dose of 1 mg/L), 0.75 m² activated carbon surface is available for 15 of the solutes which is sufficient to adsorb as a monolayer. When at least 0.11 m² of these solutes is adsorbed in the pores < 0.6 nm (which contain a surface of 0.40 m²), also Lincomycine will adsorb as a monolayer. For the higher doses of HD4000 or for the other activated carbons, the available carbon surface area is sufficient for monolayer coverage even if only the pores > 0.6 nm are included.

At pH 6, all activated carbons have a positive surface charge (Supporting information S4). The pH_{pzc} of CN1 is relatively close to the operational pH, resulting in a lower positive surface charge compared to the other activated carbons.

When comparing the enthalpy of immersion of the activated carbons in cyclohexane with their total BET surface, a good correlation is found ($r^2 = 0.84$; S5). This is to be expected, since the adsorption of both cyclohexane and nitrogen both occurs mainly via van der Waals interactions with the activated carbon surface. The correlation is less pronounced for ethylene glycol ($r^2 = 0.60$; S6) and water ($r^2 = 0.27$; S7), both of which also have polar interactions with the activated carbon surface.

Table 3: activated carbon characteristics

Activated carbon	CN1	HD4000	ROW 0.8 Supra	Centaur HSL	AC1230C	UC830
Base material	Wood	Coal	Peat	RA-coal	Coconut	Coal
BET surface (m ² /g)*	1256	729	1499	1339	1265	819
pH _{pzc}	6.8 (0/+)	8.1 (+)	10.4 (+)	8.5 (+)	9.8 (+)	8.8 (+)
Oxygen surface density (μmol/m ²)	3.11	1.14	1.51	0.69	0.81	0.67

Enthalpy of immersion (mJ/m ²)						
Water	85.26	47.58	40.28	37.53	35.29	35.31
Cyclohexane	70.62	78.14	78.34	69.55	84.15	94.80
Ethylene glycol	132.92	114.64	95.48	83.56	103.10	109.93

Surface tension components (mJ/m ²)						
γ _c ^{LW}	32.20	36.14	36.25	31.66	39.45	45.66
γ _c ⁺	7.89	4.97	2.30	1.83	2.86	2.61
γ _c ⁻	8.71	2.37	3.68	5.40	1.64	0.84

3.1 Two-phase interactions: solute-water

In order to assess the accuracy of the surface tension component values we acquired for the solutes, we investigated a simpler (2-phase) system before applying these values in (3-phase) adsorption. The stability of suspensions of solutes in water depends on the free energy of interaction (cohesion) between these solutes when immersed in water, i.e. ΔG_{sws} [21]. A high negative value for ΔG_{sws} represents strong interaction between solutes dissolved in water, which will consequently stay agglomerated and consequently have a low solubility. Solutes which are highly soluble have positive values for ΔG_{sws}, i.e., solutes which are initially

cohesive will repulse each other when dissolved in water. The solubility and ΔG_{sws} are linked as follows [6, 22]:

$$\Delta G_{\text{sws}} S_c = kT \ln s \quad (7)$$

where ΔG_{sws} (J/m^2) is the energy of cohesion for solutes dissolved in water, S_c (m^2) is the contactable surface area between two molecules of solutes, k ($1.38 \cdot 10^{-23} \text{ J/K}$) is the Boltzmann constant, T (298 K) the temperature and s (mol/mol) the solute solubility in water (expressed as mole fraction). Half of the molecular surface, as presented in Table 2, was used for the contact surface, S_c . The value of the surface tension components of the solutes, which were used to calculate ΔG_{sws} , can be found in the supporting information (S8).

The relationship between ΔG_{sws} of the 16 pharmaceuticals, and their solubility, is presented in Figure 1. For positive values of ΔG_{sws} , a plateau value for solute solubility has been reached, and there is no correlation between ΔG_{sws} and solubility. Van Oss and Giese (2004) indeed postulate that Equation (7) is only valid for $\Delta G_{\text{sws}} < 0$ [22]. For negative values of ΔG_{sws} , a linear relationship is observed between $\ln s$ and $\Delta G_{\text{sws}} * S_c / kT$, as expected based on Equation (7). However, $\ln s$ and $\Delta G_{\text{sws}} * S_c / kT$ are not exactly the same, which they should be based on this equation. This discrepancy can be related to the assumption that the contactable surface area is half of the total molecular surface area. Based on figure 1, the contactable surface area between two molecules of solutes should be lower than 50% of the total molecular surface, and be around 35%. Carbamazepine, Ibuprofen, Naproxen and Ketoprofen are an exception to this linear relationship. Their value of $\Delta G_{\text{sws}} * S_c / kT$ is far too low considering their solubility, and cannot be explained by an error in the contactable surface area alone, as that would imply that an unrealistic >150 % of the total molecular surface area is contactable surface area between two molecules of solutes. Possibly, errors in the measured contact angles for these four pharmaceuticals may have resulted in values for surface tension components and ΔG_{sws} which are not representative, although there is no indication why the contact angle measurements should be erroneous for exactly these four pharmaceuticals, and not for the others.

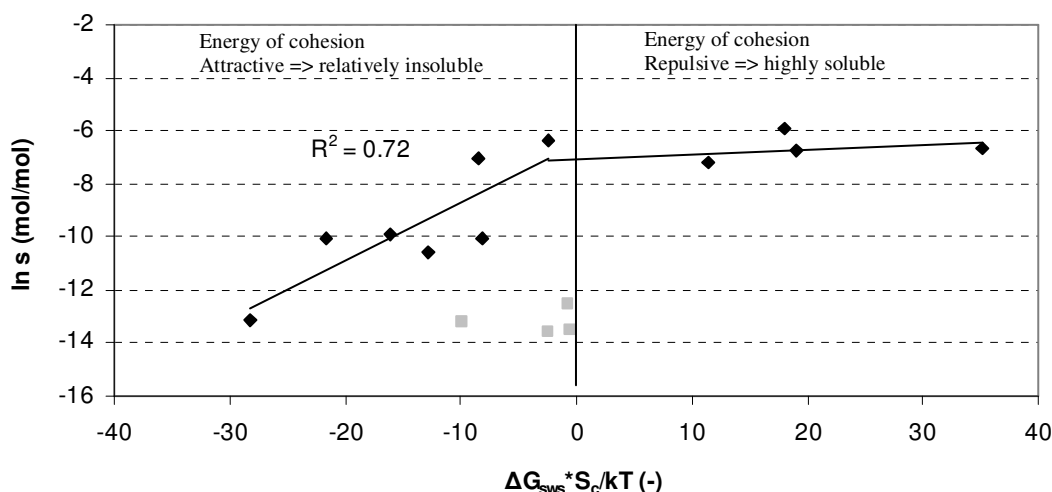


Figure 1: Relationship between energy of cohesion of solutes dissolved in water and solute solubility. Outliers: Carbamazepine, Ibuprofen, Naproxen, Ketoprofen (solubility relatively low for their ΔG_{sws}).

3.2 Two-phase interactions: activated carbon – water and activated carbon-solute

Activated carbons with a higher amount of oxygen containing functional groups are typically more hydrophilic [2, 3]. The interaction energy between activated carbon and water, i.e. ΔG_{cw} , is an indication of activated carbon hydrophobicity. It can indeed be observed that ΔG_{cw} , as calculated from the surface tension components, increases at a higher oxygen surface density

of activated carbon (Figure 3). However, care should be taken not to generalize this correlation, as no clear relation between oxygen surface density and the interaction energy of activated carbon with water (as determined by immersion calorimetry) was found when a broader set of activated carbons was used [16]. Furthermore, it is possible that not all oxygen on the activated carbon surface is released as CO or CO₂ during TPD, and water can interact with nitrogen-containing functional groups and electron-rich sites on the activated carbon basal planes.

The higher ΔG_{cw} at higher oxygen surface density is the result of increasing values for the surface tension components for electron donor – and acceptor interactions at increasing oxygen surface density (Figure 4). It has to be remarked that it is quite exceptional that the values of γ^+ and γ^- are similar for activated carbon. Other authors reported that γ^- is typically much larger than γ^+ for solutes [6], membranes [15] and biofilm [12-14]. Activated carbon, however, is known for its heterogeneity and both acidic and basic sites are present on its surface [23]. According to our TPD data, the amount of oxygen containing functional groups on the activated carbon that act as base (electron donor) or acid (electron acceptor) is of similar order of magnitude, where the amount of basic groups is typically about twice the amount of acidic groups. This was also observed when (Boehms) titration was used to determine the amount of acidic and basic groups on AC1230C and UC830 activated carbon [24]. These findings make it reasonable to expect similar values for γ^+ and γ^- for activated carbon.

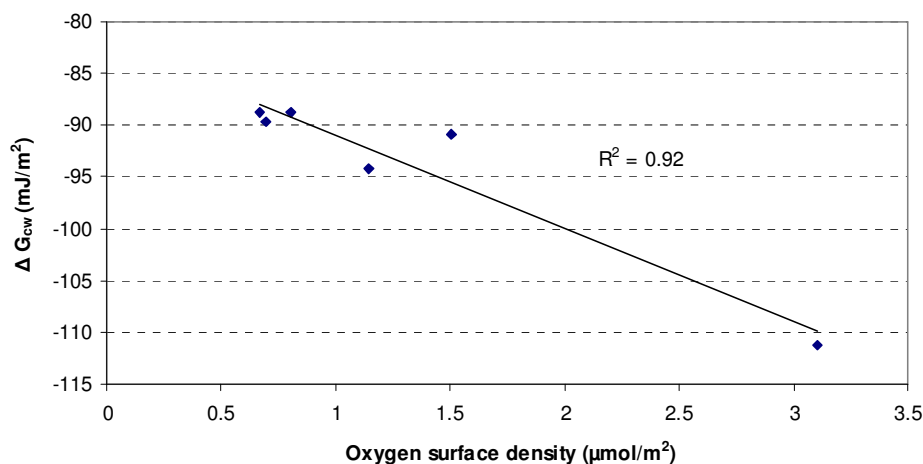


Figure 3: Relationship between oxygen surface density on activated carbon surface, and activated carbon-water interaction.

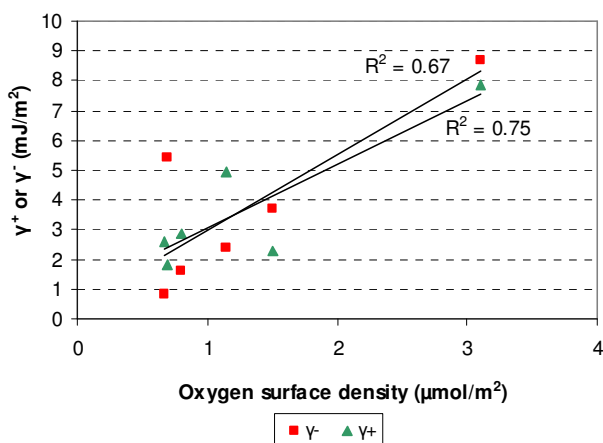


Figure 4: Dependence of activated carbon surface tension components to activated carbon oxygen surface density

The surface tension component approach allows also to determine how large the contribution of van der Waals interaction and acid-base interactions are in the total interaction. All pharmaceuticals have the possibility to form hydrogen bonds with water or with oxygen or nitrogen containing functional groups on the activated carbon surface. The contribution of acid-base interactions to the total interaction is with 25-53% (depending on the solute) significant in solute-water interaction. In solute-activated carbon interaction, van der Waals interactions typically dominate, with a contribution of 80-94% for the most hydrophobic carbon, and 65-87% for the most hydrophilic carbon (S10).

3.3 Three-phase interactions: solute/activated carbon/water

In the previous paragraph on the calculated 2-phase interactions, the validity of the surface tension components of the activated carbons and solutes was assessed, by comparing calculated interaction energies to independent physical parameters. In this paragraph, the interaction between solute and activated carbon in water (ΔG_{scw}) was calculated using the surface tension components and compared to solute carbon loading. The solute carbon loading at an equilibrium concentration of 1 nmol/L was used, as this equilibrium concentration was in the measured range of all solutes, thus eliminating the need for extrapolation. ΔG_{scw} (mJ/m²) as calculated with Equation (6) was multiplied by the molar surface and the initial molar concentration of each solute to obtain the total free energy (in mJ).

When investigating the relationship between the free energy of interaction and the activated carbon loading for individual solutes, reasonable linear correlations are found for most solutes, as shown in Figure 5 (Hydrochlorothiazide) and Figure 6 (Cyclophosphamide). The graphs for all (other) solutes are found in the supporting information (S11).

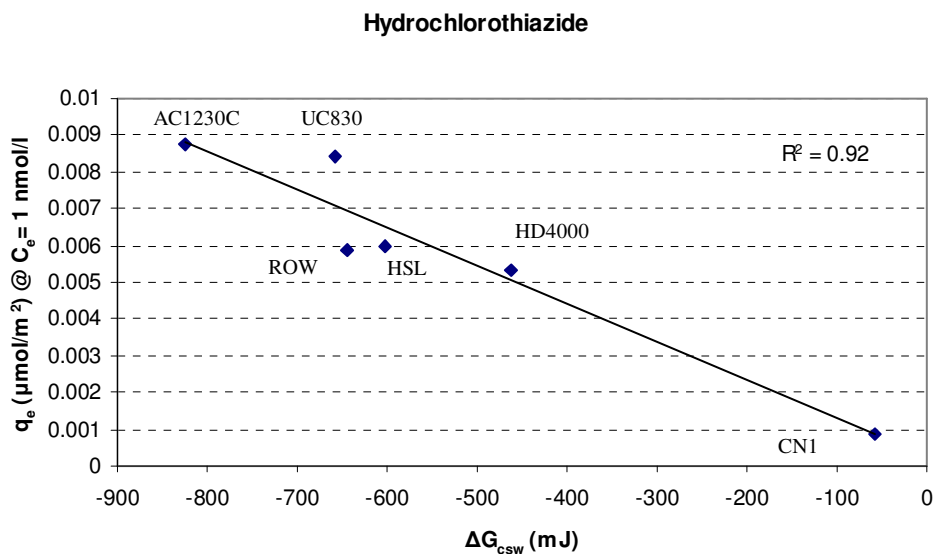


Figure 5: Relationship between ΔG_{scw} and solute surface loading at $C_e = 1 \text{ nmol}/\text{m}^2$ for Hydrochlorothiazide on 6 activated carbons.

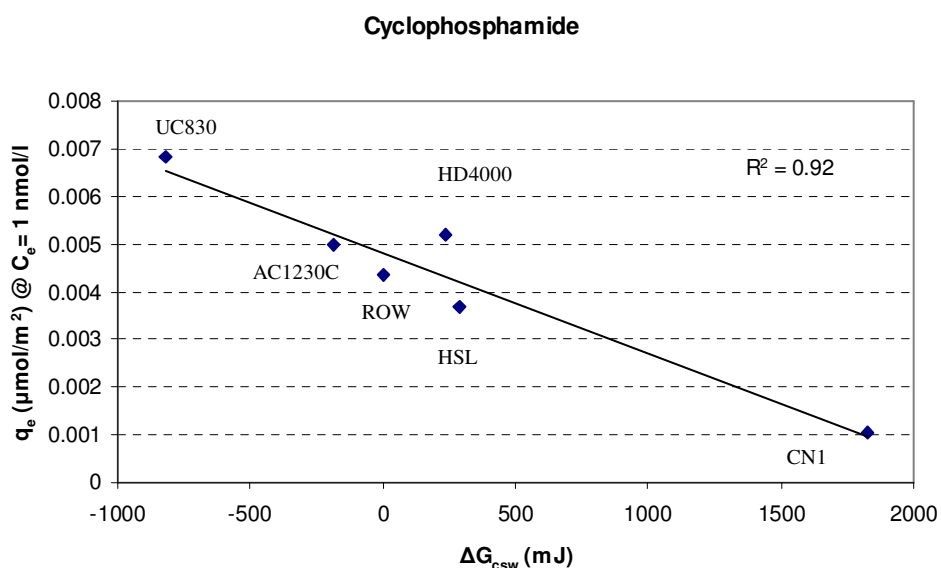


Figure 6: Relationship between ΔG_{scw} and solute surface loading at $C_e = 1 \text{ nmol}/\text{m}^2$ for Cyclophosphamide on 6 activated carbons.

The relation as shown in Figure 5 goes through the origin. This is expected, as the origin is the turning point between attraction between activated carbon surface and the solute (i.e. negative values for ΔG_{scw}) and repulsion (i.e. positive values for ΔG_{scw}). For five solutes, amongst which Cyclophosphamide (Figure 6), the relation does not go through the origin. This may indicate that adsorption mechanisms other than van der Waals or acid-base interaction can be relevant for these solutes, or that their surface tension components are over- or underestimated. For all positively charged solutes, the solute carbon loading was relatively high for CN1 activated carbon as compared to the other activated carbons. As CN1 carries the lowest positive surface charge of all activated carbons, a possible explanation is that the higher carbon loading is caused by lower charge repulsion. The opposite effect (i.e. lower

carbon loading because of lower charge attraction) was not observed for negatively charged solutes.

When the removal of all solutes on an individual activated carbon type is investigated, a clear linear relationship is found for most carbons (AC1230C in Figure 7, other carbons in supporting information S12-S16). This indicates that, although the 16 pharmaceuticals used in this work have varying properties, the main adsorption mechanisms are captured by our approach. The correlation between activated carbon loading and ΔG_{scw} is weak for CN1 ($R^2=0.07$), and this can be explained by the positive values for ΔG_{scw} for this activated carbon. At positive values for ΔG_{scw} , no adsorption takes place, irrespective of the magnitude of the positive value (see also Figure 1). As such, there is no (linear) correlation between ΔG_{scw} and the activated carbon loading for CN1. UC830 and ROW have a relatively low coefficient of determination of 0.29 and 0.62, respectively. This is mainly caused by one solute; ibuprofen. When ibuprofen is excluded, the coefficient of determination rises to 0.68 and 0.82, respectively.

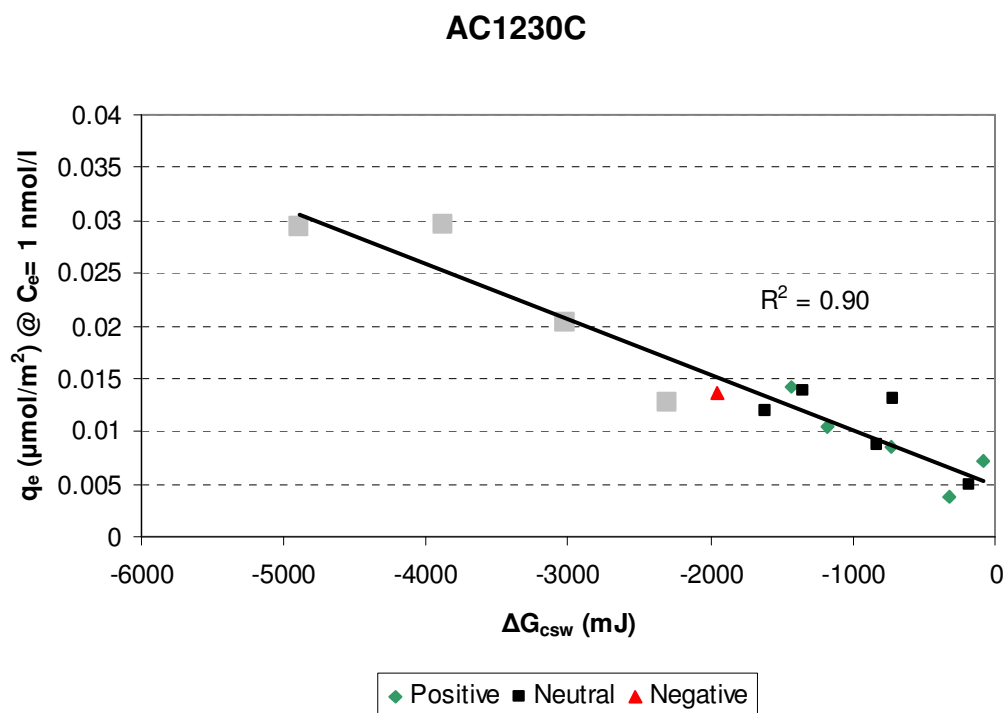


Figure 7: Relationship between the free energy of solute-carbon interaction in water and solute carbon loading at C_e 1 nmol/l for AC1230 activated carbon. Grey squares: Outliers from ΔG_{scw} .

The four pharmaceuticals which were outliers in Figure 1 are included in the correlations of Figure 7 and S12-S16. Of these four pharmaceuticals, only Ibuprofen showed relatively low removal for their ΔG_{scw} for most carbons, but most notably for UC830 and ROW 0.8 supra. Figure 8 shows the integrated data of all activated carbons, with the data of Ibuprofen shown separately. A reasonable correlation ($r^2=0.70$) is found between ΔG_{scw} and the solute activated carbon loading. The mean deviation of the measured activated carbon loadings from the linear is $0.0034 \mu\text{mol}/\text{m}^2$, while 90% of the datapoints have a deviation $<0.005 \mu\text{mol}/\text{m}^2$ (S17).

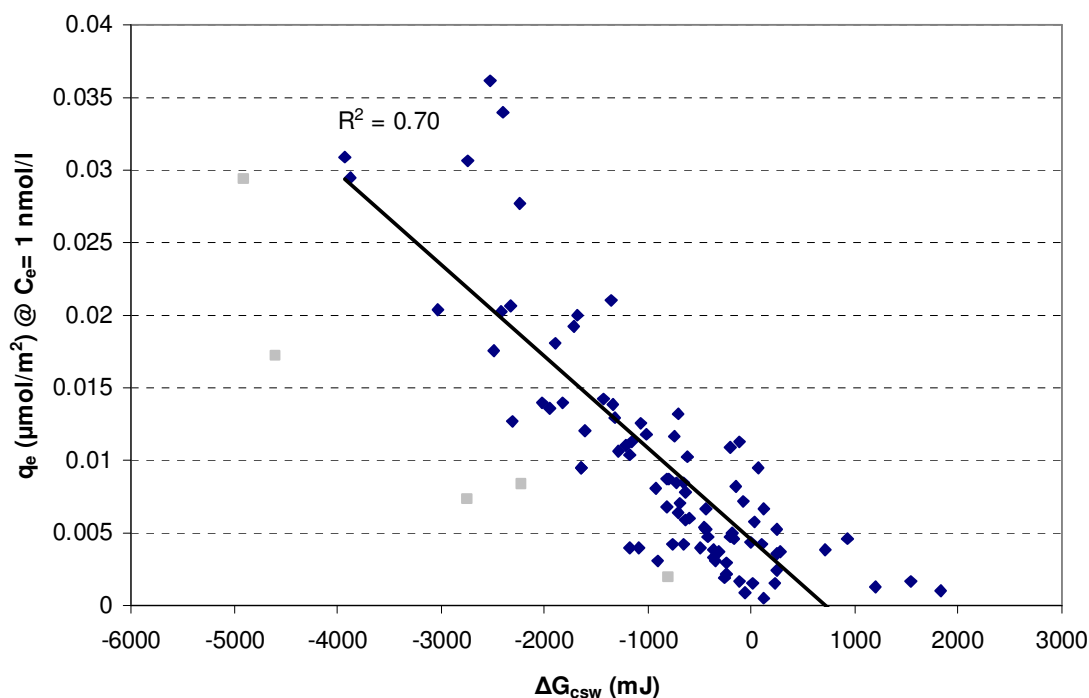


Figure 8: Relationship between the free energy of solute-carbon interaction in water and solute carbon loading at C_e 1 nmol/l for all activated carbons. The data of Ibuprofen is shown separately (grey squares).

The correlation shown in Figure 8 only describes a single point of the adsorption isotherm. However, the slopes of the linearized isotherms (i.e. the Freundlich exponent $1/n$) are reasonably similar (S18). The isotherms are approximated based on the solute carbon loading at C_e 1 nmol/L and a fixed (average) slope for all solutes on a single activated carbon, and compared to the Freundlich isotherms. We found that at C_e 0.1 and 10 nmol/L, the deviation of $\log q_e$ of the approximated isotherm was $<0.18 \mu\text{mol}/\text{m}^2$ as compared to the Freundlich isotherm for 90% of the datapoint. For C_e 0.01 and 100 nmol/L, this deviation increased to $<0.34 \mu\text{mol}/\text{m}^2$ (S19). The adsorption isotherms were measured at low initial solute concentrations and care should be taken when extrapolating these results to higher initial solute concentrations as other mechanisms may become more important, such as adsorption competition between the solutes and multilayer adsorption.

4. Conclusions

- Solute-activated carbon interactions are mainly van der Waals interactions, although the contribution of van der Waals interaction is solute and carbon dependant. For hydrophobic activated carbon, the contribution of van der Waals interactions to the total interaction varies inbetween 80-94%, while for hydrophilic activated carbon, it varies inbetween 65-87%.
- The electron donor- and acceptor surface tension components of activated carbon could be related to the density of oxygen on the activated carbon surface. Solubility of the solutes could be related to solute-solute interaction in water, as calculated with the surface tension approach. Both findings illustrate that physical phenomena can be explained with the surface tension component approach.
- The influence of solute charge on solute removal appears to be limited.

- Solute carbon loadings can be reasonably well related to the free energy for solute-activated carbon interaction in water ($r^2 = 0.70$). Six activated carbons and sixteen solutes with varying characteristics were used in this correlation were used to test how universally applicable the approach is.

Acknowledgements

This research is financially supported by VEWIN, the association of drinking water companies in the Netherlands. Any opinions, findings, conclusions or recommendations expressed in this publication are those of the authors and do not necessarily reflect the opinion of the supporting organisation. We also wish to express our gratitude to Bart van der Linden of the DelftChemTech for his support with the TPD analyses of the activated carbons.

References

- [1] Li L, P.A. Quinlivan, D.R.U. Knappe. Effects of activated carbon surface chemistry and pore structure on the adsorption of organic contaminants from aqueous solution. *Carbon* 2002; 40(12):2085-2100.
- [2] Li L, Quinlivan PA, Knappe DRU. Predicting adsorption isotherms for aqueous organic micropollutants from activated carbon and pollutant properties. *Environ Sci Technol* 2005; 39:3393-400.
- [3] Pendleton P, Wu SH, Badalyan A. Activated carbon oxygen content influence on water and surfactant adsorption. *J Colloid Interf Sci* 2002; 246:235-40.
- [4] Israelachvili JN. Intermolecular and surface forces. 2nd ed. Academic Press; 1992.
- [5] van Oss CJ, Good RJ, Chaudhury MK. Additive and nonadditive surface tension components and the interpretation of contact angles. *Langmuir* 1988; 4:884-91.
- [6] van Oss CJ. Interfacial forces in aqueous media. 2nd ed. CRC Press; 2006.
- [7] Yildirim I. Surface free energy characterization of powders. Virginia Polytechnic Institute and State University, PhD thesis, 2001.
- [8] Douillard JM, Zoungrana T, Partyka S. Surface Gibbs free energy of minerals: some values. *J Petrol Sci Eng* 1995; 14:51-7.
- [9] Medout-Marere V, Malandrini H, Zoungrana T, Douillard JM, Partyka S. Thermodynamic investigation of surface of minerals. *J Petrol Sci Eng* 1998; 20:223-31.
- [10] Chiang HL, Huang CP, Chiang PC. The adsorption of benzene and methylethylketone onto activated carbon: thermodynamic aspects. *Chemosphere*. 2002; 46:143-52.
- [11] van Oss CJ. Use of the combined Lifshitz-van der Waals and Lewis acid-base approaches in determining the apolar and polar contributions to surface and interfacial tensions and free energies. *J Adhesion Sci Technol* 2002; 16(6):669-77.
- [12] Dimitrov D, Hadjiev D, Nikov I. Optimisation of support medium for particle-based biofilm reactors. *Biocheml Eng J* 2007; 37:238-45.
- [13] Khan MMT, Ista LK, Lopez GP, Schuler AJ. Experimental and theoretical examination of surface energy and adhesion of nitrifying and heterotrophic bacteria using self-assembled monolayers. *Environ Sci Technol* 2011; 45(3):1055-60.
- [14] Pereira MA, Alves MM, Azeredo J, Mota M, Oliveira R. Influence of physico-chemical properties of porous microcarriers on the adhesion of an anaerobic consortium. *J Ind Microbiol Biot* 2000; 24(3):181-6.
- [15] Verliefde ARD, Cornelissen ER, Heijman SGJ, Hoek EMV, Amy GL, Van der Bruggen B, et al. Influence of solute-membrane affinity on rejection of uncharged organic solutes by nanofiltration membranes. *Environ Sci Technol* 2009; 43:2400-6.

- [16] De Ridder DJ, Verliefde ARD, Heijman SGJ, Gelin S, Pereira MFR, Rocha RP, et al. A thermodynamic approach to assess organic solute adsorption onto activated carbon in water. *Carbon* 2012; 50:3774-81.
- [17] Yang Y, Chun Y, Sheng G, Huang M. pH-Dependence of pesticide adsorption by wheat-residue-derived black carbon. *Langmuir* 2004; 20:6736-41.
- [18] Denoyel R, Beurroies I, Lefevre B. Thermodynamics of wetting: information brought by microcalorimetry. *J Petrol Sci Eng* 2004; 45(3-4):203-12.
- [19] Kostler S, Delgado AV, Ribitsch V. Surface thermodynamic properties of polyelectrolyte multilayers. *J Colloid Interf Sci* 2005; 286:339-48.
- [20] Denoyel R, Fernandez-Colinas J, Grillet Y, Rouquerol J. Assessment of the surface area and microporosity of activated charcoals from immersion calorimetry and nitrogen adsorption data. *Langmuir* 1993; 9:515-8.
- [21] De Ridder DJ, Verberk JQJC, Heijman SGJ, Amy GL, Van Dijk JC. Zeolites for nitrosamine and pharmaceutical removal from demineralised and surface water: Mechanisms and efficacy. *Sep Purif Technol* 2012; 89:71-77.
- [22] van Oss CJ, Giese RF. Role of the properties and structure of liquid water in colloidal and interface systems. *J Dispers Sci Technol* 2004; 25(5):631-55.
- [23] Moreno-Castilla C. Adsorption of organic molecules from aqueous solutions on carbon materials. *Carbon* 2004; 42:83-94.
- [24] Campos AAR. Removal of polar and emerging organic contaminants by alternative adsorbents. North Carolina State University, PhD thesis, 2008.

Supporting information

Chapter 4

Relation between interfacial energy and adsorption of organic micropollutants onto activated carbon

D.J. de Ridder a, *, A.R.D. Verliefde a,b, K. Schoutteten b, S.G.J. Heijman a, I. Beurroies c, R. Denoyel c, G.L. Amy a,d, J.C. van Dijk a

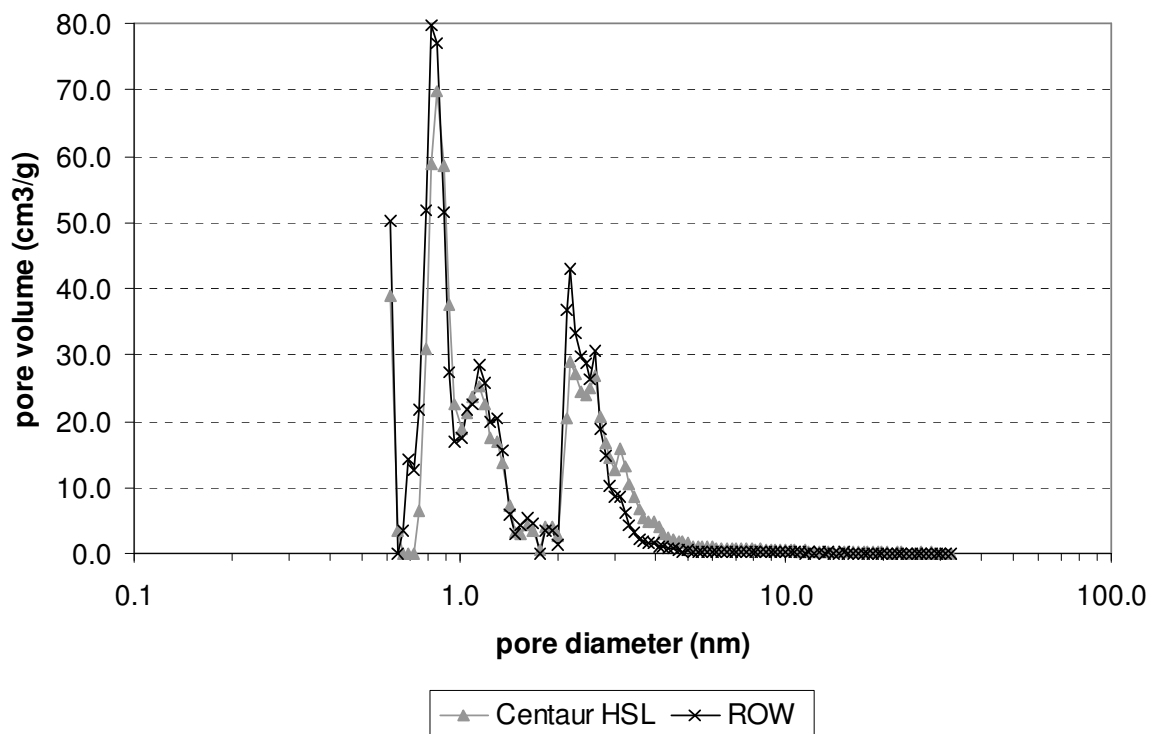


Figure S1: Pore size distribution Centaur HSL and ROW

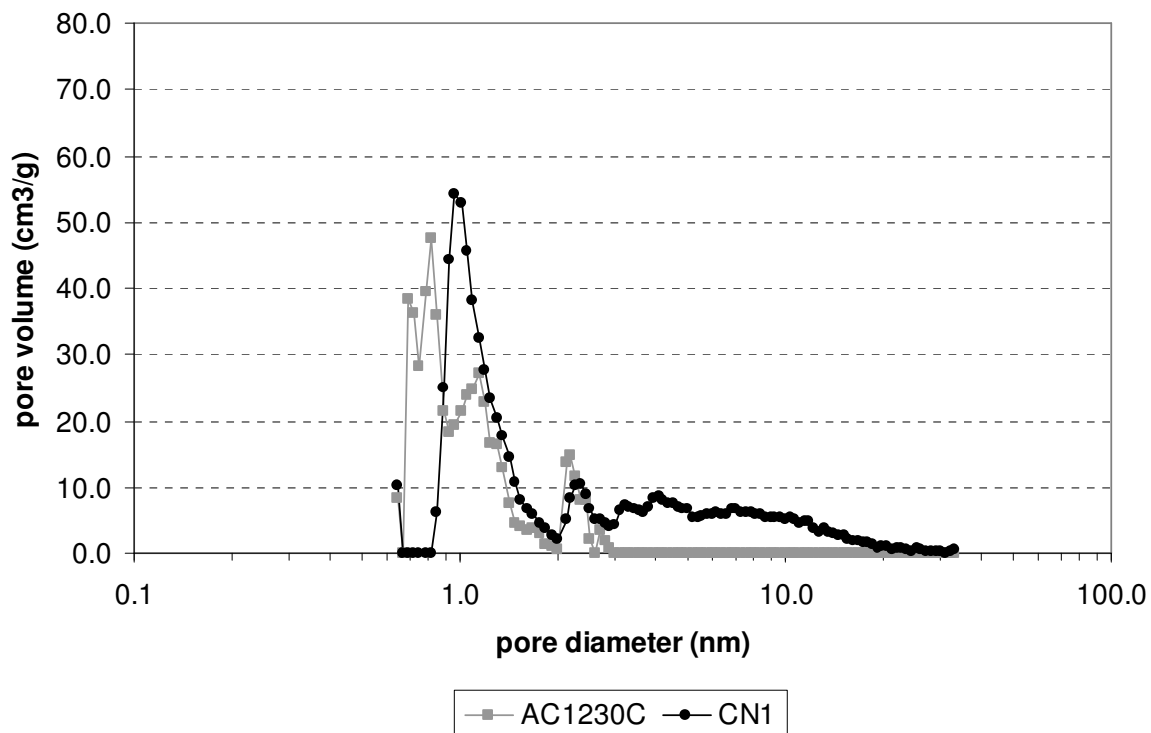


Figure S2: Pore size distribution AC1230C and CN1

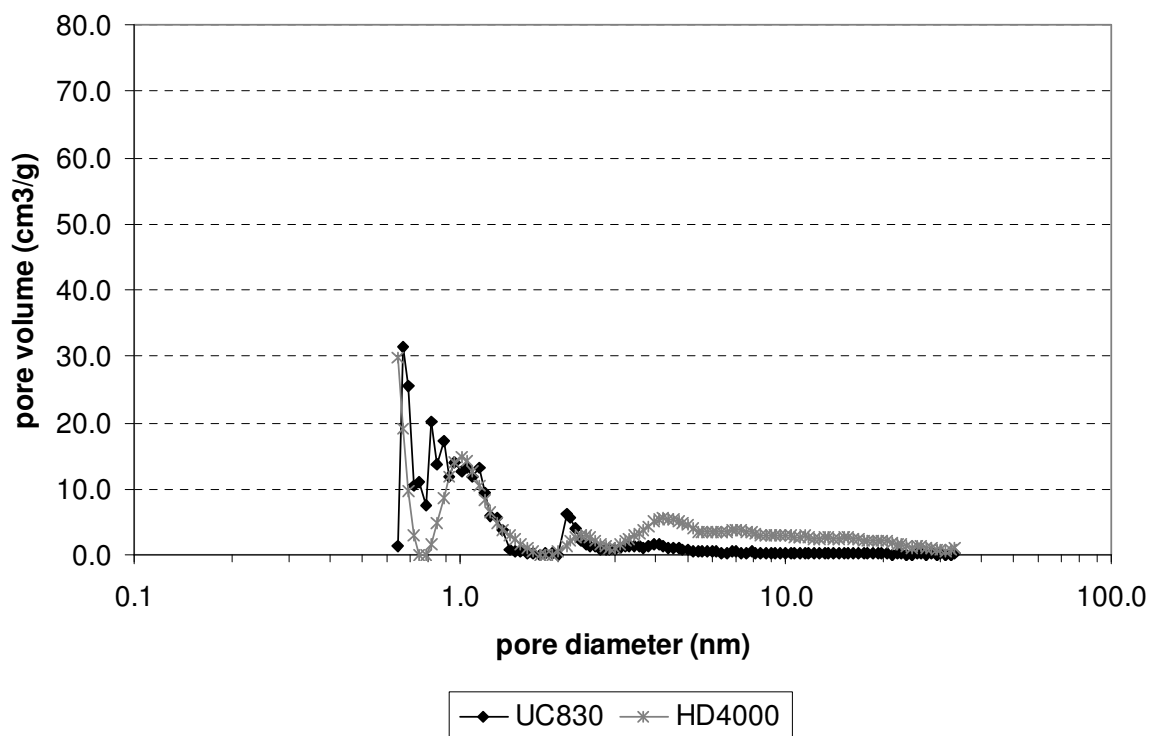


Figure S3: Pore size distribution UC830 and HD4000

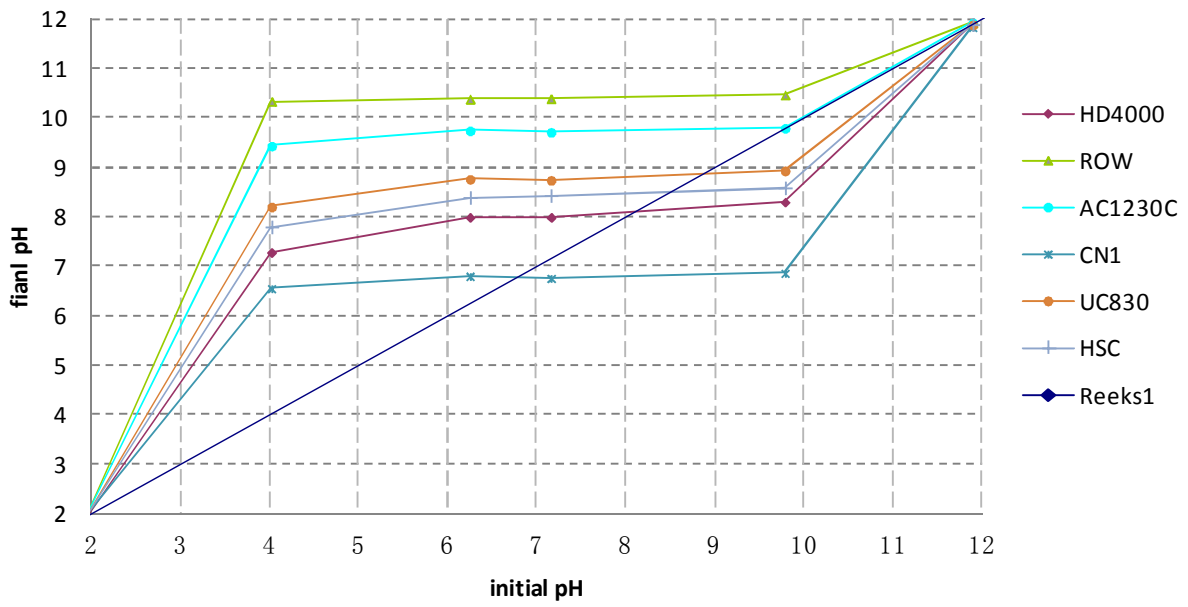


Figure S4: pH drift results of activated carbons

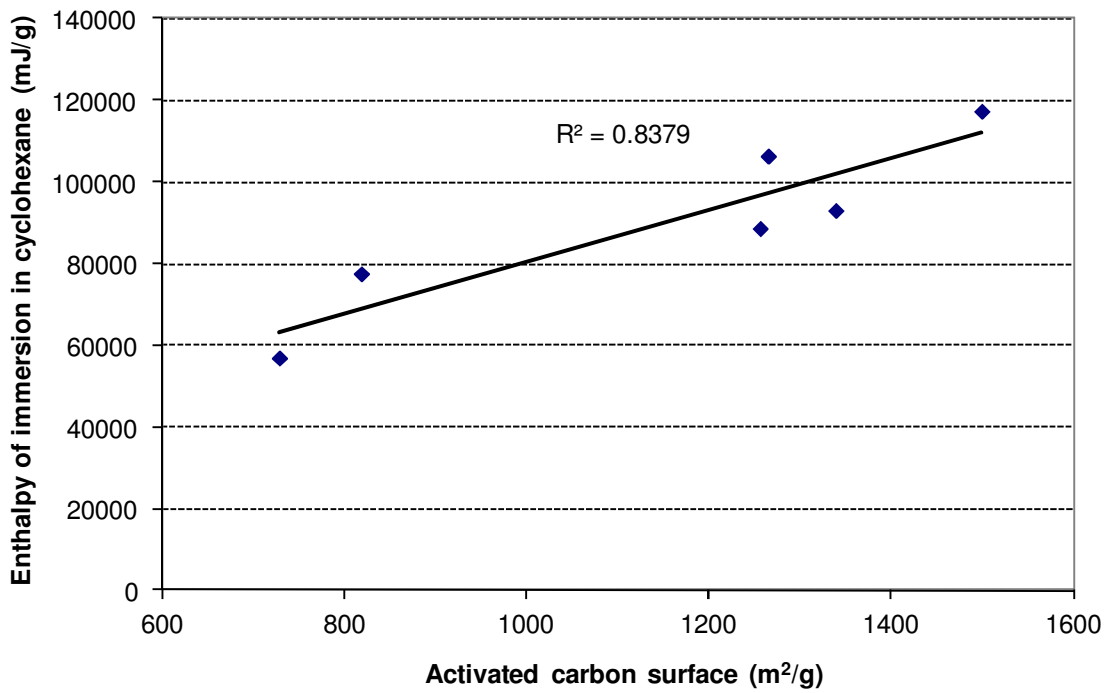


Figure S5: Relationship between activated carbon (BET) surface and enthalpy of immersion of activated carbon in cyclohexane.

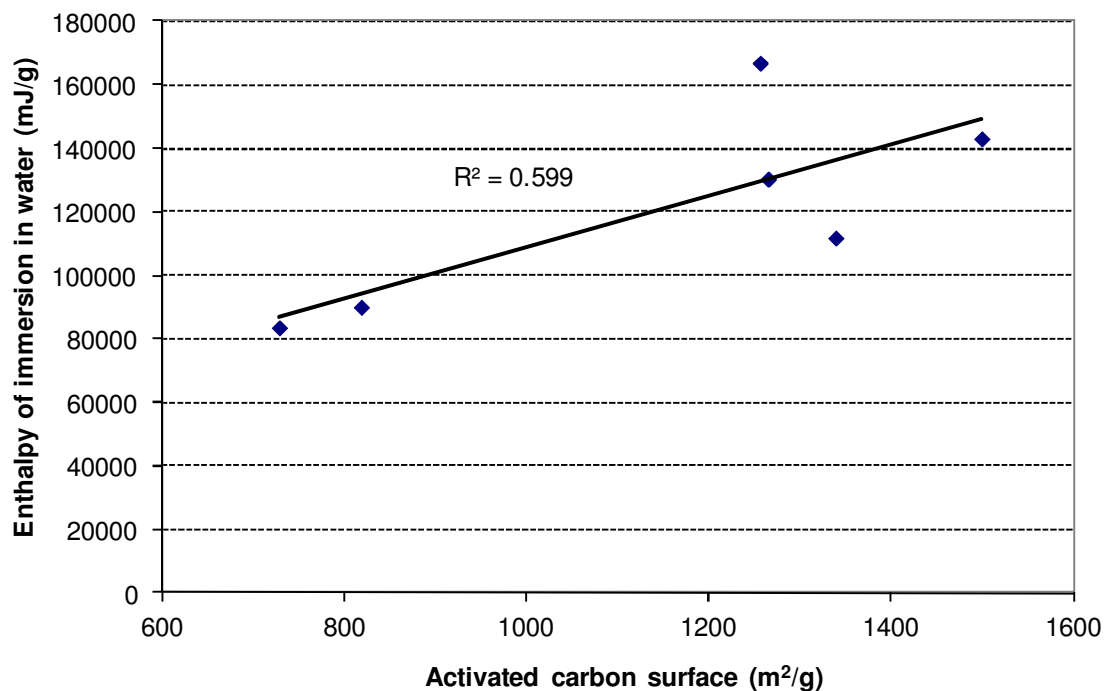


Figure S6: Relationship between activated carbon (BET) surface and enthalpy of immersion of activated carbon in ethylene glycol.

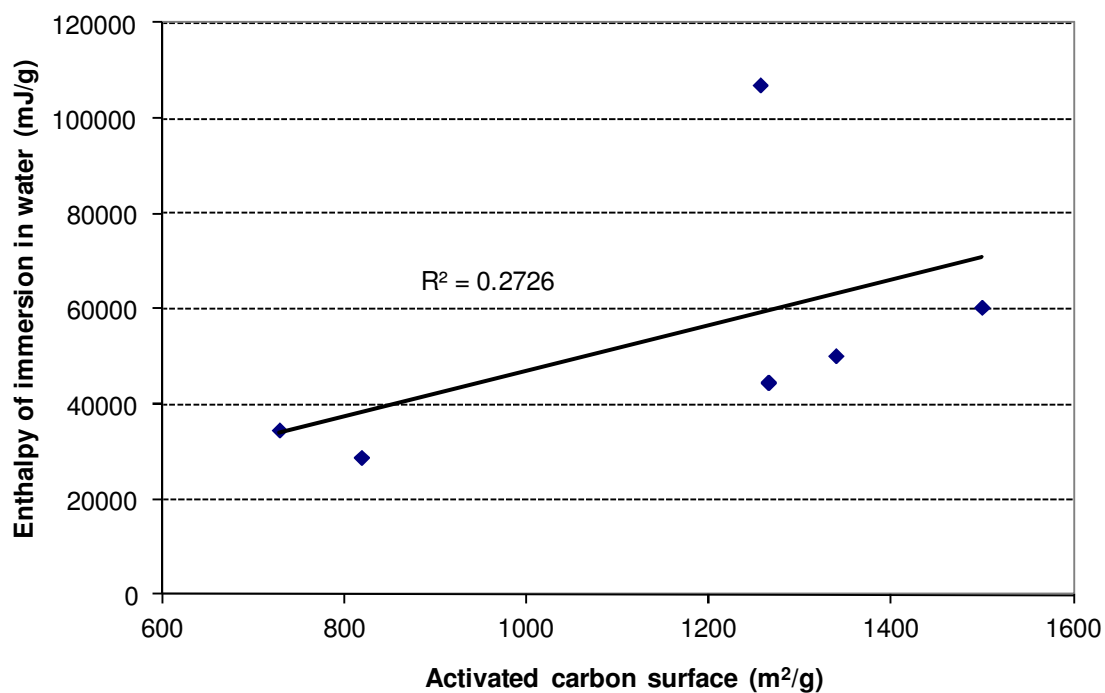


Figure S7: Relationship between activated carbon (BET) surface and enthalpy of immersion of activated carbon in water.

Table S8: Surface tension components of pharmaceuticals

Name	θ water	θ glycerol	θ diiodomethane	γ_s^{LW}	γ_s^+	γ_s^-
Atenolol	60.9	79.8	46.0	36.46	0	21.22
Metropolol	14.8	52.9	19.5	47.93	0	47.64
Lidocaine	38.9	65.9	15.6	48.95	0	33.53
Lincomycin hydrochloride	12.3	55.0	32.2	43.30	0	62.16
Trimethoprim	57.1	71.9	28.1	44.98	0	19.91
Hydrochlorothiazide	48.7	40.7	12.7	49.56	0.63	21.70
Theophylline	31.3	41.7	12.4	49.62	0	50.02
Paracetamol	49.1	59.9	18.3	48.28	0	27.82
Cyclophosphamide	23.7	56.6	25.8	45.85	0	52.23
Carbamazepine	44.9	47.1	13.7	49.37	0.06	31.07
Sulfamethoxazole	63.7	52.3	14.9	49.10	0.28	11.45
Gemfibrozil	65.4	49.5	20.7	47.59	0.80	8.60
Naproxen	49.9	61.2	23.0	46.84	0	28.02
Ketoprofen	48.1	50.8	21.1	47.45	0.02	30.25
Ibuprofen	57.0	72.0	29.6	44.37	0	20.37
Clofibric acid	67.3	61.8	12.9	43.63	0.03	13.78

Table S9: TPD results activated carbons. Activated carbon CN1 was not analysed. All quantities are expressed in $\mu\text{mol}/\text{m}^2$.

Activated Carbon	Carboxylic acid	Anhydride	Lactone	Phenol	Carbonyl	Total electron donor	Total electron acceptor
HD4000	0.17	0.08	0.08	0.23	0.58	0.91	0.41
ROW 0.8	0.36	0.04	0.32	0.17	0.61	1.34	0.53
AC1230C	0.38	0.03	0.02	0.07	0.31	0.74	0.45
UC830	0.14	0.04	0.01	0.08	0.40	0.59	0.21
Centaur HSL	0.08	0.03	0.03	0.12	0.44	0.58	0.20

Electron donor: Anhydride, Lactone, Carbonyl/quinine

Electron acceptor: Phenol

Electron donor & acceptor: Carboxylic acid

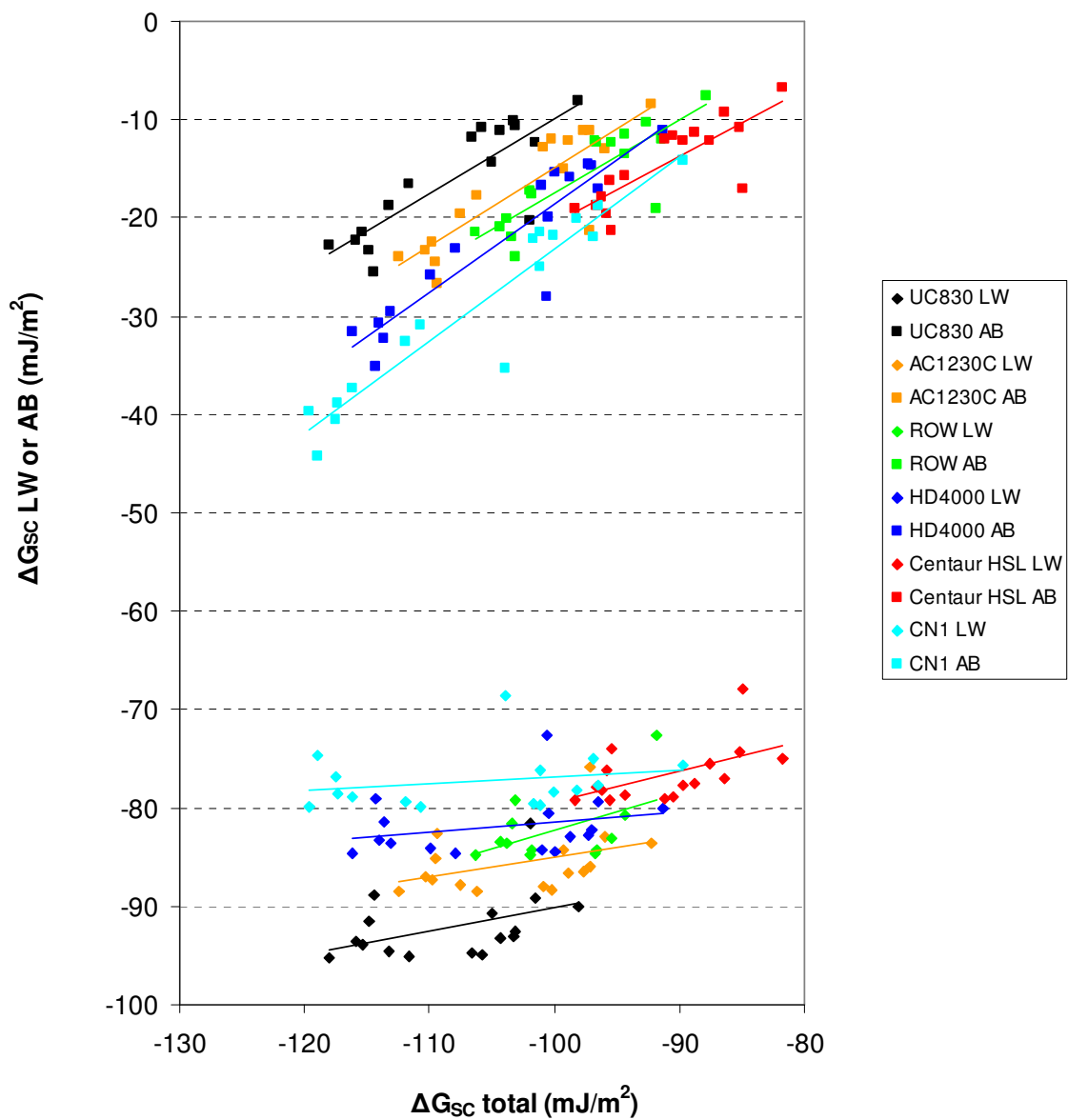
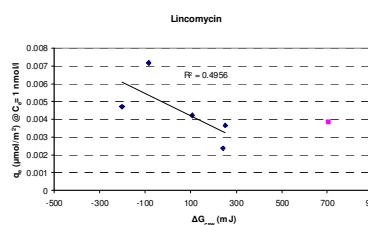
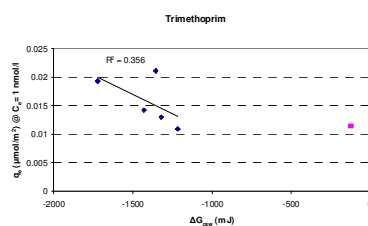
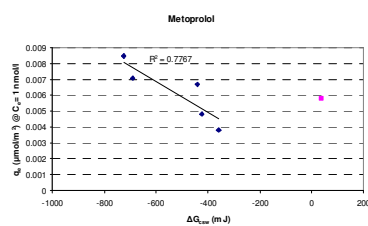
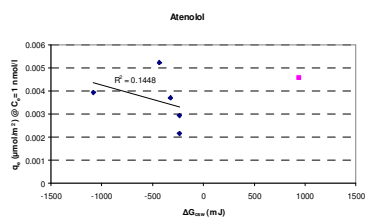
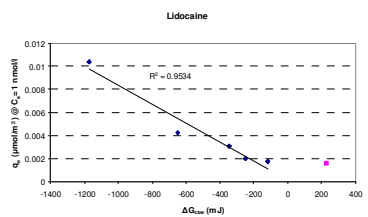
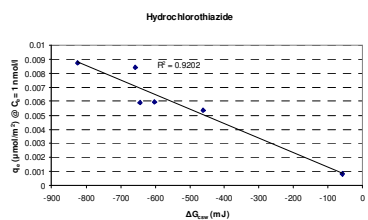
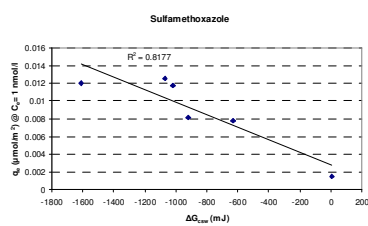
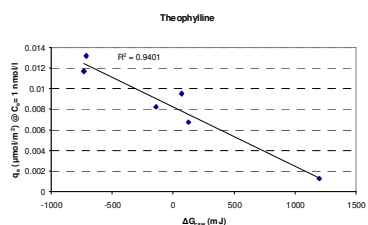
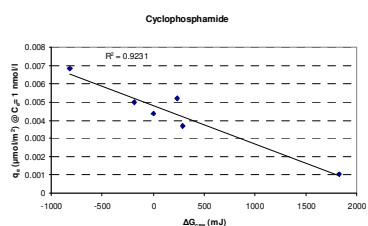
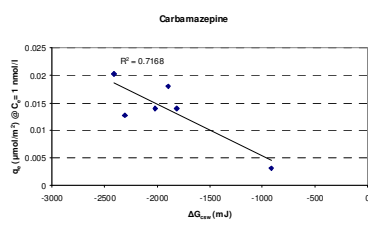
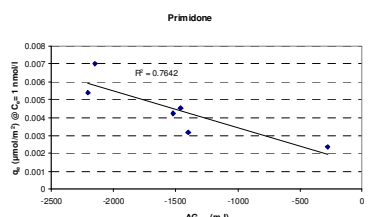
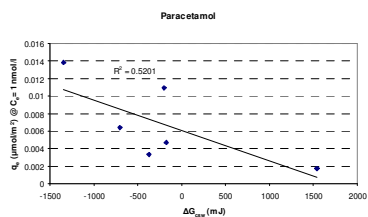


Figure S10: Contribution of van der Waals interaction and acid-base interaction for the total solute-water interaction.

Positively charged



Neutral



Negatively charged

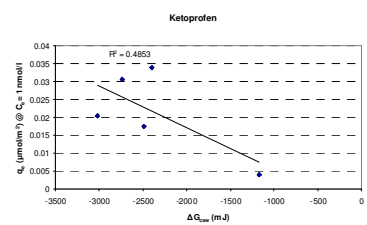
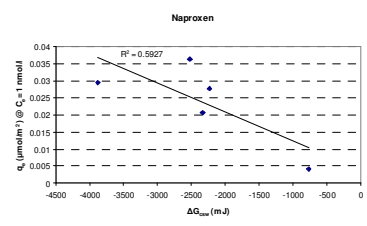
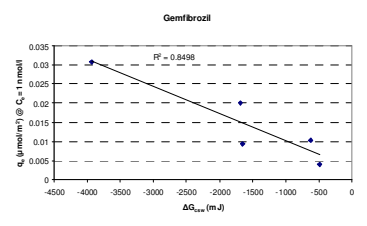
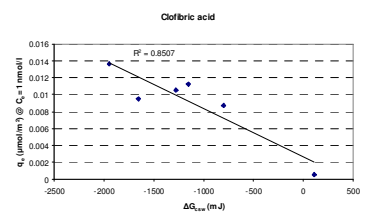
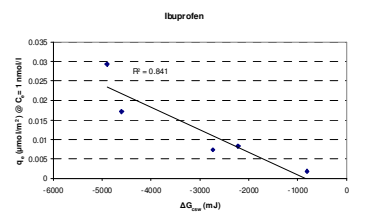


Figure S11: Relationship between ΔG_{scw} , multiplied by solute surface and initial molar concentration, and solute surface loading at $C_e = 1 \text{ nmol/m}^2$.

UC830

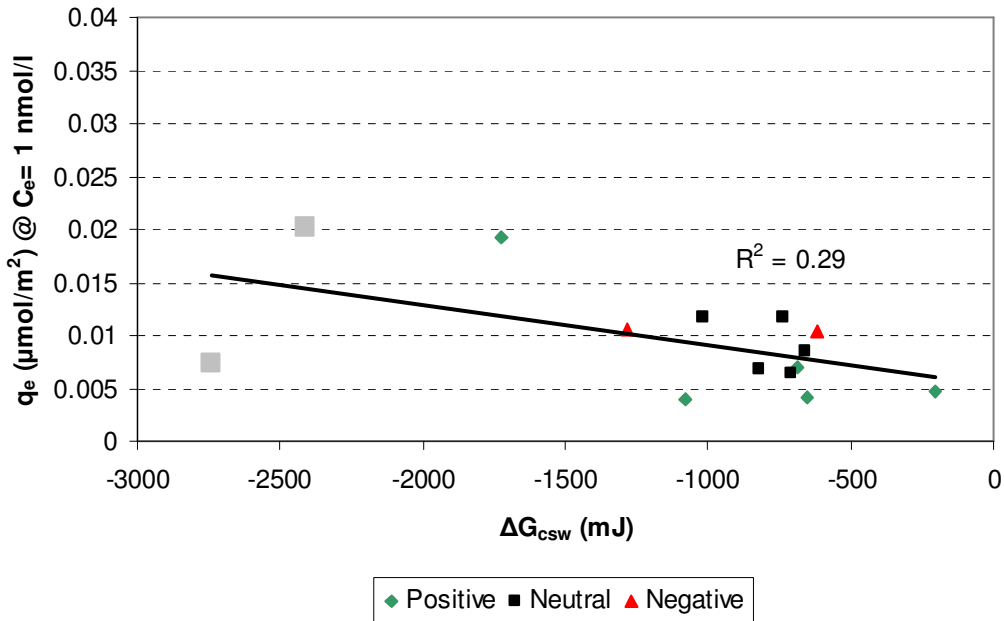


Figure S12: Relationship between the Gibbs free energy of solute-carbon interaction in water and solute carbon loading at C_e 1 nmol/l for UC830 activated carbon. Grey squares: Outliers from ΔG_{sWS} .

HD4000

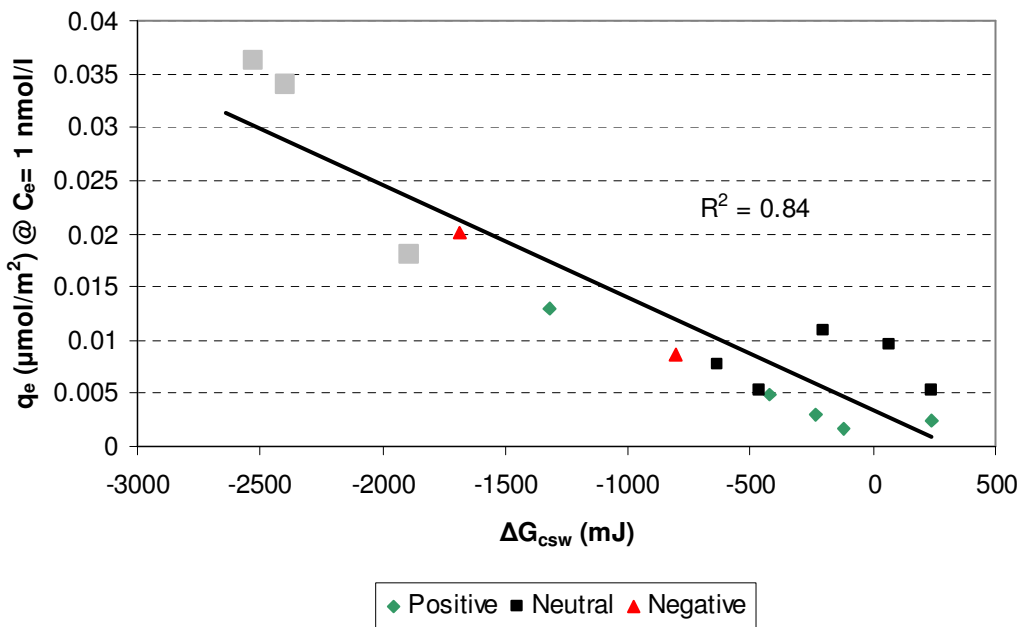


Figure S13: Relationship between the Gibbs free energy of solute-carbon interaction in water and solute carbon loading at C_e 1 nmol/l for HD4000 activated carbon. Grey squares: Outliers from ΔG_{sWS} .

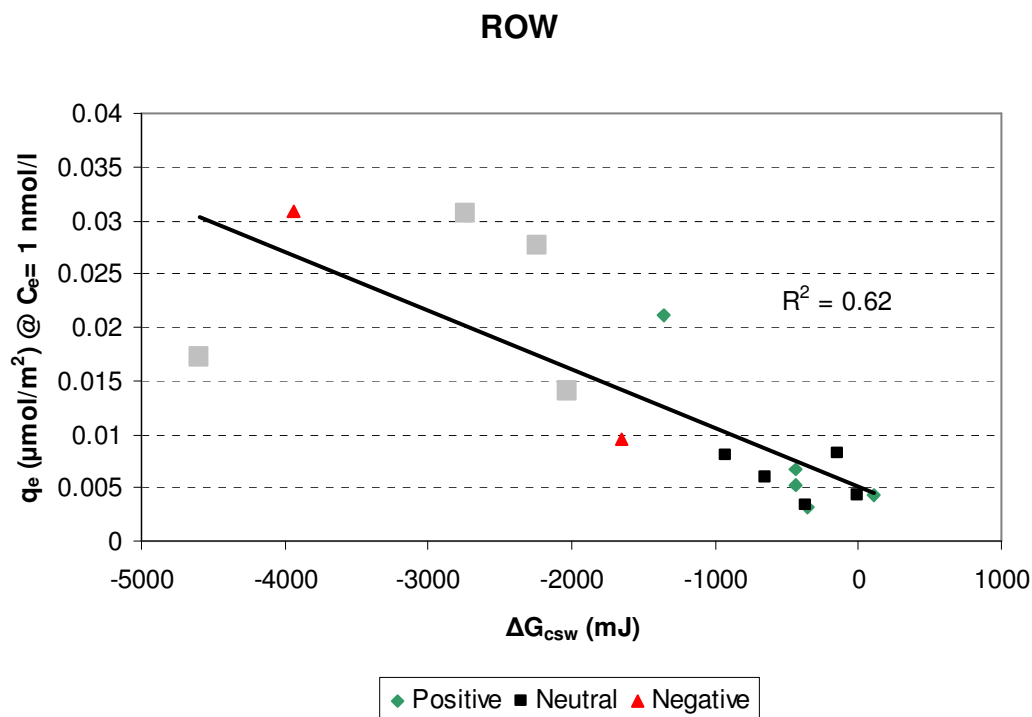


Figure S14: Relationship between the Gibbs free energy of solute-carbon interaction in water and solute carbon loading at C_e 1 nmol/l for ROW 0.8 Supra activated carbon. Grey squares: Outliers from ΔG_{sWS} .

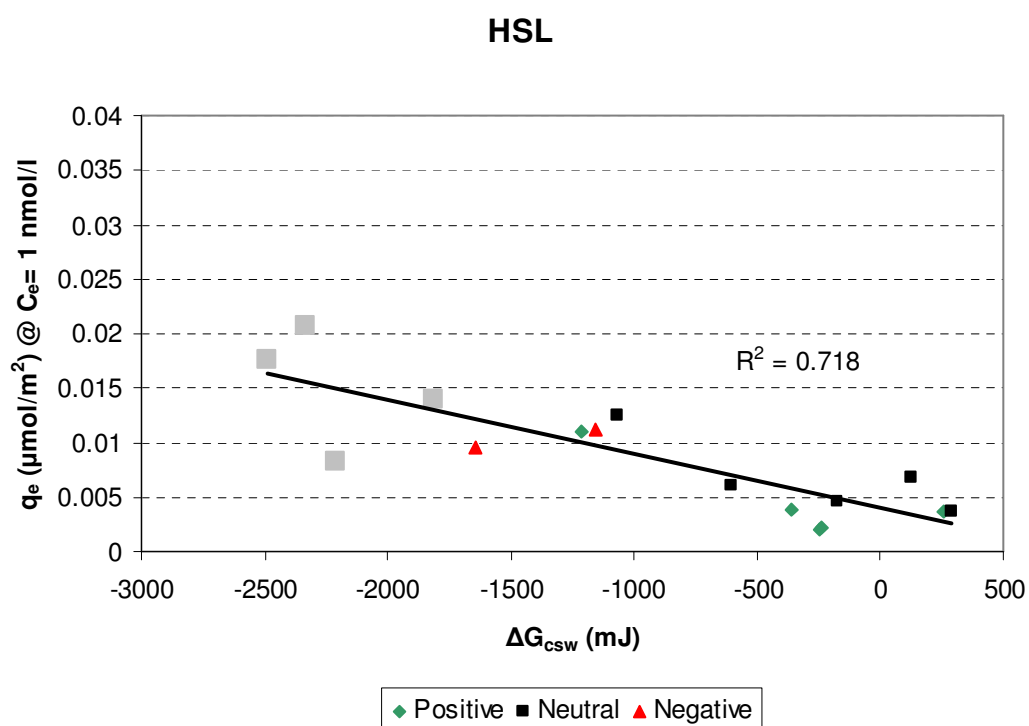


Figure S15: Relationship between the Gibbs free energy of solute-carbon interaction in water and solute carbon loading at C_e 1 nmol/l for Centaur HSL activated carbon. Grey squares: Outliers from ΔG_{sWS} .

CN1

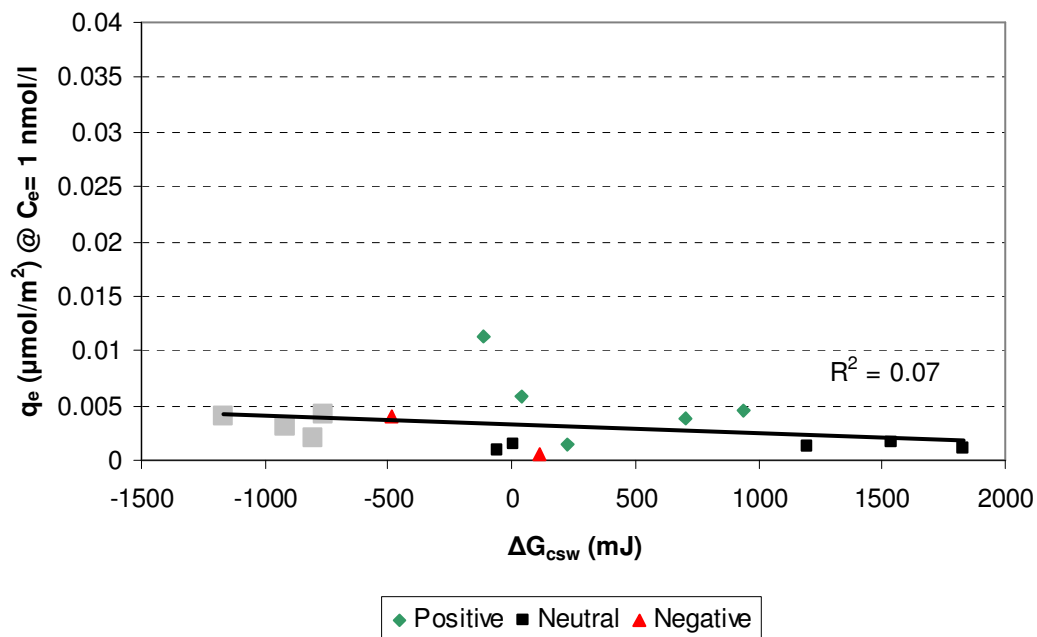


Figure S16: Relationship between the Gibbs free energy of solute-carbon interaction in water and solute carbon loading at C_e 1 nmol/l for CN1 activated carbon. Grey squares: Outliers from ΔG_{SWS} .

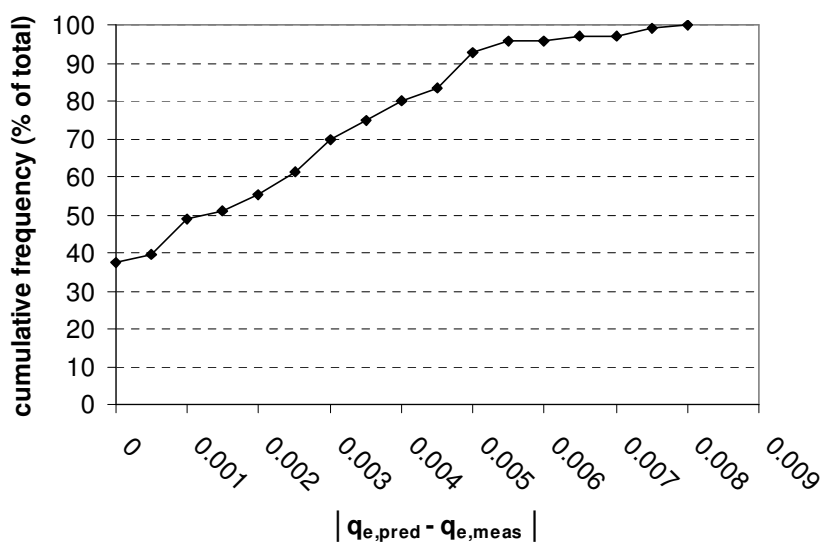


Figure S17: Cumulative frequency of the absolute difference between measured and predicted activated carbon loadings.

Table S18: Freundlich exponent (1/n) of the solute isotherms

Name	UC830	HD4000	AC1230C	CN1	HSL	ROW
Atenolol	0.28	0.13	0.36	0.34	0.38	0.36
Metoprolol	0.48	0.41	0.39	1.00*	0.54	0.44
Lidocaine	0.23	0.11	0.32	0.58	0.40	0.26
Lincomycin hydrochloride	0.34	0.11	0.27	0.65	0.46	0.23
Trimethoprim	0.56	0.58	0.48	1.42*	0.65	0.58
Hydrochlorothiazide	0.31	0.27	0.25	0.42	0.32	0.34
Theophylline	0.40	0.33	0.36	0.39	0.41	0.44
Paracetamol	0.34	0.34	0.39	0.29	0.35	0.58
Cyclophosphamide	0.33	0.21	0.39	0.55	0.42	0.48
Carbamazepine	0.42	0.26	0.32	0.39	0.54	0.43
Sulfamethoxazole	0.39	0.32	0.25	0.31	0.42	0.54
Gemfibrozil	0.61	0.44	0.01*	0.53	0.56	0.73*
Naproxen	0.52	0.21	0.21	0.41	0.34	0.48
Ketoprofen	0.38	0.34	0.20	0.42	0.28	0.35
Ibuprofen	0.54	0.21	0.19	0.45	0.42	0.60
Clofibric acid	0.31	0.29	0.34	0.39	0.49	0.45
Average	0.40	0.28	0.32	0.44	0.43	0.44

*not included in average

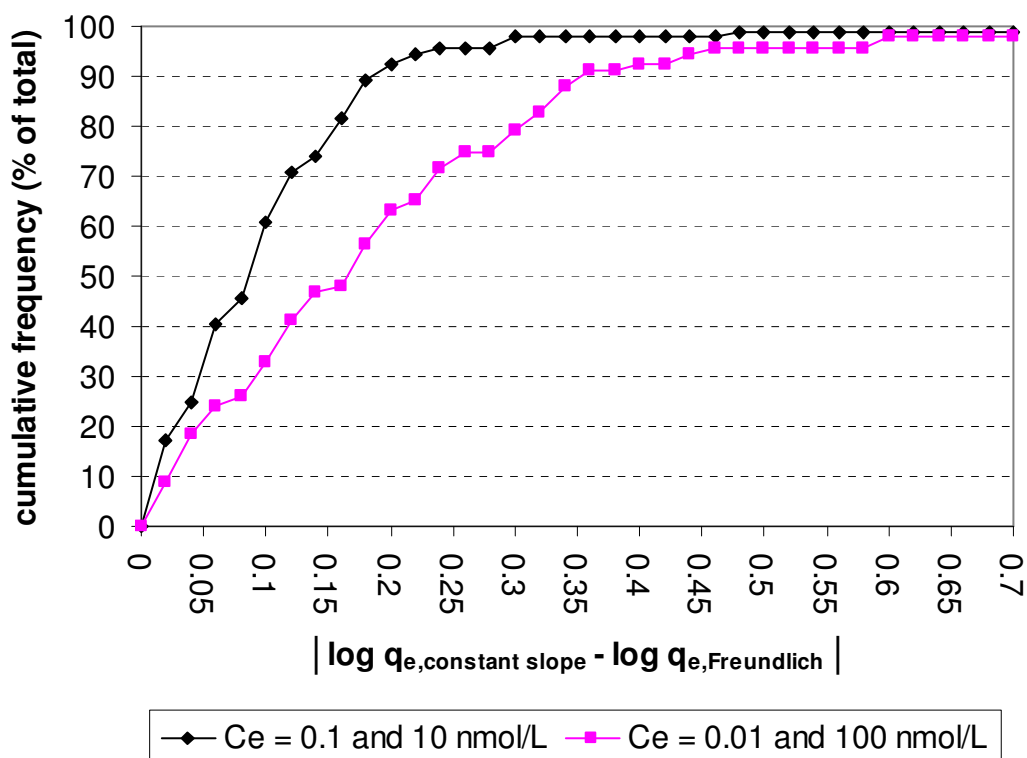


Figure S19: Cumulative frequency of the absolute difference between q_e as described by the Freundlich isotherm and as derived from the "constant slope" approximation for different values of $\log C_e$.

Chapter 5

Influence of Natural Organic Matter on Equilibrium Adsorption of Neutral and Charged Pharmaceuticals onto activated carbon

D.J. de Ridder¹*, A.R.D. Verliefde¹2)4), S.G.J. Heijman¹), J.Q.J.C. Verberk¹), L.C. Rietveld¹3), L.T.J. van der Aa¹3), G.L. Amy¹5)6), J.C. van Dijk¹)

1) Delft University of Technology, P.O. box 5048, 2600 GA Delft, The Netherlands

2) UNESCO Centre for Membrane Science & Technology, University of New South Wales, NSW 2052, Sydney, Australia

3) Waternet, P.O box 94370, 1090 GJ, Amsterdam, The Netherlands

4) KWR Watercycle Research Institute, P.O. Box 1072, 3430BB Nieuwegein, The Netherlands

5) UNESCO-IHE, P.O. Box 3015, 2601 DA Delft, The Netherlands

6) King Abdullah University of Science and Technology, Thuwal, Saudi Arabia

*corresponding author. E-mail: d.j.deridder@tudelft.nl, fax : 0031 (0)152784918, tel : 0031(0)152781718

Water science and technology 63 (2011) 416-423

Abstract

Natural organic matter (NOM) can influence pharmaceutical adsorption onto granular activated carbon (GAC) by direct adsorption competition and pore blocking. However, in the literature there is limited information on which of these mechanisms is more important and how this is related to NOM and pharmaceutical properties.

Adsorption batch experiments were carried out in ultrapure, waste- and surface water and fresh and NOM preloaded GAC was used. Twenty-one pharmaceuticals was selected with varying hydrophobicity and with neutral, negative or positive charge. The influence of NOM competition and pore blocking could not be separated. However, while pore blocking was lower for wastewater preloaded GAC than for surface water preloaded GAC, up to 50% lower pharmaceutical removal was observed. This was contributed to higher hydrophobicity of wastewater NOM, indicating that NOM competition may influence pharmaceutical removal more than pore blocking. Preloaded GAC was negatively charged, which influenced removal of charged pharmaceuticals significantly. At a GAC dose of 6.7 mg/l, negatively charged pharmaceuticals were removed for 0-58%, while removal of positively charged pharmaceuticals was between 32-98%. Charge effects were more pronounced in ultrapure water, as it contained no ions to shield the surface charge. Solutes with higher log D could compete better with NOM, resulting in higher removal.

1. Introduction

Trace concentrations of pharmaceuticals and personal care products (PPCP) have been detected in natural water sources in the U.S. and Europe (Zwiener, 2007; Snyder, 2008; Ternes et al., 2002; Westerhoff et al., 2005; Mompelat et al., 2009). The main pathway for PPCPs to enter surface water is via wastewater effluent, and PPCPs may potentially cause adverse ecological effects at the concentrations found in surface waters (Hernando et al., 2006). When treating surface water to produce drinking water, various techniques can be applied to remove PPCPs, such as ozonation, activated carbon filtration chlorination or irradiation with UV (Westerhoff et al., 2005; Snyder, 2008; Ternes et al., 2002). Although it is unlikely that PPCPs pose significant threats to human health at the concentrations at which they are detected in finished drinking water (Snyder, 2008), drinking water companies aim to reduce PPCP concentrations even further out of precaution.

Activated carbon is widely used to remove organic micropollutants, and several researchers have investigated its efficacy for the removal of PPCP on fresh activated carbon in natural water (Westerhoff et al., 2005; Ternes et al., 2002; Redding et al., 2009). Pharmaceutical hydrophobicity and charge are recognized as important solute properties that influence their removal. The influence of preloading granular activated carbon (GAC) with natural organic matter (NOM) and/or co-adsorption with NOM was not investigated explicitly by these authors. NOM can reduce PPCP removal by the following mechanisms: (1) natural organic matter (NOM) competes for available adsorption surface area and adsorption sites, and (2) NOM blocks (micro)pores, which reduces the available surface area (Newcombe and Drikas, 1997; Matsui et al., 2002; Pelekani and Snoeyink, 1999; Kilduff et al., 1998). Direct competition with larger NOM fractions is lower because of size exclusion within GAC grains (Worch, 2008).

NOM adsorption, and thus its ability to compete for available adsorption surface area, is influenced by charge interactions (Newcombe and Drikas, 1997). NOM is negatively charged at neutral pH, and electrostatic repulsion or attraction can occur between NOM and GAC. GAC surface charge depends on the quantity of acid and basic functional groups, and the pKa value at which these dissociate and protonate, respectively (Moreno-Castilla, 2004). When the amount of dissociated and protonated functional groups is equal, the net surface charge is zero. The pH value at which a net zero charge is obtained (pHpzc) depends on the GAC type, and can vary between 3.4 and 8 (Newcombe and Drikas, 1997; Bjelopavlic et al., 1999; Fairey et al., 2006). Most GAC types presented by these authors have pHpzc values between 6.5 and 8, indicating that GAC surface can be slightly positively charged or negatively charged at neutral pH.

Electrostatic repulsion is less influential at lower pH values as the negative charge of NOM is reduced and the net surface charge of GAC becomes less negative, or becomes positive. A high ionic strength can reduce the effect of electrostatic repulsion or attraction (Newcombe and Drikas, 1997; Fairey et al., 2006). When a layer of NOM has been adsorbed on GAC, the surface becomes negatively charged due to NOM coverage, with increasing negative charge at higher NOM loading (Newcombe, 1994). This may promote electrostatic repulsion reducing adsorption of NOM and anionic pharmaceuticals.

Although interaction mechanisms are proposed in the literature to explain the influence of NOM on pharmaceutical removal, it is not clear which of the interaction mechanisms is more dominant, how this is related to NOM and pharmaceutical characteristics, and how this changes when NOM has already adsorbed onto GAC. Insight into these relationships is required, however, to predict pharmaceutical removal in the presence of NOM a-priori. A-priori prediction models can be useful to determine if new pharmaceuticals are likely to be removed or not in an activated carbon filter, without requiring extensive field testing.

This study aimed to relate NOM composition (based on liquid chromatography with organic carbon detection (LC-OCD) analysis) and pharmaceutical hydrophobicity and charge to their removal. The second objective was to investigate the influence of NOM competition and pore blocking separately. Adsorption experiments were carried out in ultrapure water and two natural water types containing different NOM mixtures. In order to separate NOM competition and pore blocking, the following configurations were investigated:

Natural water, fresh GAC; mainly NOM competition is expected

Ultrapure water, NOM preloaded GAC; NOM competition and pore blocking are expected

Natural water, NOM preloaded GAC; stronger NOM competition and similar pore blocking are expected as in the experiment with ultrapure water

Furthermore, the change in available adsorption surface area as a consequence of preloading was measured.

2. Materials and Methods

Equilibrium batch experiments were conducted with an equilibrium time of 8 weeks. Three water matrices were used; Buffered ultrapure water, treated surface water and treated wastewater. Whole GAC grains were used, either fresh or preloaded with NOM. All pharmaceuticals had an initial concentration of 2 µg/l. During the experiment, the samples were stored in a climate room at 12°C and stirred continuously with a magnetic stirrer (LD-746, Labenco, Netherlands) at 84 rpm. For each adsorption isotherm determination, five GAC doses were used (from 6.7 to 88.9 mg/l) and a blank measurement was included. The blank solution was spiked with pharmaceuticals, but no GAC was dosed.

Surface water, wastewater and fresh and preloaded GAC were obtained from Waternet, watercycle company for Amsterdam and surrounding areas. The surface water originated from Weesperkarspel water treatment plant and was taken after coagulation, storage (about 100 days), filtration, ozonation and pellet softening. The wastewater originated from waste water treatment plant Horstermeer after primary sedimentation, activated sludge and secondary sedimentation. Both surface water and wastewater were filtered through a 1.2 µm polypropylene filter (Sartopure PP2 maxicap, Sartorius, Netherlands) and a 0.45 µm nylon filter (Polycap AS, Whatman, Netherlands) before use. The ultrapure water was generated on-site from tap water, using ion exchange and nanofiltration treatment. Ultrapure water samples were buffered with 1mM NaH₂PO₄.H₂O.

Twenty-one pharmaceuticals (see Table 1) were obtained from Sigma-Aldrich and were analytical grade. The pharmaceuticals were selected based on solute charge and were ordered in three charge groups: negatively charged, neutral and positively charged. The selected solutes have similar molecular weight, but varied in hydrophobicity. Hydrophobicity was expressed by log D. Log D is equivalent to log K_{ow} (octanol-water partitioning coefficient), which is corrected for molecule dissociation/protonation according to Equations [1] and [2]:

$$\text{Acids: } \log D = \log K_{ow} - \log(1 + 10^{(pH - pKa)}) \quad [1]$$

$$\text{Bases: } \log D = \log K_{ow} - \log(1 + 10^{(pKa - pH)}) \quad [2]$$

Table 1: Solute characteristics

	MW (g/mol)	pKa	Log D (pH 7.4)	Log D (pH 8.1)
Negatively charged				
Clofibrac acid	214	3.35	0.57	0.57
Ibuprofen	206	4.47	1.97	1.97
Ketoprofen	254	4.29	1.12	1.12
Gemfibrozil	250	4.45	2.77	2.77
Diclofenac	296	4.08	2.51	2.51
Naproxen	230	4.84	1.18	1.18
Fenoprofen	242	4.21	1.9	1.9
Bezafibrate	361	3.44	2.25	2.25
Neutral				
Cyclophosphamide	261	n/a	0.63	0.63
Phenazon	188	n/a	0.4	0.4
Carbamazepine	236	n/a	2.4	2.4
Pentoxiphylline	278	n/a	0.29	0.29
Aminopyrine	231	n/a	1	1
Positively charged				
Salbutamol	239	9.27	-1.24	-0.56
Sotalol	272	9.44	-1.76	-1.12
Metoprolol	267	9.49	-0.12	0.47
Atenolol	266	9.43	-1.84	-1.19
Clenbuterol	277	9.29	0.1	0.78
Terbutaline	225	8.86	-0.57	0.07
Pindolol	248	9.26	-0.12	0.56
Propranolol	259	9.58	1.48	1.99

All pharmaceuticals were dosed as a mixture. This may result in lower removal in ultrapure water as compared with single solute isotherms. In surface water and wastewater, mutual competitions effects between pharmaceuticals are expected to be negligible; the TOC concentration in natural water is 2,500 times higher than the concentrations of the pharmaceuticals. Similarly, a high TOC to pharmaceutical ratio is expected when considering adsorption competition in NOM-preloaded GAC.

The various NOM fractions of the natural waters were quantified using LC-OCD. First they are separated based on size with liquid chromatography (LC) and then quantified with organic carbon detection (OCD), a procedure similar to regular TOC analyses. The NOM fraction that does not elute from the LC column after 200 minutes is identified as hydrophobic organic carbon (HOC). In addition, the specific UV adsorption (SUVA) at 254 was determined, which is a measure of the aromaticity of NOM.

Fresh and preloaded Norit GAC830 P granular activated carbon was used. Preloading was done using Weesperkarspel surface water or Horstermeer waste water effluent for at least 6 months. In order to use preloaded GAC with characteristics similar to field practice, the GAC was not dried before use. Both fresh and preloaded GAC was sieved wet and the fraction 0.6 – 0.71 mm was collected. After sieving, the required amount of GAC was weighed in its wet condition. When equilibrium was reached, the GAC was collected and dried at 105 °C for 24 hours, after which its dry weight was determined.

GAC characterization measurements were done by Norit (Amersfoort). Total available surface area on fresh and preloaded GAC was determined by nitrogen adsorption, and calculated as BET (Brunauer, Emmett, Teller) surface area. Micro-, meso- and macropore volumes were determined by nitrogen adsorption and calculated with the BJH method (Barrett, Joyner, Helena). In addition to nitrogen adsorption, adsorption of iodine and methylene blue was measured on fresh and preloaded GAC. The adsorbed amount of iodine and methylene blue are indications of the available micro pore and macro pore surface, respectively (Bestani, 2008). Both measurements should be regarded as indicative. Iodine adsorption can be related to nitrogen adsorption (Mianowski et al., 2007), although there may still be up to 20% difference in the surface area estimated based on their adsorption. Methylene blue is also a cation; both pore size and charge effects may influence its adsorption. Pharmaceutical analysis was done by Technologiezentrum Wasser (TZW) using LC/MS/MS. The analysis method is described in (Sacher et al., 2001). The limit of quantification of this method was 0.02 µg/l for all pharmaceuticals when 2 liter of sample volume was used. The accuracy of measured concentrations was estimated to be +/- 20% by TZW, indicating a higher accuracy when low concentrations are measured, i.e., when pharmaceuticals are adsorbed effectively. This yields the error margins shown in Table 2.

Table 2: Error margins

Measured removal	0-20%	20-40%	40-60%	60-80%	80-100%
Error margin	20-15%	15-11%	11-8%	8-4%	4-0%

3. Results and Discussion

3.1 Water Quality

Total carbon concentrations were similar for both water types (table 3). However, in waste water higher levels of hydrophobic organic carbon were detected. Five NOM size-fractions were obtained from LC-OCD analyses, and humic substances represented the largest fraction. Wastewater contained higher concentrations of the large biopolymers. Concentrations of NOM fractions with similar molecular weight as the pharmaceuticals (neutrals, acids) were higher in wastewater (0.96 mg/l) than in surface water (0.69 mg/l). The average molecular weight of humic substances in wastewater was lower than that of the surface water. This indicates that wastewater has a higher potential for direct adsorption competition than surface water.

Table 3: NOM characteristics for natural water types

	Surface water	%TOC	Waste-water	%TOC	Molecular weight (g/mol)
TOC (ppb-C)	5459	100	5659	100	
DOC (ppb-C)	5337	97.8	5509	97.3	
HOC (hydrophobic) (ppb-C)	9	0.2	480	8.5	
Biopolymers (ppb-C)	69	1.3	295	5.2	>>20,000
Humic substances (ppb-C)	3538	64.8	2652	46.9	
With SUVA (L(mg*m))	2		3.9		
With mol. weight (g/mol)	566		428		
Building blocks (ppb-C)	1035	19	1125	19.9	300-500
Neutrals (ppb-C)	615	11.3	956	16.9	<350
Acids (ppb-C)	72	1.3	0	0	<350
SUVA (L(mg*m))	1.64		3.21		
pH	8.1		7.4		

1) After ozonation

2) Fraction with eluting times > 200 min.

3.2 GAC Characterization

All GAC samples were dried before use. For preloaded GAC, drying changes the characteristics of the NOM adsorbed onto the surface (Gorham et al., 2007), forming larger, ring-shaped aggregates. As such, the pore volume distribution measured here may vary from the actual situation.

It was observed that the total pore volume of fresh GAC 830P mainly consist of pores < 1 nm (~50%) and to a lesser degree of pores in the ranges 1-25 nm and >25 nm (~20% and 30%, respectively)(see Table 4).

Table 4: Characterisation of fresh and preloaded GAC 830P

Analysis	Unit	Fresh	Preloaded (SW)		Preloaded (WW)	
		Value	Value	Change (%)*	Value	Change (%)*
Iodine number	N/0.1 L/g	880 (±2.5)	530 (±2.5)	-40	685 (±2.5)	-22
MB adsorption	g/100g	21.4 (±0.5)	13.6 (±0.5)	-36	11.7 (±0.5)	-45
Pore volume 25-48000 nm	cm ³ /g	0.213	0.21	-1	0.215	+1
Pore volume 1-25 nm	cm ³ /g	0.131	0.206	+57	0.110	-16
Pore volume < 1 nm	cm ³ /g	0.372	0.287	-23	0.287	-23
B.E.T. Surface	m ² /g	924 (±13)	666 (±13)	-28	705 (±13)	-24

*compared to fresh GAC

The BET surface area of surface water (SW) preloaded GAC and wastewater (WW) preloaded GAC is similar, and yields a reduction of 24-28 % with respect to virgin GAC. SW preloaded GAC appears to have slightly less accessible surface area based on BET surface area measurements, and this is confirmed by the iodine number. This can be related to the larger fraction of medium-sized humic substances in surface water, which had a larger average size than those in wastewater.

Methylene blue (MB) adsorption was slightly lower on wastewater preloaded GAC. As wastewater contains higher concentrations of large biopolymers (MW>20,000 g/mol), this might be related to partial pore blocking of the pore mouth by these molecules, blocking pore access for methylene blue, but not for iodine or nitrogen. However, the differences in methylene blue adsorption can also be related to differences in surface charge.

The mesopore volume measured on surface water preloaded GAC was unrealistic, as the measured volume exceeded that of fresh GAC. This cannot be explained by the narrowing of macro pores, as the macro pore volume remained unchanged.

3.3 Effect of GAC Preloading and Water Quality on Equilibrium removal

The pH levels of the surface water and wastewater were 8.1 and 7.4, respectively. This variation of pH will have limited effect on the charge of the pharmaceuticals. Negatively charged solutes are fully dissociated at both pH values. Of the positively charged solutes, terbutaline (pKa 8.8) is protonated for 83% at pH 8.1. Protonation of the other pharmaceuticals and protonation at pH 7.4 is higher.

The point of zero charge was not determined for the fresh GAC, but lies typically between 7 and 8 (Bjelopavlic et al., 1999). In this range, the surface charge of fresh GAC is expected to be slightly negatively charged at pH 8.1, and neutral or slightly positively charged at pH 7.4. Preloaded GAC obtains a significant negative surface charge (Newcombe, 1994). As such, charge interactions are expected to be limited on fresh GAC, and significant on preloaded GAC. Hydrophobic interaction is expected to be more significant for negatively charged solutes than for neutral or positively charged solutes, based on log D values.

3.3.1 Surface Water Experiments

In ultrapure water and using freshly regenerated GAC, most solutes were each removed at more than 85% at even the lowest GAC dose (Figure 1). When GAC was preloaded with either surface water, a strong decrease in removal of negatively charged solutes was observed, while for positively charged solutes, removal was barely affected. This can be explained by the negative surface charge that the GAC surface obtained due to NOM preloading, which resulted in the attraction of positively charged solutes and repulsion of the negatively charged solutes. Within the charged groups, more hydrophobic solutes (higher log D) generally showed higher removal. However, log D only partially explained differences within a charge group; the neutral Carbamazepine, and the negatively charged diclofenac and gemfibrozil showed lower removal than expected based on their log D values. The lower removal of carbamazepine might be related to its bulkier shape, with a cross section of approximately 5.8 Å. This may prevent access to (partially blocked) pores which are accessible to other solutes. No explanation was found for the relatively low removal of diclofenac and gemfibrozil. Despite the low log D values of positively charged solutes, their removal was higher than neutral and negatively charged solutes, demonstrating the relevance of charge interactions. In surface water, using freshly regenerated GAC, charge interactions were limited; negatively charged solutes showed only slightly lower removal than neutral solutes, which showed only slightly lower removal than positively charged solutes. This can be related to the lower surface charge of fresh GAC and to charge shielding by ions. Except for clofibrac acid, ibuprofen, and cyclophosphamide, all solutes within charge groups showed similar removal. In surface water using preloaded GAC, charge interactions were important. However, they were lower than when using ultrapure water due to charge shielding effects by ions present in natural water. Removal was reduced for positively charged solutes (up to 30%) and increased for negatively charged solutes (up to 18%).

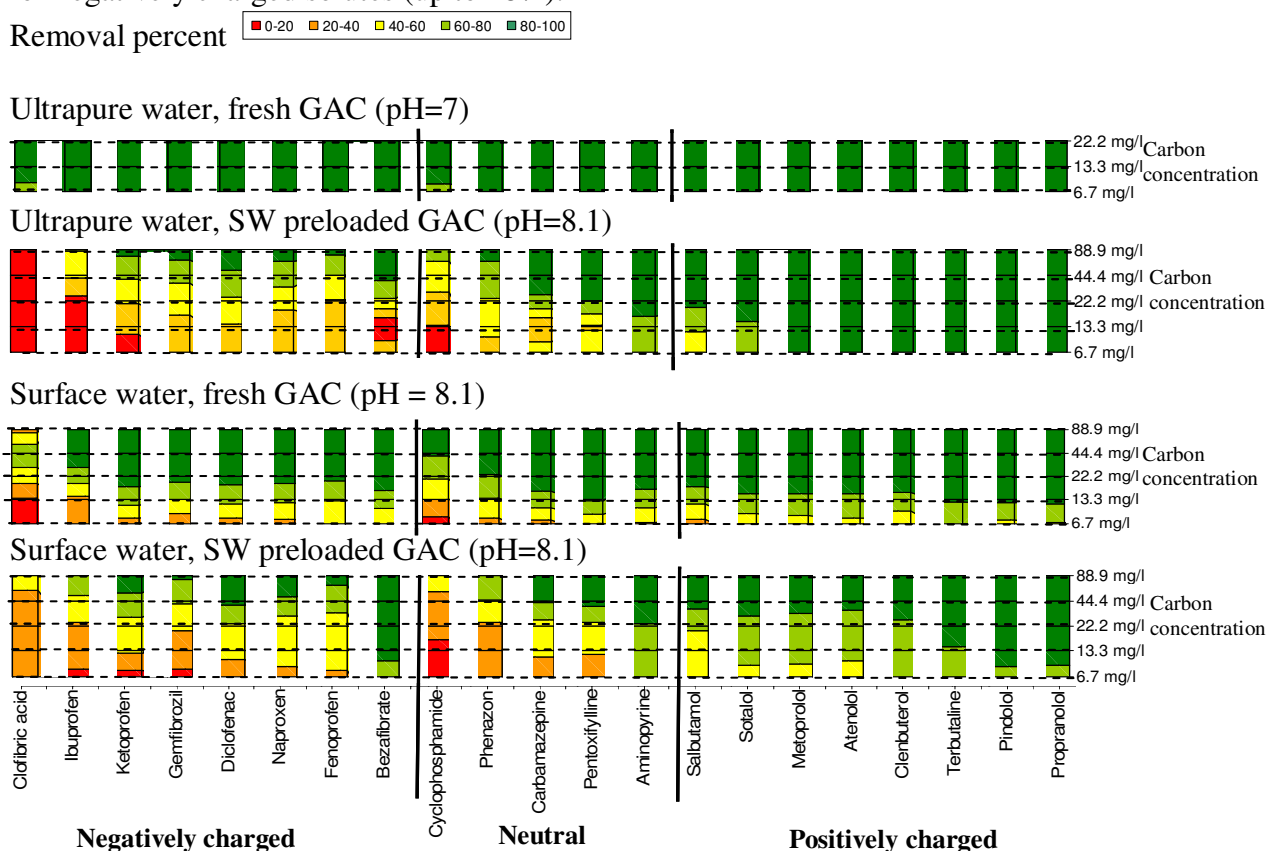


Figure 1: Pharmaceutical equilibrium removal on 6.7-88.9 mg/l fresh or preloaded GAC in ultrapure water and treated surface water

3.3.2 Wastewater experiments

In blank wastewater samples (GAC dose 0 mg/l), five pharmaceuticals were present in low concentrations after an equilibrium time of 8 weeks. This can be caused by binding with the NOM present in the water phase during the experiment, or by interference of NOM with the Solid phase extraction (SPE) concentration step in the analysis. These solutes were excluded in Figure 2.

In ultrapure water, pharmaceuticals were removed less effectively on wastewater preloaded GAC than with surface water preloaded GAC, with a typical reduction of removal of 10-50% for charged and neutral pharmaceuticals at a GAC concentration of 6.7 mg/l. This reduction cannot be contributed differences in pore blocking, as Table 4 indicates that pore blocking is even lower on wastewater preloaded GAC as compared with surface water preloaded GAC. Based on SUVA and HOC fraction from the LC-OCD analysis, wastewater NOM is more hydrophobic than surface water NOM. As a consequence, competition of pharmaceuticals with NOM is higher for wastewater preloaded NOM than for surface water preloaded NOM. This indicates that the hydrophobicity of the preloaded NOM has a greater effect on pharmaceutical removal than does pore blocking.

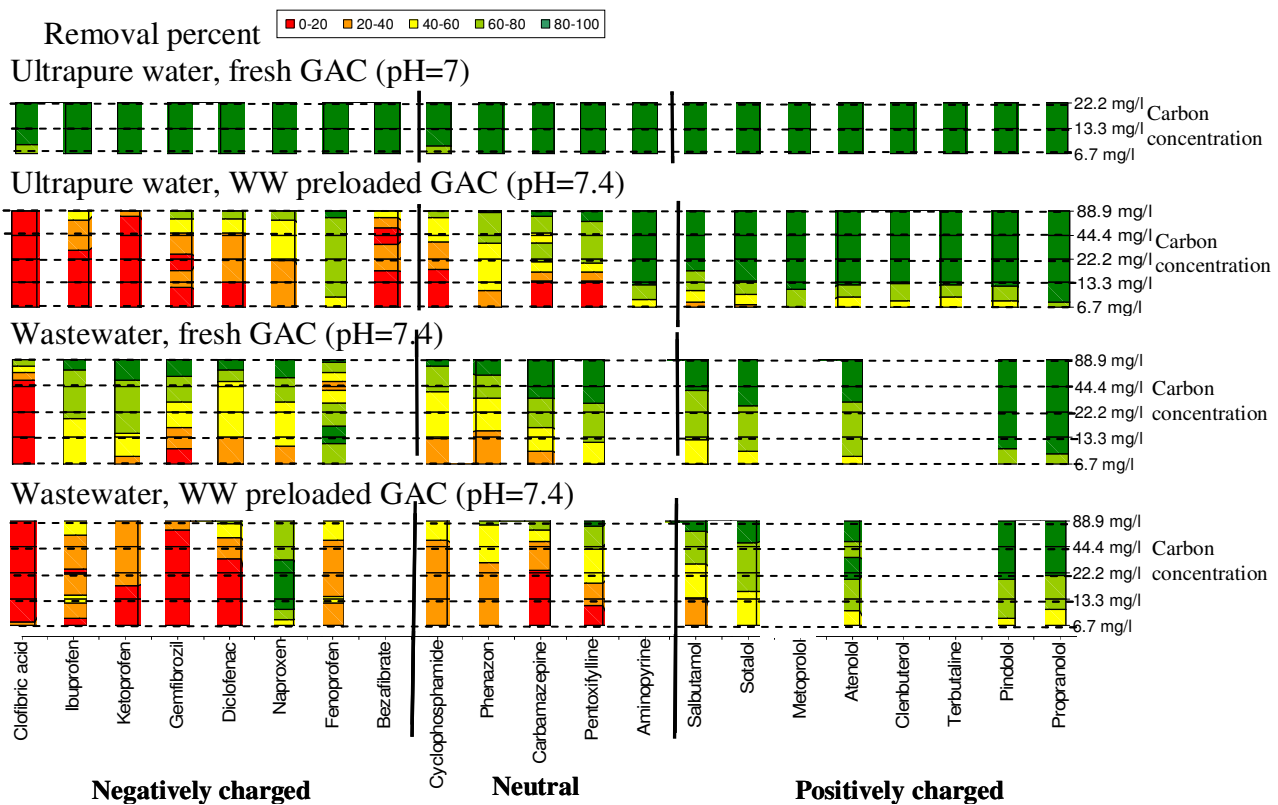


Figure 2: Pharmaceutical equilibrium removal on 6.7-88.9 mg/l fresh or preloaded GAC in ultrapure water and wastewater

4. Conclusions

The influence of NOM competition and pore blocking could not be separated. With respect to virgin carbon, the reduction of available surface area is similar for both preloaded carbons (24-28% reduction), with a slightly lower reduction of surface area for wastewater preloaded GAC.

Wastewater NOM contained fractions with smaller molecular weight and higher SUVA than surface water NOM, indicating a higher potential for adsorption competition. When comparing pharmaceutical removal on wastewater preloaded GAC and surface water preloaded GAC, 10-50% lower pharmaceutical removal was observed for wastewater preloaded GAC at a GAC dose of 6.7 mg/l. This effect was related to higher competition with wastewater NOM, and may indicate that NOM competition influences pharmaceutical removal more than pore blocking under the experimental conditions applied in this paper. More variations in GAC type and natural water type are needed to generalize this finding. Log D and charge interaction both had significant influence on pharmaceutical removal and should be considered when constructing a-priori prediction models. Preloaded GAC obtains a negative surface charge as a consequence of accumulation of NOM on its surface. The negatively charged pharmaceuticals had higher log D values than positively charged pharmaceuticals (0.57 to 2.77 versus -1.7 – 1.48, respectively). When only hydrophobic interactions are considered, higher removal of negatively charged solutes is expected. However, considerably higher removal of positively charged solutes was observed on preloaded carbon compared to removal of negatively charged solutes (32-98% removal vs 0-58% removal, respectively, at 6.7 mg/l GAC). This indicates that charge interactions are a dominant removal mechanism on preloaded carbon.

Within a charge group, pharmaceuticals with higher log D values showed higher removal. Charge shielding by ions in natural water could reduce the influence of charge interaction, by increasing removal of negatively charged solutes by up to 18% and reducing removal of positively charged solutes by up to 30%.

Acknowledgements

This research is based upon work supported by VEWIN, the association of drinking water companies in the Netherlands, and Waternet. Any opinions, findings, conclusions or recommendations expressed in this publication are those of the authors and do not necessarily reflect the views of the supporting organization.

References

- Bestani, B., N. Benderdouche, B. Benstaali, M. Belhakem, A. Addou. (2008). Methylene blue and iodine adsorption onto an activated desert plant, *Bioresource Technology*, 99, 8441-8444,
- Bjelopavlic, M., Newcombe, G., and Hayes, R. (1999). Adsorption of NOM onto activated carbon: effect of surface charge, ionic strength, and pore volume distribution, *Journal of colloid and interface science*, 210, 271-280,
- Fairey, J. L., Speitel Jr., G. E., and Katz, L. E. (2006). Impact of natural organic matter on monochloramine reduction by granular activated carbon: the role of porosity and electrostatic surface properties, *Environmental science and technology*, 40, 4268-4273,
- Gorham, J. M., Wnuk, J. D., Shin, M., and Fairbrother, H. (2007). Adsorption of natural organic matter onto carbonaceous surfaces: atomic force microscopy study, *Environmental science and technology*, 41, 1238-1244,
- Hernando, M. D., Mezcuca, M., Fernandez-Alba, A. R., and Barcelo, D. (2006). Environmental risk assessment of pharmaceutical residues in wastewater effluents, surface waters and sediments, *Talanta*, 69, 334-342,

- Kilduff, J. E., Karanfil, T., and Weber, W. J. (1998). Competitive effects of nondisplaceable organic compounds on trichloroethylene uptake by activated carbon. II. Model verification and applicability to natural organic matter, *Journal of colloid and interface science*, 205, 280-289,
- Matsui, Y., Knappe, D. R. U., and Takagi, R. (2002). Pesticide adsorption by granular activated carbon adsorbers. 1. Effect of natural organic matter preloading on removal rates and model simplification, *Environmental science and technology*, 36, 3426-3431,
- Mianowski, A., Owczarek, M., and Marecka, A. (2007). Surface area of activated carbon determined by the iodine adsorption number, *Energy sources, part A*, 29, 839-850,
- Mompelat, S., Le Bot, B., and Thomas, O. (2009). Occurrence and fate of pharmaceutical products and by-products, from resource to drinking water, *Environment international*, 35, 803-814,
- Moreno-Castilla, C. (2004). Adsorption of organic molecules from aqueous solutions on carbon materials, *carbon*, 42, 83-94,
- Newcombe, G. (1994). Activated carbon and soluble humic substances: adsorption, desorption, and surface charge effects, *Journal of colloid and interface science*, 164, 452-462,
- Newcombe, G., and Drikas, M. (1997). Adsorption of NOM onto activated carbon: electrostatic and non-electrostatic effects, *Carbon*, 35, 1239-1250,
- Pelekani, C., and Snoeyink, V. L. (1999). Competitive adsorption in natural water: role of activated carbon pore size, *Water research*, 33, 1209-1219,
- Redding, A. M., Cannon, F. S., Snyder, S. A., and Vanderford, B. J. (2009). A QSAR-like analysis of the adsorption of endocrine disrupting compounds, pharmaceuticals, and personal care products on modified activated carbons, *Water research*, 43, 3849-3861,
- Sacher, F., Lange, F. T., Brauch, H.-J., and Blankenhorn, I. (2001). Pharmaceuticals in groundwaters. Analytical methods and results of a monitoring program in Baden-Württemberg, Germany, *Journal of chromatography A*, 938, 199-210,
- Snyder, S. A. (2008). Occurrence, treatment, and toxicological relevance of EDCs and Pharmaceuticals in water, *Ozone science and engineering*, 30, 65-69,
- Ternes, T. A., Meisenheimer, M., McDowell, D., Sacher, F., Brauch, H.-J., Haist-Gulde, B., Preuss, G., Wilme, U., and Zulei-Seibert, N. (2002). Removal of pharmaceuticals during drinking water treatment, *Environmental science and technology*, 36, 3855-3863,
- Westerhoff, P., Yoon, Y., Snyder, S., and Wert, E. (2005). Fate of endocrine-disruptor, pharmaceutical, and personal care product chemicals during simulated drinking water treatment processes, *Environmental science and technology*, 39, 6649-6663,
- Worch, E. (2008). Fixed-bed adsorption in drinking water treatment: a critical review on models and parameter estimation, *Journal of Water Supply: Research and Technology-Aqua*, 57, 171-183,
- Zwiener, C. (2007). Occurrence and analysis of pharmaceuticals and their transformation products in drinking water treatment, *Analytical and Bioanalytical Chemistry*, 287, 1159-1162,

Chapter 6

Zeolites for nitrosamine and pharmaceutical removal from demineralised and surface water: mechanisms and efficacy

D.J. de Ridder¹*, J.Q.J.C. Verberk¹), S.G.J. Heijman¹), G.L. Amy^{1,2}) J.C. van Dijk¹)

1) Delft University of Technology, P.O. box 5048, 2600 GA Delft, The Netherlands

2) King Abdullah University of Science and Technology, Thuwal, Saudi Arabia

* Corresponding author

Email: d.j.deridder@tudelft.nl

Telephone: +31 (0)15 2786588

Postal address: see affiliation 1)

Separation and Purification Technology 89 (2012) 71-77

Abstract

Zeolites with a high Si/Al ratio can be used as selective adsorbents in water treatment, targeting organic micropollutants which are removed poorly with activated carbon. Due to size exclusion, many Natural Organic Matter (NOM) components cannot access the pores, thus limiting adsorption competition between organic micropollutant and NOM. Furthermore, zeolite channel diameters are close to molecule diameters, which results in strong van der Waals interaction.

MOR200 and ZSM5, the two most hydrophobic zeolites, showed the highest removal of neutral nitrosamines in demineralised water, with higher efficacy than activated carbon. DAY and MOR30, which were relatively hydrophilic zeolites, did not show appreciable removal of any of the nitrosamines. When nitrosamines were adsorbed from surface water, there was no influence of competition with, or pore blockage by, NOM components on nitrosamine removal for ZSM5 zeolite, in contrast to activated carbon.

Repulsion of negatively charged pharmaceuticals was significant for ZSM5, which had a Si/Al ratio of 80. MOR200 had a Si/Al ratio of 200, indicating a lower Al content than ZSM5 and, as such, a lower negative surface charge. Charge effects were not observed for MOR200. A relationship was found between the Stokes diameter of the pharmaceuticals and nitrosamines, and their removal by ZSM5 and MOR200, indicating that a “close fit” adsorption mechanism is more likely than hydrophobic interaction in these zeolites.

Due to their selective nature, adsorption on zeolites should only be considered as an additional treatment step to existing processes, dedicated for the removal of specific organic micropollutants. Less specific treatment techniques, such as activated carbon filtration, are still required to ensure a broad barrier for organic micropollutants in water treatment.

Keywords: zeolite, adsorption, nitrosamine, pharmaceutical

1. Introduction

Zeolites are a group of minerals which can be used in water treatment as a selective ion exchange resin for NH_4^+ removal or as a selective adsorbent [1]. This selectivity can be attributed to the small pore size and small variation in pore size distribution. Zeolites consist of a framework of SiO_4 and AlO_4 in a tetrahedral structure, which are linked together by oxygen atoms. These tetrahedral structures can be ordered in various distinct ways, such as the MFI, Mordenite (MOR) or Faujasite (FAU) frameworks (Figure 1).

The most well known zeolites with the MFI framework are ZSM5 zeolite and silicalite. This framework consists of straight channels with dimensions $5.3 \times 5.6 \text{ \AA}$ ($0.53 \times 0.56 \text{ nm}$). These

channels are interconnected with slightly smaller channels, with dimensions 5.1*5.5 Å. The framework of Mordenite zeolite consists of straight, parallel channels of 6.5*7.0 Å and 2.6*5.7 Å. There are no interconnecting channels in the MOR framework. Y Zeolite is of the family of zeolites with the Faujasite framework type. In this framework, 3-dimensional “cages” are connected with each other, having an internal diameter of about 13 Å and four openings with a diameter of 7.4 Å.

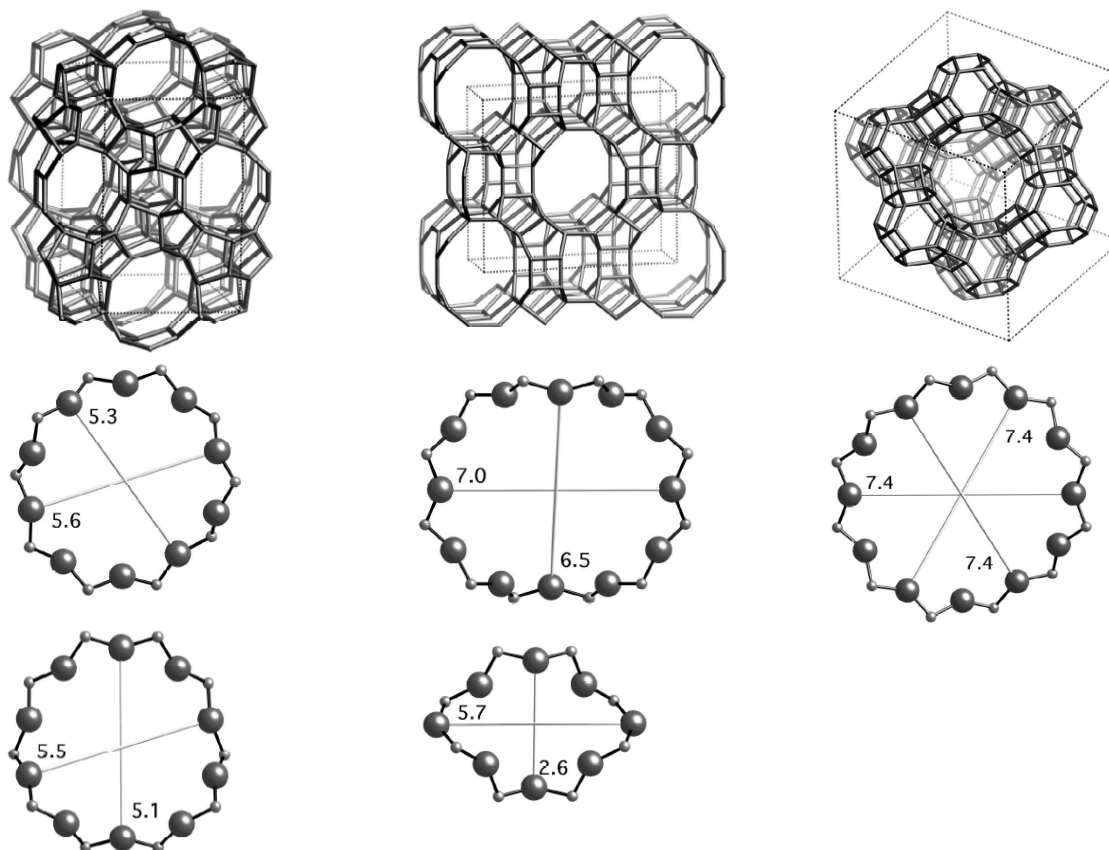


Figure 1: Zeolite frameworks MFI (left), MOR (middle) and FAU (single cage) (right)
 Source: Baerlocher et al. (2001) (www.iza-structure.org/databases)

Zeolites can be interesting to use for adsorption of organic micropollutants, as they have some distinct advantages over activated carbon:

Most of the natural organic matter (NOM) components present in water cannot enter pores <10 Å [2, 3]. As such, adsorptive competition of NOM with organic micropollutants is minimal for zeolites [4-6]. Adsorption kinetics can however be slower in the presence of NOM [5].

Zeolites are stable over a wide range of temperatures and acidic conditions. As such, in contrast to carbon, the loss of material during regeneration is not to be expected [7].

It should be stressed that activated carbon is effective for adsorption of a broad range of solutes (barrier-function), while zeolites are selective. Due to their selectivity, zeolites should not be regarded as a replacement for activated carbon, but rather as additional, dedicated adsorbent for a limited amount of target solutes. Target solutes can be solutes which require high removal due to high influent concentrations and/or strict effluent regulations, or which show poor removal with activated carbon.

Various authors have related zeolite hydrophobicity to aluminum content where a higher aluminum content indicates higher affinity for water [8-10]. Specific mechanisms for zeolite-water interaction are proposed by Bolis and Busco (2006);

electron pair donor-acceptor interaction between aluminum and pollutant. This occurs at Lewis acid sites and has the highest bonding energy (109-160 kJ/mol)

H bond donor-acceptor interaction. This can occur at Brønsted acid sites (Si-OH+-Al-) and silanol sites (Si-OH), with a bonding energy of 65 kJ/mol and 49 kJ/mol, respectively.

Silanol sites are created by defects in the zeolite framework and can explain that even all-silica zeolites can adsorb water.

Generally, the removal of organic micropollutants from aqueous solution is enhanced when zeolites with high Si/Al ratio (i.e. hydrophobic zeolites) are used [7, 10-13]. However, it was found that above a Si/Al ratio of 90, the removal of MTBE on ZSM5 zeolite did not improve [4].

The channel dimensions of the zeolites are another important aspect affecting solute removal. Besides size exclusion effects, it was also observed that solutes, which do fit in the channels of ZSM5, MOR or Y zeolite, were removed more effectively when they fit tightly, because of larger van der Waals interactions [7, 14]. An alternative or additional explanation is that in the small channels of ZSM5 zeolite (about 5.5 Å) water is unable to form a structure which is typical for its liquid form and is actually present as vapor, making it easier for solutes to transport through the channels of ZSM5. In the larger cages of Y zeolite, water is still present in its liquid form [15].

In the literature, only limited solutes were used to investigate the importance of zeolite hydrophobicity or zeolite channel diameter. As such it is difficult to separate and generalize removal mechanism in order to assess the adsorption efficacy for other solutes. A broader set of solutes was used by [16], and differences in solute adsorption were attributed mainly to the close-fit mechanism.

Nitrosamines, among which NDMA is the most well known, are potent carcinogens [17].

They can enter the environment via industrial waste disposal, or can be formed during chlorination. A wide range of pharmaceuticals have been detected in surface waters at trace levels, and mainly originate from discharges of treated municipal wastewater [18, 19].

This research aims to investigate the influence of solute size and hydrophobicity on adsorption on zeolites. For this purpose, a broad set of nitrosamines and pharmaceuticals is selected that vary in these aspects. Furthermore, the influence of NOM on nitrosamine adsorption is investigated.

2. Materials and methods

A set of seven neutral nitrosamines was selected with differences in hydrophobicity and molecular size (Table 1). An additional set of 15 neutral, positively or negatively charged pharmaceuticals, varying in hydrophobicity and size, is shown in Table 2. Solute molecular weight (MW) and log Kow values were obtained from Chem ID plus. Hydrophobicity was expressed as log D to include the influence of solute charge, according to [20]:

$$\text{Acids: } \log D = \log K_{ow} - \log(1 + 10^{(pH - pKa)})$$

$$\text{Bases: } \log D = \log K_{ow} - \log(1 + 10^{(pKa - pH)})$$

For neutral solutes, log Kow and log D are equal. For charged solutes, these equations were used up to a difference of 2 pH units from the solute pKa values.

The molecule's Stokes diameter was calculated with:

$$D_{Stokes} = \frac{2k_B T}{6\pi\eta D_L}$$

Where k_B ($1.38 \cdot 10^{-23}$ J/K) is the Boltzmann constant, T (K) is the temperature, η (m^2/s) is the kinematic viscosity of water, D_L (cm^2/s) is the diffusion coefficient.

The diffusion coefficient was calculated with the Gnielinski correlation [21]:

$$D_L = \frac{13.26 \cdot 10^{-5}}{\mu^{1.14} V^{0.589}}$$

Where μ (centipoise (= 0.001 N s/ m^2)) is the dynamic viscosity of water and V (cm^3/mol) is the molar volume of the solute. The molar volume and molecule dimensions (dimensions of the closest fitting “box” around the molecule) were calculated using Hyperchem 7.0 after geometric optimization.

Table 1: Nitrosamine properties

Name	CAS	Log D (pH 6)	MW (g/mol)	Stokes diameter (Å)	Dimensions (Å*Å*Å)
N-Nitrosodimethylamine (NDMA)	62-75-9	-0.57	74.0	2.6	1.8*3.8*4.0
N-Nitrosomorpholine (NMOR)	59-89-2	-0.44	116.0	3.0	3.1*4.6*5.1
N-Nitrosomethylethylamine (NEMA)	10595-95-6	0.04	88.15	2.9	2.7*3.5*5.3
N-Nitrosopiperidine (NPIP)	100-75-4	0.36	114.0	3.1	3.1*4.7*5.7
N-Nitrosodiethylamine (NDEA)	55-18-5	0.48	102.0	3.1	2.8*4.1*6.3
N-Nitrosodi-n-propylamine (NDPA)	621-64-7	1.36	130.0	3.5	3.7*4.2*7.6
N,N-Dibutylnitrosamine (NDBA)	924-16-3	2.63	158.0	4.0	3.6*4.2*9.9

Table 2: Pharmaceutical properties

Name	CAS	Log D (pH 6)	pKa (charge)	MW (g/mol)	Stokes diameter (Å)	Dimensions (Å*Å*Å)
Atenolol	29122-68-7	-1.84	9.43 (+)	266	4.9	3.8*6.7*14.4
Metropolol	56392-17-7	-0.12	9.49 (+)	257	5.1	4.1*6.2*16.1
Metformine	1115-70-4	-4.60	11.9 (+)	129	3.4	1.8*4.4*7.6
Lidocaine	137-58-6	0.44	8.0 (+)	234	4.6	5.8*5.9*8.7
Lincomycine	154-21-2	-1.14	7.7 (+)	407	5.8	5.3*7.2*15.6
Paracetamol	103-90-2	-1.54	9.38 (+)	151	3.5	1.9*4.5*9.2
Ifosfamide	3778-73-2	0.86	n/a (0)	261	4.3	5.2*6.0*7.8
Cyclophosphamide	50-18-0	0.63	n/a (0)	261	4.2	4.5*5.6*8.0
Carbamazepine	298-46-4	2.45	n/a (0)	236	4.3	4.7*6.3*9.0
Primidone	125-33-7	0.91	n/a (0)	218	4.1	4.7*6.1*8.5
Sulfamethoxazole	723-46-6	0.41	5.7 (-/0)	253	4.3	4.5*6.7*8.5
Gemfibrozil	25812-30-0	3.21	4.45 (-)	250	4.8	4.5*6.7*10.8
Naproxen	22204-53-1	1.47	4.3 (-)	230	4.3	4.4*5.4*11.4
Phenazon	60-80-0	-1.62	1.4 (-)	188	3.9	3.1*5.3*9.5
Ketoprofen	22071-15-4	1.56	4.45 (-)	254	4.6	4.7*6.1*10.2
Clofibric acid	882-09-7	0.56	4 (-)	214	4.1	3.8*5.7*9.8

Equilibrium adsorption was determined with batch experiments. Experiments were conducted in demineralised water and in surface water obtained from Weesperkarspel treatment plant (Waternet, the Netherlands), after coagulation, flocculation and sand filtration. This water had a TOC content of 5.4 mg C/l, a SUVA of 1.64 L/mg*m, and a pH value of 8.1. The pH value of demineralised water was 6.0.

ZSM-5 zeolite (CBV8014) and DAY zeolite (CBV780) were obtained from Zeolyst. Both Mordenite zeolites (MOR30 (HSZ-660HOA) and MOR200 (HSZ-690HOA)) were obtained from Tosoh Corporation. All zeolites were in powdered form. Granular activated carbon (GAC 830P) was obtained from Norit, and was ground to powder before use. Basic properties of the (ground) adsorbents used in this study are shown in Table 3. Zeolite hydrophobicity is determined by microcalorimetry (Parr 6755 solution calorimeter), measuring the temperature increase when 1 g of adsorbent is contacted with 100 ml water. Additionally, water vapour uptake experiments were carried out, where the adsorbents are placed in a moisture-conditioned room for 26 days. In preparation for these experiments, the zeolites and carbon were dried for at least 3 hours at 105 °C.

The initial concentration of each of the nitrosamines was 15 µg/l, and the initial concentration of each of the pharmaceuticals was 2 µg/l. The set of nitrosamines and the set of pharmaceuticals were dosed as a mixture. The adsorbent concentration was varied between 10 and 200 mg/l for the nitrosamines set, and between 2.5 and 1000 mg/l for the pharmaceutical set. A blank measurement (0 mg/l adsorbent dosed) was included in each isotherm series. The samples were mixed using a magnetic stirrer. After 24 hours, samples were filtrated through a 1.2 µm glassfiber filter and sent to an external laboratory (Nitrosamines: TZW, Karlsruhe, GC/MS/MS)(Pharmaceuticals: HWL, Haarlem, UPLC/MS/MS) for analysis.

Table 3: Adsorbent characteristics

Adsorbent	Surface area (m ² /g)	Cation	Si/Al ratio	Pore diameter (Å)	Heat of Immersion (mJ/m ²)	H ₂ O vapour uptake (mg/m ²)
Mordenite (MOR30)	400	H+	30	6.5	19.2	0.57
Mordenite (MOR200)	420	H+	200	6.5	12.3	0.45
ZSM5	425	NH ₄ ⁺	80	5.3	7.3	0.53
DAY	780	H+	80	7.4	32.6	0.67
GAC830P	807	-	-	range	24.6	0.66

3. Results and discussion

3.1 Hydrophobicity

Based only on Si/Al ratios, MOR200 is expected to be the most hydrophobic zeolite and MOR30 the least hydrophobic. Although ZSM5 and DAY have the same Si/Al ratio, ZSM5 is expected to be more hydrophobic due to the smaller pore size [15]. The results of the water vapour uptake test and calorimetric measurements, as shown in Table 3, partly confirm these expectations. MOR200 is indeed more hydrophobic than MOR30, as indicated by its lower heat of immersion and water vapour uptake, and ZSM5 is indeed more hydrophobic than DAY. There is some disagreement when comparing ZSM5 and MOR200, as heat of immersion measurements indicate that ZSM5 would be more hydrophobic, while water vapour uptake indicate that MOR200 is more hydrophobic. Calorimetric measurements are fast (typically 15-30 minutes). ZSM5 is the zeolite with the smallest pore size. Possibly, the complete surface of ZSM5 was not wetted in the timeframe of the experiment, and thus did not produce heat. GAC830P is less hydrophobic than MOR30, but more hydrophobic than DAY.

3.2 Removal of nitrosamines in demineralised water

NDMA and NEMA, two of the smallest and most hydrophilic nitrosamines, were not adsorbed onto any of the adsorbents. NMOR could only be removed by ZSM5, NPIP only by ZSM5 and MOR200, and the larger and more hydrophobic nitrosamines NDEA, NDPA, NDPA were removed by ZSM5, MOR200 and GAC830P. The hydrophilic zeolites MOR30

and DAY were unable to remove any of the nitrosamines. The experimental results are summarized in Table 4, where the Freundlich parameters as calculated from the adsorption isotherms are given.

Table 4: Freundlich parameters KF (($\mu\text{g/g}$)/(μg)ⁿ) and nF (-) of adsorption isotherms of nitrosamines in demineralised water

Nitrosamine	ZSM5	MOR200	GAC830P
NDMA	n/a 1)	n/a 1)	n/a 1)
NEMA	n/a 1)	n/a 1)	n/a 1)
NMOR	KF=17 ; nF=1.04	KF=2 ; nF=1.7	n/a 1)
NPIP	KF=491 ; nF=1.11	KF=187 ; nF=0.99	n/a 1)
NDEA	KF=303 ; nF=1.06	KF=43 ; nF=0.65	KF=28 ; nF=1.02
NDPA	KF=9.04*104 ; nF=1.2	KF=1574 ; nF=0.91	KF=832 ; nF=0.54
NDBA	Only 2 datapoints, removal >NDPA	Complete removal	KF=4141 ; nF=0.48

No removal observed at maximum adsorbent dose

Other authors confirmed low removal of NDMA on GAC [22-25]. In pilot studies with GAC, it was found that the moment of breakthrough was shortest for NDMA, followed by NMOR, followed by NDEA [22]. This was explained by differences in hydrophobicity by the authors. When deriving interaction energies between nitrosamines and the ZSM5 zeolite framework using molecular modeling, NDMA was found to have the lowest interaction energy [26]. The interaction energies of NEMA and NDEA with the zeolite surface were similar, and higher than NDMA. According to our findings, NDEA is adsorbed more effectively than NEMA. Based on the higher octanol-water partitioning coefficient of NDEA, expulsion from the water phase to the zeolite surface is thermodynamically more favorable for NDEA than for NEMA.

The dominant removal mechanism, i.e. hydrophobic interaction or close fit of the solute in the adsorbent pore channel, cannot be strictly separated based on the set of nitrosamines used as the larger nitrosamines are also the more hydrophobic ones.

MOR30 is more hydrophilic than MOR200, while the zeolite framework is the same. As such, differences in nitrosamine removal can be attributed mainly to differences in zeolite hydrophobicity. Due to higher affinity of water with the surface of MOR30 as compared to MOR200, the water present inside the zeolite pores might be harder to displace and allow nitrosamine molecules to diffuse inside the pore. The activated carbon GAC830P is relatively hydrophilic compared to MOR200 and ZSM5, and shows lower nitrosamine removal. However, MOR30 shows no nitrosamine removal at all, while it is more hydrophobic than GAC830P. Possibly, the larger influence of solute hydrophobicity for solute removal onto MOR 30 zeolite is related to pore structure. Mordenite zeolite holds singular, straight channels, while activated carbon consists of a network of interconnected pores. These pores can be blocked by water clusters that form around active sites, which are typically oxygen-containing functional groups for activated carbon [27, 28]. When a pore of mordenite is blocked by a water cluster, a larger part of the adsorption surface is potentially made unavailable as compared to activated carbon, as there are no alternative diffusion routes for the pollutants.

3.3 Influence of surface water

To assess the influence of NOM on nitrosamine removal, equilibrium batch experiments in surface water were executed with ZSM5, the zeolite with the smallest pore size and high nitrosamine removal, and the activated carbon GAC830P. In Figure 2, it can be observed that the results for the equilibrium batch experiments in demineralised water and surface water are similar for ZSM5. This indicates that NOM components are effectively excluded from the zeolite pores, and do not block the zeolite pores. The limited influence of NOM for solute removal onto zeolites was also confirmed by other authors [4-6, 16]. Figure 3 shows that NOM has a clear impact on nitrosamine removal on GAC830P, lowering the equilibrium carbon load by 0.2-0.6 log units.

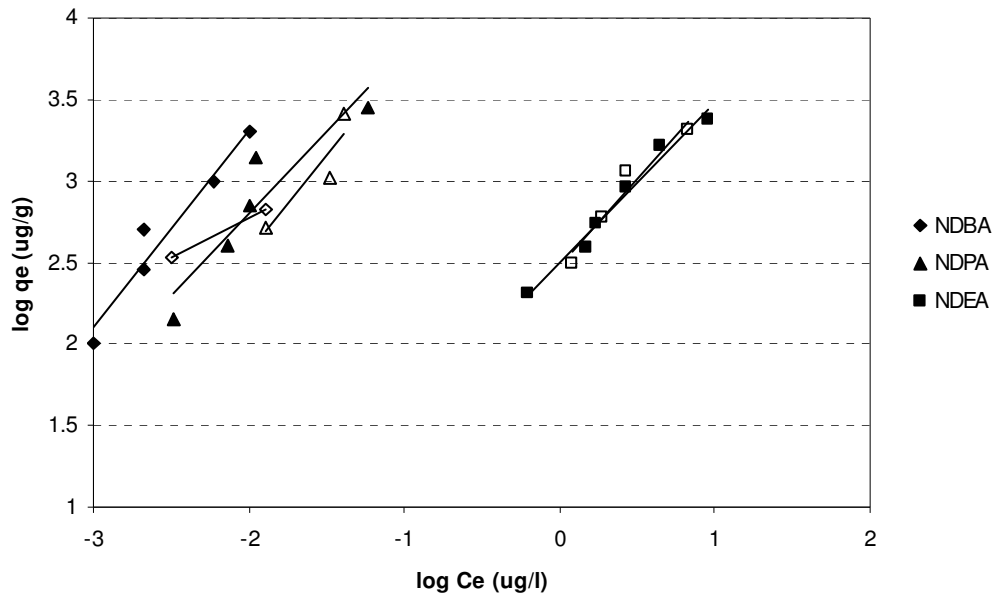


Figure 2: Nitrosamine adsorption isotherms for ZSM5 in demineralised water (open symbols) and surface water (closed symbols).

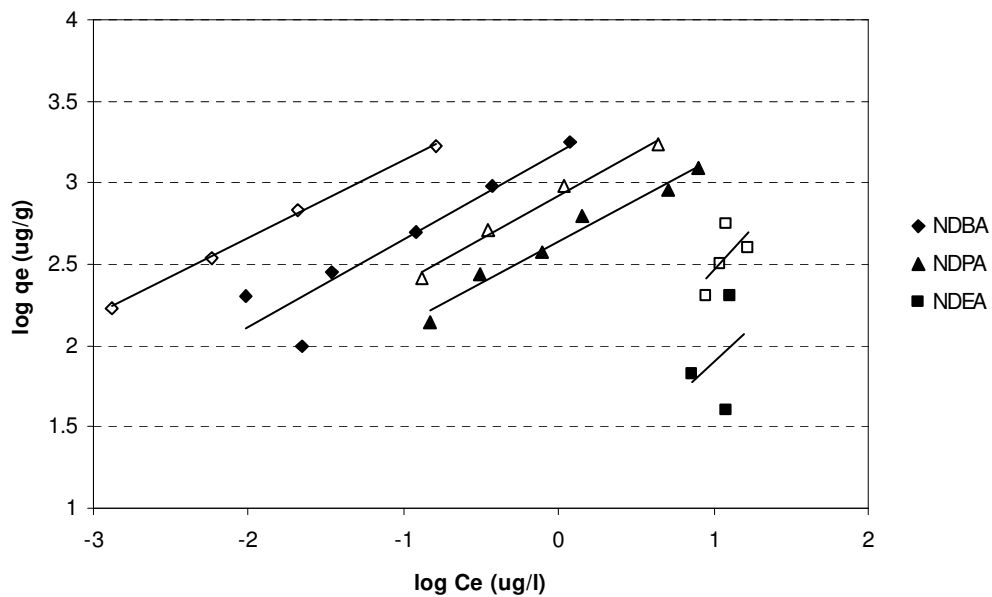


Figure 3: Nitrosamine adsorption isotherms for GAC830P in demineralised water (open symbols) and surface water (closed symbols).

3.4 Removal of pharmaceuticals on ZSM5 and MOR200 in demineralised water

The Freundlich parameters derived from the equilibrium adsorption experiments with the set of pharmaceuticals are presented in Table 5. The adsorption isotherm for Metformine, Lidocaine and Paracetamol gave an S-shaped pattern. For these solutes, the Freundlich parameters cannot be determined from a log-log plot, and they were estimated by fitting the C_e vs q_e plot.

Table 5: Freundlich parameters KF (($\mu\text{g/g}$)/(μg)ⁿ) and nF of adsorption isotherms of pharmaceuticals in demineralised water

Pharmaceutical	ZSM5	MOR200
Atenolol	Complete removal	Complete removal
Metropolol	Complete removal	Complete removal
Metformine	KF: 1122 nF: 0.7 1)	KF:630 nF: 0.60 1)
Lidocaine	KF:133 nF: 0.84	KF: 5012 nF: 0.55 1)
Lincomycine	KF: 2339 nF: 1.18	KF: 145 nF: 0.68
Paracetamol	No appreciable removal	KF: 8 nF: 0.7 1)
Ifosfamide	KF: 459 nF: 0.88	KF: 51 nF: 0.81
Cyclophosphamide	KF: 22 nF: 0.90	KF: 132 nF: 0.82
Carbamazepine	No appreciable removal	KF: 31 nF: 0.80
Primidone	No appreciable removal	No appreciable removal
Sulfamethoxazole	KF: 63 nF: 1.18	KF: 36 nF: 0.91
Gemfibrozil	KF: $9.20 \cdot 10^{-5}$ nF: 0.4	Only 2 datapoints, high removal
Naproxen	No appreciable removal	KF: 597 nF: 0.39
Phenazon	Only 2 datapoints, limited removal	KF: 1054 nF: 0.41
Ketoprofen	Only 2 datapoints, limited removal	KF: 230 nF: 0.48
Clofibric acid	No appreciable removal	KF: 52 nF: 0.55

1) Freundlich parameters determined by fitting the Freundlich model to an S-shaped adsorption isotherm

From Table 5, it can be observed that negatively charged solutes, i.e. Gemfibrozil, Naproxen, Phenazon, Ketoprofen and Clofibric acid are not removed when using ZSM5, while their removal on MOR200 is comparable to that of neutral or positively charged solutes. This can be related to the lower Si/Al ratio of ZSM5, which implies a higher Al content, and thus a higher negative surface charge which repels negatively charged solutes. Positively charged solutes are removed well on both zeolites, with exceptional high removal of Atenolol and Metropolol.

Previous experiments with fresh GAC830P in surface water (reference [29]) showed better performance than ZSM5 zeolite in the adsorption of the five negatively charged solutes and the neutral cyclophosphamide and carbamazepine, with KF values ranging from 43 to 160. However, MOR200 outperformed GAC830P for all solutes.

When relating solute log D values to zeolite surface load (log q_e), no clear relationship was found (see supporting information S1, S2). However, as shown in Figure 4 and 5, a relationship was found between the solute Stokes diameter and zeolite surface load. Both figures include the measured surface loads of nitrosamines and pharmaceuticals at an equilibrium concentration of 1 $\mu\text{g/l}$. In addition, the solutes which were completely removed or not removed at all, are indicated with an error bar which represents a higher surface load than the highest measured datapoint, or lower surface loading than the lowest measured datapoint, respectively. For nitrosamines, both Figure 4 and 5 give a positive correlation between the solute Stokes diameter and the solute surface load. This is in agreement with the close-fit mechanism. For pharmaceuticals, this is also observed for MOR200 (Figure 4). This is less evident for ZSM5 (Figure 5), but this can be explained by charge interaction which reduces the removal of negatively charged solutes, as shown in Figure 6.

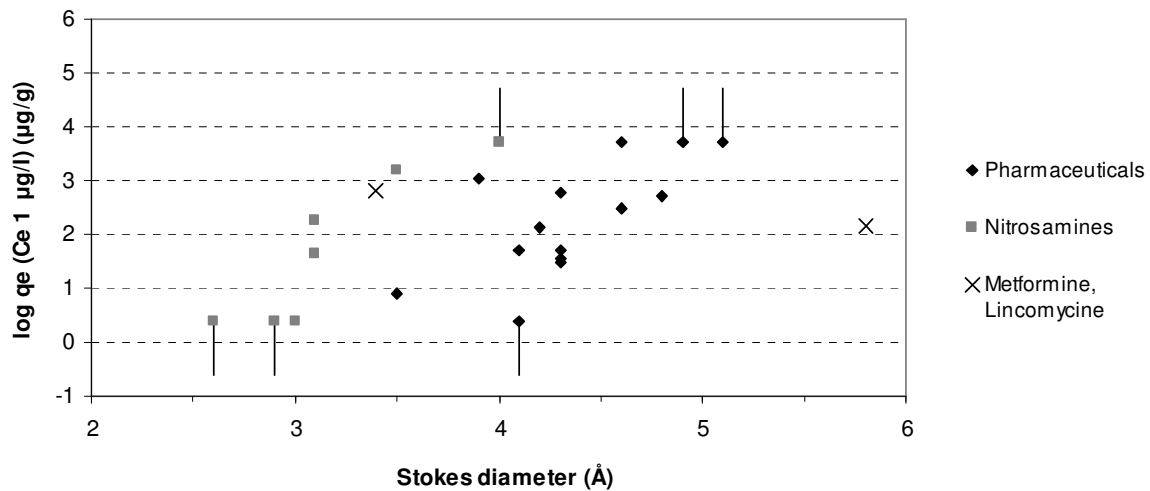


Figure 4: MOR200 surface load of nitrosamines and pharmaceuticals vs solute diameter. Solutes with either complete removal or no removal are indicated with error bars.

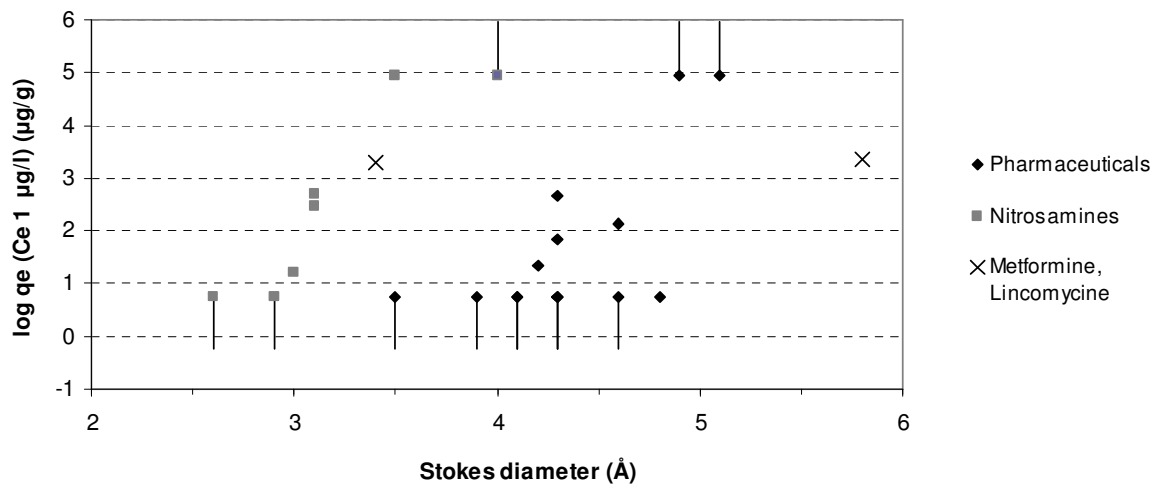


Figure 5: ZSM5 surface load of nitrosamines and pharmaceuticals vs solute diameter. Solutes with either complete removal or no removal are indicated with error bars.

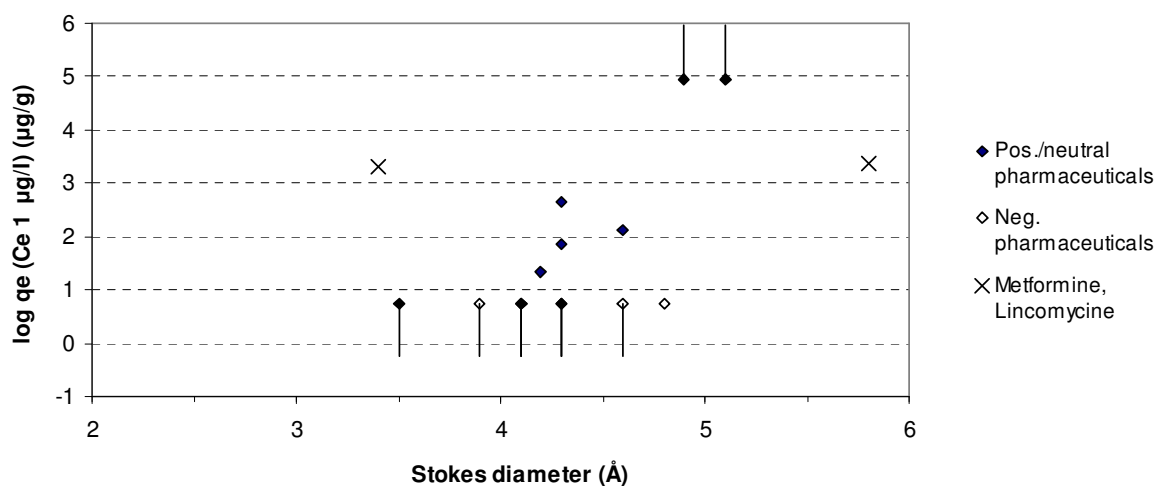


Figure 6: ZSM5 surface load of pharmaceuticals vs solute diameter.

Metformine and Lincomycine (both positively charged) are outliers for both zeolites, giving a higher and lower removal respectively than expected based on their Stokes diameter. Metformine shows relative high removal compared to the other pharmaceuticals given its Stokes diameter, but agrees rather well with the relation found for the nitrosamines. It is expected that this is related to the assumptions made when calculating the Stokes diameter for solutes; i.e. that solutes can be represented as a sphere. For small, compact molecules such as the nitrosamines and Metformine, this assumption might be more realistic than for the more extended pharmaceutical molecules which may approach cylindrical shapes instead of spheres. As such, the Stokes diameter may overestimate the effective size of pharmaceuticals considering pore entrance.

Lincomycine is the largest solute, and with a Stokes diameter of 5.8 Å, it is expected to fit in the pores of MOR200 (7.0 Å), but not in the pores of ZSM5 (5.6 Å). As Lincomycine also gives relatively low removal by MOR200 given its Stokes diameter, it is hypothesed that the optimal solute size for a close fit removal mechanism should be smaller than the pore size. This enables the water molecules (Stokes diameter 1.5 Å) that are originally present in the pores to pass the solute, thus enabling the solute to diffuse into the pores.

For ZSM5, the optimal solute diameter appears to be closer to the actual pore diameter than for MOR200. This might be related to the zeolite framework; ZSM5 is an interconnected framework, where water molecules can be displaced via several routes. MOR200 has single channel pores.

It was found that ZSM5 is still able to adsorb pharmaceuticals with a Stokes diameter >4.1 Å, and MOR200 those with a Stokes diameter >5.5 Å. Based on the Stokes diameter of water (1.5 Å), and the respective zeolite pore sizes, water molecules would not be able to pass these pharmaceutical molecules, and thus low removal would be expected. This is not observed, again supporting the statement that the Stokes diameter over-estimates the “real” diameter of the cylindrically shaped pharmaceuticals.

3.5. Practical applications

Zeolites are a specific adsorbent, and their specificity appears to depend mainly on zeolite pore size/shape, combined with molecule size/shape, although a minimum Si/Al ratio of 100-200 is required to limit the effect of pore blockage by water clusters. Size specificity limits the range of solutes that can be removed, but because of that, the solutes that can be removed benefit from lower adsorption competition. The zeolites in this study were effective to remove pharmaceuticals with a Stokes diameter of 5 Å, and nitrosamines with a Stokes diameter of 3.5 Å. The smallest nitrosamines (a.o. NDMA) could not be removed effectively with ZSM-5 or Mordenite. Following the findings of this research, it is expected that a zeolite with pore openings of 3 - 4 Å would be required for NDMA removal. Various zeolites are available with pore openings in this range, such as MCM-35, Merlinoite, Phillipsite, VPI-9, Yugawaralite.

4. Conclusions

MOR200 and ZSM5, the two most hydrophobic zeolites, showed the highest removal of neutral nitrosamines in demineralised water, with higher efficacy than activated carbon. DAY and MOR30, which were relatively hydrophilic zeolites, did not show appreciable removal of any of the nitrosamines. When nitrosamines were adsorbed from surface water, there was no influence of competition with, or pore blockage by, NOM components on nitrosamine removal for ZSM5 zeolite, in contrast to activated carbon.

Repulsion of negatively charged pharmaceuticals was significant for ZSM5, which had a Si/Al ratio of 80. MOR200 had a Si/Al ratio of 200, indicating a lower Al content than ZSM5 and, as such, a lower negative surface charge. Charge effects were not observed for MOR200.

A relationship was found between the Stokes diameter of the pharmaceuticals and nitrosamines, and their removal by ZSM5 and MOR200, indicating that a “close fit” adsorption mechanism is more likely than hydrophobic interaction in these zeolites.

Acknowledgements

This research is financially supported by VEWIN, the association of drinking water companies in the Netherlands. Any opinions, findings, conclusions or recommendations expressed in this publication are those of the authors and do not necessarily reflect the opinion of the supporting organisation.

References

- [1] D.R.U. Knappe, A. Rossner, S.A. Snyder, C. Strickland, Alternative adsorbents for the removal of polar organic contaminants, AWWA research foundation, 2007.
- [2] C. Pelekani, V.L. Snoeyink, Competitive adsorption in natural water: role of activated carbon pore size, *Water Res.*, 33 (1999) 1209-1219.
- [3] K. Ebie, F. Li, Y. Azuma, A. Yuasa, T. Hagishita, Pore distribution effect of activated carbon in adsorbing organic micropollutants from natural water, *Water Res.*, 35 (2001) 167-179.
- [4] D.R.U. Knappe, A. Rossner, Effectiveness of high-silica zeolites for the adsorption of methyl tertiary-butyl ether from natural water, *Water Sci. Technol.*, 5 (2005) 83-91.
- [5] H.-W. Hung, T.-F. Lin, Adsorption of MTBE from contaminated water by carbonaceous resins and mordenite zeolite, *J. Hazard. Mater.*, B135 (2006) 210-217.
- [6] H.-W. Hung, T.-F. Lin, C. Baus, F. Sacher, H.-J. Brauch, Competitive and hindering effects of natural organic matter on the adsorption of MTBE onto activated carbons and zeolites, *Environ. Technol.*, 26 (2005) 1371-1382.
- [7] M.A. Anderson, Removal of MTBE and other organic contaminants from water by sorption to high silica zeolites, *Environ. Sci. Technol.*, 34 (2000) 725-727.
- [8] V. Bolis, C. Busco, Thermodynamic study of water adsorption in high-silica zeolites, *J. Phys. Chem.*, 110 (2006) 14849-14859.
- [9] D.H. Olsen, W.O. Haag, W.S. Borghard, Use of water as a probe of zeolitic properties: interaction of water with HZSM-5, *Microporous Mesoporous Mater.*, 35-36 (2000) 435-446.
- [10] T. Kawai, T. Yanagihara, K. Tsutsumi, Adsorption characteristics of chloroform on modified zeolites from gaseous phase as well as its aqueous solution, *Colloid Polym. Sci.*, 272 (1994) 1620-1626.
- [11] J.H. Zhu, D. Yan, J.R. Xai, L.L. Ma, B. Shen, Attempt to adsorb N-nitrosamines in solution by use of zeolites, *Chemosphere*, 44 (2001) 949-956.
- [12] F. Wei, J.Y. Yang, L. Gao, F.N. Gu, J.H. Zhu, Capturing nitrosamines in tobacco-extract solution by hydrophobic mesoporous silica, *J. Hazard. Mater.*, 172 (2009) 1482-1490.
- [13] S. Li, V.A. Tuan, R.D. Noble, J.L. Falconer, MTBE adsorption on all-silica beta zeolite, *Environ. Sci. Technol.*, 37 (2003) 4007-4010.
- [14] A. Erdem-Senatarlar, J.A. Bergendahl, A. Giaya, R.W. Thompson, Adsorption of methyl tertiary butyl ether on hydrophobic molecular sieves, *Environ. Eng. Sci.*, 21 (2004) 722-729.
- [15] A. Giaya, R.W. Thompson, Water confined in cylindrical micropores, *J. Chem. Phys.*, 117 (2002) 3464-3475.
- [16] A. Rossner, S.A. Snyder, D.R.U. Knappe, Removal of emerging contaminants of concern by alternative adsorbents, *Water Res.*, 43 (2009) 3787-3796.
- [17] W.A. Mitch, J.O. Sharp, R.R. Trussel, R.L. Valentine, L. Alvares-Cohen, D.L. Sedlak, N-Nitrosodimethylamine (NDMA) as a drinking water contaminant: A review, *Environ. Eng. Sci.*, 20 (2003) 389-404.

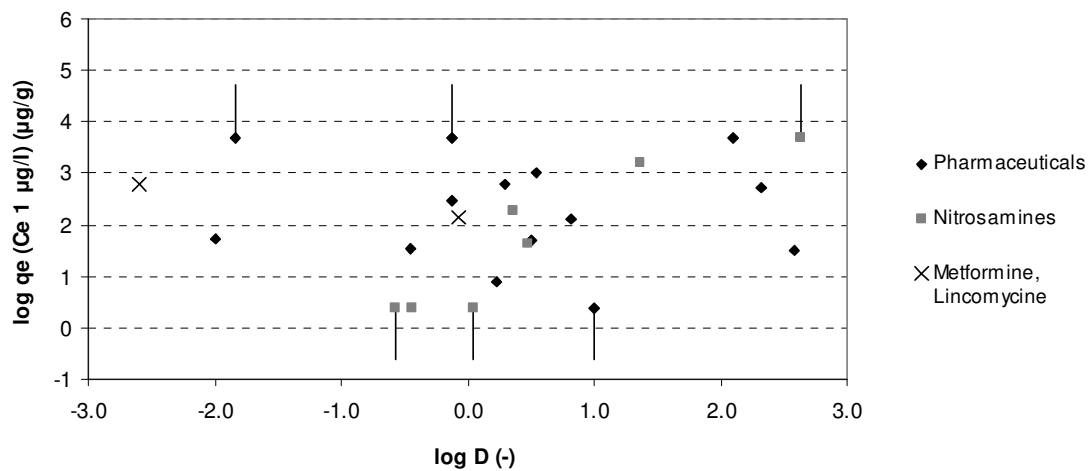
- [18] S.A. Snyder, P. Westerhoff, Y. Yoon, D.L. Sedlak, Pharmaceuticals, Personal Care Products, and Endocrine Disruptors in water: Implications for the water industry, *Environmental Eng. Sci.*, 20 (2003) 449-469.
- [19] S.A. Snyder, Occurrence, treatment, and toxicological relevance of EDCs and pharmaceuticals in water, *Ozone: Sci. Eng.*, 30 (2008) 65-69.
- [20] R.P. Schwarzenbach, P.M. Geschwend, D.M. Imboden, *Environmental Organic Chemistry*, Wiley-interscience, 2003.
- [21] M.E. Jarvie, D.W. Hand, S. Bhuvendralingam, J.C. Crittenden, D.R. Hokanson, Simulating the performance of fixed-bed granular activated carbon adsorbers: Removal of synthetic organic chemicals in the presence of background organic matter, *Water Res.*, 39 (2005) 2407-2421.
- [22] L. Ho, C. Grasset, D. Hoefel, M.B. Dixon, F.D.L. Leusch, G. Newcombe, C.P. Saint, J.D. Brookes, Assessing granular media filtration for the removal of chemical contaminants from wastewater, *Water Res.*, 45 (2011) 3461-3472.
- [23] X. Dai, L. Zou, Z. Yan, M. Millikan, Adsorption characteristics of N-nitrosodimethylamine from aqueous solution on surface-modified activated carbons, *J. Hazard. Mater.*, 168 (2009) 51-56.
- [24] E.C. Fleming, J.C. Pennington, B.G. Wachob, R.A. Howe, D.O. Hill, Removal of N-nitrosodimethylamine from waters using physical-chemical techniques, *J. Hazard. Mater.*, 51 (1996) 151-164.
- [25] S. Kommineni, W.P. Ela, R.G. Arnold, S.G. Huling, B.J. Hester, E.A. Betterton, NDMA treatment by sequential GAC adsorption and Fenton-driven destruction, *Environ. Eng. Sci.*, 20 (2003) 361-373.
- [26] A. Pinisakul, C. Kritayakornupong, V. Ruangpornvisuti, Molecular modeling of nitrosamines adsorbed on H-ZSM-5 zeolite: An ONIOM study, *J. Mol. Modell.*, 14 (2008) 1035-1041.
- [27] J.K. Brennan, K.T. Thomson, K.E. Gubbins, Adsorption of water in activated carbons: effects of pore blocking and connectivity, *Langmuir*, 18 (2002) 5438-5447.
- [28] M.F. Tennant, D.W. Mazyck, The role of surface acidity and pore size distribution in the adsorption of 2-methylisoborneol via powdered activated carbon, *Carbon*, 45 (2007).
- [29] D.J.de. Ridder, A.R.D. Verliefde, S.G.J. Heijman, J.Q.J.C. Verberk, L.C. Rietveld, L.T.J.van der Aa, G.L. Amy, J.C.v. Dijk, Influence of natural organic matter on equilibrium adsorption of neutral and charged pharmaceuticals onto activated carbon, *Water Sci. Technol.*, 63 (2011) 416-423.

Supporting information

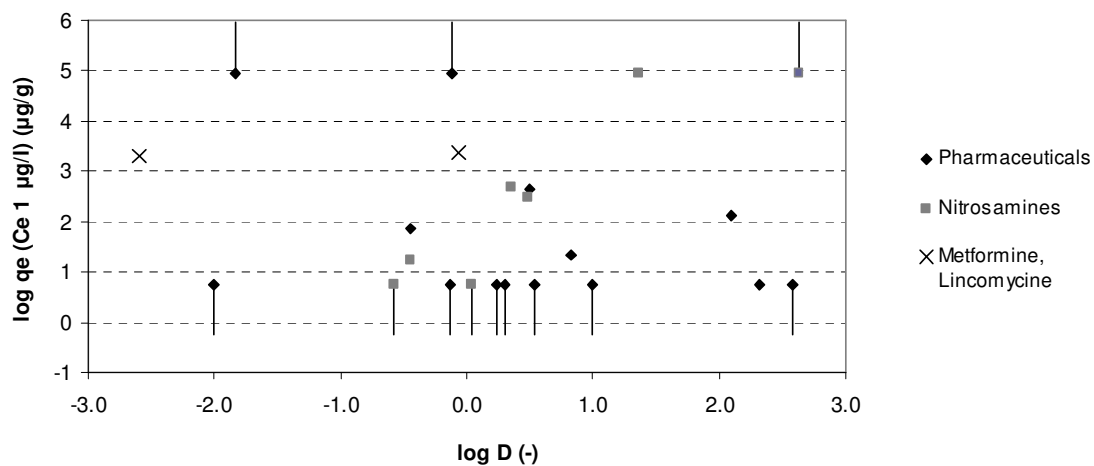
Chapter 6

Zeolites for nitrosamine and pharmaceutical removal from demineralised and surface water: mechanisms and efficacy

D.J. de Ridder¹*, J.Q.J.C. Verberk¹), S.G.J. Heijman¹), G.L. Amy^{1,2}) J.C. van Dijk¹)



S1: MOR200 surface load of nitrosamines and pharmaceuticals vs log D. Solutes with either complete removal or no removal are indicated with error bars.



S2: ZSM5 surface load of nitrosamines and pharmaceuticals vs log D. Solutes with either complete removal or no removal are indicated with error bars.

Chapter 7

Conclusions and recommendations

Relevant solute and activated carbon properties

Research question: What solute and activated carbon properties can be related to adsorption mechanisms to determine removal efficacy? (Chapters 2, 3, 4)

When investigating adsorption of a wide range of solutes onto F400 activated carbon in dematerialized water, solute removal could be related to $\log D$, the octanol-water partitioning coefficient, corrected for the pH value at which the experiments are performed. This indicates that hydrophobic partitioning is an important mechanism for solute removal. This finding is not particularly surprising, as other authors draw similar conclusions [1-3]. Aromatic solutes are typically stronger adsorbed than aliphatic solutes, as aromatic solutes can form pi-pi bonds between the aromatic ring of the solute and an aromatic ring in the activated carbon basal plane.

Molecule size and charge did not affect adsorption significantly. However, it was found that the presence or absence of hydrogen bond donor/acceptor groups had a strong influence for relatively hydrophilic solutes, e.g., for solutes with a $\log D$ of 1.0, the carbon loading of solutes with hydrogen bond d/a groups was 1.5 log units higher than for the solutes without. This difference is reduced for solutes with higher $\log D$ values, and does not exist at a $\log D$ of 3.7, where hydrophobic partitioning is the dominating mechanism for solute adsorption. The stronger adsorption of solutes with hydrogen bond d/a groups is caused by hydrogen bond formation between the solute and functional groups on the activated carbon surface.

Given the importance of hydrophobic partitioning and hydrogen bond formation between solute and activated carbon, the methods used to characterize activated carbon should be related to the affinity of activated carbon with water, and to characterization of the different functional groups responsible for hydrogen bond formation. Therefore, a wide range of activated carbons was selected. Water vapour uptake provided information on the total amount of water molecules that are adsorbed, and this related to the total oxygen surface density of activated carbon. However, this did not give information about the interaction strength of water with the activated carbon surface. Contact angle measurements and immersion calorimetry can give information about the interaction strength of water with activated carbon, where immersion calorimetry proved to be more accurate as it characterizes both the internal and external activated carbon surface, where contact angle measurements mainly characterize the external surface. This interaction strength between water and activated carbon correlated more strongly to only a fraction of the oxygen containing functional groups, i.e., carbonylic and phenolic functional groups, rather than the total, indicating that not all oxygen containing functional groups adsorb water with equal strength. When following the thermodynamic equation explaining the interaction energy between a solute and activated carbon in water, the interaction energies between activated carbon-water, solute-water, solute-activated carbon and water with itself (i.e. its cohesion) have to be determined (equation 1)

$$W_{scw} = W_{sc} + W_{ww} - W_{sw} - W_{cw} \quad (1)$$

Here, W_{ij} (mJ/m^2) is the work required per unit area to separate two phases i and j and subscripts c , s , and w refer to activated carbon, solute and water, respectively. Activated carbon hydrophobicity is included in W_{cw} , solute hydrophobicity in W_{sw} , and interaction between solute and activated carbon in W_{sc} .

Two solutes, 1-hexanol and 1,3-dichloropropene, were selected as probe compounds to test this equation. These were selected as they have similar $\log K_{ow}$ values (2.03 and 2.04, respectively), but 1-hexanol is able to form hydrogen bonds with functional groups on the activated carbon surface, while 1,3-dichloropropene is unable to do so. Immersion calorimetry was used to determine W_{cw} and W_{sc} , while W_{ww} and W_{sw} could be calculated based on surface tension values found in the literature. The work of adhesion (W_{scw}) was compared to the activated carbon loading of 1-hexanol and 1,3-dichloropropene, as determined with equilibrium batch experiments. It was indeed confirmed that 1-hexanol had higher interaction energy with activated carbon (W_{sc}) than 1,3-dichloropropene, confirming our hypothesis that hydrogen bond formation is an important (and almost never accounted for) adsorption mechanism.

Immersion calorimetry can only be used when the solutes are liquids. Many solutes are solid at room temperature, raising the need for a different method to determine solute-activated carbon interaction. For this, the surface tension component approach was used, where interactions between activated carbon, solute and water are defined by van der Waals interaction and acid-base interactions. Amongst others, hydrogen bond formation is an acid-base reaction. Six activated carbons and sixteen solutes were used. The surface tension components of activated carbon were determined using immersion calorimetry, while those of the solutes were determined using contact angle measurements on plates of compressed powder.

To check the validity of the surface tension components, it was first investigated if they could represent simpler activated carbon or solute properties. The acid-base surface tension components of activated carbon correlated to the activated carbon oxygen content. Solute-water interaction correlated well to solubility, although four solutes deviated from the trend. When calculating the Gibbs energy of solute adsorption onto activated carbon in water, based on the surface tension components of each of these three, reasonable correlations ($r^2=0.70$) are found with the experimentally determined carbon loading for single solutes on the six different activated carbons.

Influence of natural organic matter

Research question: What is the influence of natural organic matter on solute adsorption? (Chapter 5)
--

In practice, solutes are removed from natural waters, rather than from demineralised water. Natural organic matter (NOM) present in natural waters can influence solute adsorption by either competing for adsorption sites, or restricting access to (micro)pores. In order to separate these two mechanisms, activated carbon was preloaded with natural organic matter in an attempt to maximize pore blockage, and experiments with fresh activated carbon, but in natural water, were done to maximize adsorption competition. Two different water types, surface water and waste water, were used.

Competition with NOM and pore blockage due to NOM could not be strictly separated when comparing solute removal on fresh or NOM-preloaded activated carbon in natural water and demineralised water. When activated carbon is preloaded by NOM, the available surface for adsorption is reduced due to pore blockage, but NOM also adsorbs onto this surface, forcing solutes to compete with its adsorbed state, rather than with its dissolved state. A reduction of BET surface of 28% and 24% was observed for activated carbon that was preloaded with surface water and waste water, respectively. For surface water preloaded activated carbon, blockage of micropores (as reflected by the iodine number) was more extensive, which could

be related to the higher fraction of humic substances ($MW \approx 1000 \text{ g/mol}$). For waste water preloaded activated carbon on the other hand, (partial) blockage of mesopores (as reflected by methylene blue adsorption) was more extensive, which could be related to the higher fraction of biopolymers ($MW > 20,000$) in waste water.

In contrast to the previous experiences with fresh activated carbon and demineralised water, charge interactions did affect solute adsorption significantly. NOM has a negative charge at neutral pH, and after preloading with NOM, the surface of activated carbon obtains a negative charge as well. This resulted in reduced adsorption of negatively charged solutes and increased absorption of positively charged solutes. The influence of charge repulsion or attraction on solute removal onto preloaded activated carbons was strongest in demineralised water. This influence was lower in surface- or waste-water, due to charge shielding by ions. Compared to adsorption on fresh activated carbon in demineralised water, the reduction in solute adsorption as a result of NOM competition and pore blockage is dramatic. Where both positively and negatively charged solutes are removed to 80-100% in the NOM-free case with a carbon concentrations of 6.7 mg/l, the removal of positively charged solutes is reduced to 32-98%, and the removal of negatively charged solutes is reduced to 0-58% when the carbon is preloaded.

Zeolites as alternative adsorbent

Research question: Are zeolites an effective alternative adsorbent to remove organic micropollutants that are removed poorly on activated carbon? (Chapter 6)

Following the large impact that NOM has on solute adsorption for activated carbon, there is a strong interest for alternative adsorbents that can exclude NOM from entering the pores, thus preventing the negative influence that NOM has on solute adsorption. For this purpose, it is investigated if high-silica zeolites, which have pore diameters of only 0.5 to 0.7 nm, can be effective adsorbents for a wide range of solutes.

It was found that Mordenite (Si/Al 200) and ZSM5 (Si/Al 80), the two most hydrophobic zeolites, showed higher removal of neutral nitrosamines in dematerialized water than activated carbon. Dealuminated Y zeolite and Mordenite (Si/Al 30) were more hydrophilic and showed no appreciable removal of any of the nitrosamines. When nitrosamines were adsorbed from surface water, there was no influence of competition with, or pore blockage by, NOM components on nitrosamine removal for ZSM5 zeolite, in contrast to activated carbon. Repulsion of negatively charged pharmaceuticals was significant for ZSM5, which had a Si/Al ratio of 80. MOR200 had a Si/Al ratio of 200, indicating a lower Al content than ZSM5 and, as such, a lower negative surface charge. Charge effects were not observed for MOR200. A relationship was found between the Stokes diameter of the pharmaceuticals and nitrosamines, and their removal by ZSM5 and MOR200, indicating that a "close fit" adsorption mechanism is more likely than hydrophobic interaction for these zeolites

QSAR model

From this thesis, it can be concluded that using a thermodynamic approach to describe adsorption processes can yield reasonable predictions of solute carbon loadings, includes both solute and activated carbon characteristics, and provides more insight into adsorption mechanisms than an indicative parameter such as solute log D or activated carbon oxygen content does. Some experimental effort is still required; while the activated carbons only have to be characterized only once, each new solute has to be characterized as well. This experimental effort and the costs involved are lower than when batch experiments are performed to derive an equilibrium adsorption isotherm.

As the model was developed using fresh activated carbon and demineralised water, and equilibrium adsorption is predicted, the model can give a “best case” removal efficacy. It can also be used in a relative way, comparing the adsorption efficacy of different solutes. As such, the model would be valuable for screening purposes to identify which activated carbon type would be most suitable for specific solutes, or which solutes adsorb poorly or strongly on a specific activated carbon type. The former screening can support drinking water companies in their decision which activated carbon type they should choose. The latter screening can support policy makers to ban certain products, or support drinking water companies to stop the intake of surface water when solutes are poorly removed by adsorption onto activated carbon. Pharmaceuticals which showed relative poor adsorption were Metformine, Lincomycine and Cyclophosphamide.

Model improvement is required for the following aspects:

- The current dependent (i.e. predicted) variable, q_e at a specific C_e , only describes a single point on the adsorption isotherm, rather than describing the whole isotherm. A possible improvement is to use the model only for the low solute concentrations in the initial linear part of the isotherm. Alternatively, the adsorption isotherm of one solute can be measured, and adjusted for other solutes based on their q_e at a specific C_e , relative to this solute. Of course, the shape of the isotherm should then be similar for the solutes, and additional research is required to determine what factors affect the isotherm shape.
- Adsorption competition between solutes is not included in the current model. A commonly used method to model competition is the Ideal Adsorbed Solute Theory (IAST). As model input, (predicted) single solute isotherms are needed.
- The effect of NOM is not included. Here, more extensive research is needed to first determine which NOM fractions are dominant for adsorption competition, which are dominant for pore blockage, and how this is influenced by activated carbon surface chemistry and pore size distribution. Immersion calorimetry can be helpful to determine the surface tension components of NOM preloaded activated carbon as well, but an important analytical difficulty is that many activated carbon characterisation techniques (such as pore size distribution and immersion calorimetry) require the carbon sample to be dry. Drying may affect NOM characteristics, and open up pores that are blocked under wetted conditions. Adsorption of probe solutes with various sizes from water can be used as an alternative for determining the pore size distribution with N_2 adsorption.
- The model is not a real QSAR, for which the only required input is a molecule's chemical structure. It can be attempted to relate the solute surface tension components to molecule fragments. This can for example be done by using a similar approach as is done for biodegradability in BioWin, where the molecule is divided into fragments, which each have a certain contribution to biodegradability.

Practical conclusions

In this thesis, the activated carbon loading is expressed in $\mu\text{mol}/\text{m}^2$ to be able to compare the efficacy of the different carbons based on surface interactions. In practice, the main interest is in the total capacity of activated carbon, rather than the capacity per unit of surface, so all activated carbon loadings were recalculated to $\mu\text{mol}/\text{g}$ for a practical comparison.

Both hexanol and 1,3-dichloropropene were removed most effectively by F400 activated carbon (2021 and 742 $\mu\text{mol}/\text{g}$, respectively). For hexanol, the solute with a hydrogen bond donor group, the runner-ups were SN4 (2016 $\mu\text{mol}/\text{g}$), AC1230C (1705 $\mu\text{mol}/\text{g}$) and ROW 0.8 Supra (1596 $\mu\text{mol}/\text{g}$), while for 1,3-dichloropropene, the solute without hydrogen bond donor/acceptor groups, the runner-ups were SN4 (699 $\mu\text{mol}/\text{g}$), F600 (610 $\mu\text{mol}/\text{g}$) and W35

(595 $\mu\text{mol/g}$). 1,3-dichloropropene carbon load was 466 $\mu\text{mol/g}$ for AC1230C and 479 $\mu\text{mol/g}$ for ROW 0.8 Supra.

When comparing the adsorption of 16 pharmaceuticals onto 6 activated carbons in Chapter 4, AC1230C and ROW 0.8 Supra are included, but F400 and SN4, both of which are more effective for the adsorption of hexanol and 1,3-dichloropropene, are not included. All 16 pharmaceuticals were aromatic and did have hydrogen bond donor/acceptor groups. As expected from the previous experiences with hexanol adsorption, AC1230C and ROW proved to be more effective than the other 4 activated carbons. AC1230C was the most effective activated carbon for 9 of the 16 solutes, and ROW was the most effective for 7 out of 16 solutes. UC830 was effective for many solutes when compared in carbon loading per surface, but due to its relative low surface area (819 m^2/g , compared to 1265 m^2/g for AC1230C and 1499 m^2/g for ROW 0.8 Supra), its carbon loading per gram of activated carbon was lower. Based on equilibrium experiments with fresh powdered activated carbons in demineralised water, F400 and SN4 proved to be most effective for both solutes with and without hydrogen bond donor/acceptor groups. AC1230C and ROW were effective for both solute classes as well, although F600 and W35 outperformed these activated carbons for solutes without hydrogen bond donor/acceptor groups.

The influence of natural organic matter and adsorption kinetics are, however, not included in this comparison, and these can affect the performance of an activated carbon reactor as well. As such, additional testing is still required for choosing the most effective activated carbon for specific process conditions.

Zeolites are known for their specific adsorption or ion exchange capacity, due to size exclusion. The exclusion of NOM is a big advantage of the zeolites. Longer filter run times are possible as compared with activated carbon as competition with NOM is avoided. Furthermore, zeolites are more stable than activated carbon, and it is expected that there will be no material losses during regeneration. A disadvantage of zeolites is that these are also more specific in the types of solutes that can be removed by them. Larger solutes will be excluded from the pores, and for solutes that can enter the zeolite pores, removal efficacy depended on solute size via the “close fit mechanism”. Also, natural (cheap) zeolites typically have low Si/Al ratios. This makes them excellent for ion exchange purposes, but useless for adsorption. Zeolites with higher Si/Al ratios have to be chemically produced, and are consequently more expensive. When water companies have specific organic micropollutants that adsorb poorly onto activated carbon, zeolites might be a solution. Any effects of NOM competition will be nullified, and based on a “close fit mechanism”, a zeolite can be selected with pore sizes that are close to the size of the specific organic micropollutant. In our research, the zeolite ZSM5 had a pore size of 0.5 nm. This zeolite was not effective to remove NDMA, a typical problematic organic micropollutant in drinking water treatment, as the diameter of NDMA is smaller (i.e 0.35 nm). However, zeolites exist with pores in the 0.3-0.4 nm range, such as MSM-35, Merlinoite, Phillipsite, VPI-9 and Yugawaralite. An important precondition is, however, that these zeolites can be produced with high Si/Al ratios (Si/Al >80).

Commercial high-silica zeolites are typically offered in powdered form, but can also be prepared as pellets or beads. Operation with a fixed zeolite bed could be beneficial if the solutes that are difficult to remove with the existing processes are of the same size. Such a fixed bed is expected to have a long filter run time, as only a limited amount of solutes are able to access the zeolite pores and adsorb. A great application would be for the treatment of contaminated groundwater, as the contamination is specific (e.g., MTBE), and contamination plumes can affect the source water for extended periods of time. When target solutes vary in size, one zeolite type will not suffice and a dual zeolite bed would be necessary. When high concentrations of problematic solutes are more incidental, zeolites can also be dosed as

powder, on a temporal basis. This does, however, require careful monitoring of the intake water quality.

References

- [1] Chiou CT. A physical concept of soil-water equilibria for nonionic organic compounds. *Science*. 1979;106:831-2.
- [2] Westerhoff P, Y. Yoon, S. Snyder, E. Wert. Fate of endocrine-disruptor, pharmaceutical and personal care product chemicals during simulated drinking water treatment processes. *Environmental science and technology*. 2005;39:6649-63.
- [3] Hu J-J, T. Aizawa, Y. Magara. Evaluation of adsorbability of pesticides in water on powdered activated carbon using octanol-water partitioning coefficient. *water science and technology*. 1997;35(7):219-26.

Acknowledgements

The last four years “and a bit” have been a voyage of discovery. I’d like to thank Bas for the frequent discussions and direction during this period, and just for listening to my ranting when there was yet another setback at the pilot plant at Leiden-Noord. Arne, you have been a great sparring partner as well, and your surface tension component approach has been the basis for two chapters in this thesis which I consider to be the backbone of my work.

Jasper, you encouraged me to think outside the carbon-box. While cyclodextrins proved to be a bit of a disappointment, the zeolites proved to be promising for removing solutes that adsorbed less effectively on activated carbon. Also, your encouragement to find wisdom outside the boundaries of Delft led to many memorable travels for a short work visit or to present at conferences abroad.

Hans, thanks for giving me the opportunity to even start the PhD; after recently being fired at that time, I can imagine that I didn’t exactly make a motivated impression at the job solicitation, to put it mildly. Fortunately, that turned around and if all goes well, you can cross off another (or your last?) PhD candidate from your list and gain more time to enjoy your retirement. Gary, thanks for discussing my research, be it in Delft or in the hot Saudi desert. KAUST has been an experience of a lifetime, and even though the hard and sometimes troublesome work there may not have resulted directly in a publication, it has been a necessary “shotgun approach” to get a grip on the elusive activated carbon characterization.

Luuk, thanks for involving me in PRIOMF and integrated filtration techniques, and for voicing your trust in me, together with Jules, by making the postdoc in Ghent possible.

Victor and Andrew, thanks for sharing your ideas on QSARs. Even though I drifted to thermodynamics to explain adsorption rather than using statistical approaches, your input has been highly valued and enabled to make a balanced decision on how to proceed with my research.

Theo and Nicole, it was great to be involved in the prioritization of organic micropollutants, and experience how the drinking water companies can be supported in a political way. While, as an engineer, my framework of thinking is usually more short-term (i.e. pollutant X is found, treatment techniques Y, Z can be used to remove it), it is refreshing to also see the longer term solutions to the micropollutant problem (i.e. cooperation between EU member states to reduce emissions).

Tonny and Patrick, thanks for your support in the lab. I have heard that it is becoming quite fancy now the renovation is well on its way. Patrick, it was an “unparalleled pleasure” to meet you each time in the lab and you were a great help in getting familiar on the tough subject of thermodynamics. And a big thank you to the Frenchies; Sofien, Francois, Armand and Simon, who helped me out with the lab work.

Jenny, it was a pleasure co-working with you, and I hope that our discussions on adsorption have been helpful to give your research direction.

Maarten, you were one of my first roommates and it was inspiring to see that showering people and cycling in a water tank could be job descriptions for new trainees as well, rather than the boring isotherm experiments that I had in store for them. It was also great to see that our “party flag” brainstorm idea to indicate how water flows when somebody is swimming was actually used in one of your experiments. Doris, it has been a privilege to be your roommate for more than half of my PhD. It has been a pleasure training for the 10 km with you, experiencing your creativity, and sharing personal thoughts. Mustafa, the short period that you were my last roommate was great as well (especially with those candy buckets), and

your last minute introduction to facebook, including some high-end professional photography, offered an opportunity to stay in touch with you and other colleagues.

Cheryl, I don't know what your secret is, but your always cheerful presence brightens up everyone around you. And your tip to check out the "big bang theory" was pure gold. Sheldon will be glad to have yet another fan.

There are many more of you that enriched my PhD period in your own way; Annelies, Anke, Petra, Marjolein, Guido, Sam, Diana, David, Sheng, Gang, Ran, Peter, Xuedong, Sandra, Jojanneke, Matthieu, Marco, Kerusha, Karin, Rene, Harmen, Weren, Ignaz, Maria, Pawel, Guenda, our secretaries Mieke and Jennifer and of course the staff of the section of sanitary engineering. Your names are accumulated like the end of a movie where the credits are shown. Visitors of a movie just see a list of names (if they even stay to watch the credits at all), but the crew involved in making the movie connects memories which each of the names.

My thoughts go out to my friends and family as well. I'm not sure if my attempts to explain what I was actually doing made any sense to you, but I'll give it a final try before the defence. And once again, prof. Diederik Stapel is not my promoter.

Curriculum Vitae

Personal information:

Surname: De Ridder
Name: David Johannes
Date of birth: 28 juni 1982
Place of birth: Utrecht

Current employment:

Postdoctoral researcher at the University of Ghent

Previous employment/education:

2008-2012

PhD student at the Delft University of Technology. The research involved in identifying and modeling the mechanisms of adsorption of organic micropollutants onto activated carbon and zeolites (i.e. this thesis).

2006-2008

Junior scientific researcher at Kiwa Water Research. Main activities; set-up of research programs, participate in practical execution and interpret and report experimental results.

Projects have been carried out on the following topics:

relationship sludge accumulation and nitrification in rapid sand filters

Start up of manganese removal on a rapid sand filter

PAC/ceramic MF for removal of micropollutants

Particle removal as final polishing step

2000-2006

Study Civil engineering at Delft University of Technology. In the Msc phase, the specialization for water management / sanitary engineering was chosen.

March 2006-June 2006; Msc thesis

The Msc thesis is divided into a research- and a design part.

Research: the role of nitrate, bicarbonate and DOC on hydroxyl radical formation in the UV/H₂O₂ process has been investigated. This research has been carried out at PWN, a Dutch water company.

Design: A global design has been made for a UV/H₂O₂ installation at treatment plant "De Hooze Boom" (Oasen), with regard to MTBE removal.

September-november 2004; Traineeship

During my traineeship I optimized the backwash program of the rapid sand filters at pumping station Katwijk (DZH). The proposed improvement has been implemented.

1994-2000

VWO, Christelijk Lyceum in Zeist. Diploma 2000

Courses taken: Dutch, English, Greek, History, Mathematics B, Physics, Chemistry, Economics I.

Publications

D.J. de Ridder, M. McConville, A.R.D. Verliefde, L.T.J. van der Aa, S.G.J. Heijman, J.Q.J.C. Verberk, L.C. Rietveld, J.C. van Dijk, Development of a predictive model to determine micropollutant removal using granular activated carbon. *Drinking water engineering and science*, 2, 57-62, 2009.

D.J. de Ridder, L. Villacorte, A.R.D. Verliefde, J.Q.J.C. Verberk, S.G.J. Heijman, G.L. Amy, J.C. van Dijk, Modeling equilibrium adsorption of organic micropollutants onto activated carbon. *Water research* 44, 3077-3086, 2010.

L. Ding, H.-P. Deng, X. Han, L. Dong, P. Wang, D.J. de Ridder, Adsorption characteristics of phosphate from aqueous solutions by sponge iron: Isotherm, Kinetics and thermodynamic studies. *Fresenius Environmental Bulletin*, 19, 2548-2561, 2010.

D.J. de Ridder, A.R.D. Verliefde, S.G.J. Heijman, J.Q.J.C. Verberk, L.C. Rietveld, L.T.J. van der Aa, G.L. Amy, J.C. van Dijk, Influence of natural organic matter on equilibrium adsorption of neutral and charged pharmaceuticals. *Water science and technology*, 63, 416-423, 2011.

D.J. de Ridder, J.Q.J.C. Verberk, S.G.J. Heijman, G.L. Amy, J.C. van Dijk, Zeolites for nitrosamine and pharmaceutical removal from demineralised and surface water: mechanisms and efficacy. *Separation and Purification Technology*, 89, 71-77, 2012.

D.J. de Ridder, A.R.D. Verliefde, S.G.J. Heijman, S. Gelin, M.F.R. Pereira, R.P. Rocha, J.L. Figueiredo, G.L. Amy, J.C. van Dijk, A thermodynamic approach to assess organic solute adsorption onto activated carbon in water. *Carbon*, 50, 3774-3781, 2012.

Submitted publications

D.J. de Ridder, A.R.D. Verliefde, K. Schoutteten, S.G.J. Heijman, R. Denoyel, G.L. Amy, J.C. van Dijk, Relation between interfacial energy and adsorption of organic micropollutants onto activated carbon. Accepted in *Carbon*

In Preparation

C. Gobbo, D.J. de Ridder, R. Eelkema, S. J. Marrink, J. van Esch, A.H. de Vries, Design from random conformations and understanding of the mechanism of self-formation in molecular assemblies. In preparation for *Nature Nanotechnology*